BEHAVIOUR OF COMPOSITE SANDWICH DECKS AT HIGH TEMPERATURES

María Isabel García Puchades

Master of Civil Engineering

Composite Construction Laboratory
School of Architecture, Civil and Environmental Engineering
EPFL, École Polytechnique Fédéral de Lausanne

Switzerland, 2016

ABSTRACT

Structures made of FRP composites have been shown to provide efficient and economical applications in bridges and piers. They are being increasingly used due to their several advantages when compared to traditional materials, namely, the lightness, strength, good insulation properties, low maintenance and improved performance when submitted to aggressive environments. However, fire behaviour has been recently identified by several authors as the most critical gap for these materials to be fully exploited.

In bridge construction, decks are the most vulnerable element in the bridge system due to its exposition to the direct actions of wheel loads, chemical attack, temperature/moisture effects, fatigue and fire. In addition, composites used in civil infrastructure pose an unusually high hazard since polymers are highly flammables and release copious amounts of heat, smoke and fumes when they smoulder and burn. Furthermore, when they are exposed to high temperature (typically over 100ºC) the polymer matrix will soften, and this can cause distortion, buckling and failure.

Within this general context, and using as a case study the new Avançon Bridge in Bex (Switzerland), this Master thesis delves into the thermal, mechanical and thermomechanical response of a GFRP-balsa sandwich bridge deck at elevated temperatures. By the development of a numerical model using the finite element (FE) program Abaqus, the thermomechanical response will be studied considering the non-linear response of the structure with temperature dependent material properties.

RÉSUMÉ

Les structures en composites de PRF ont montré que fournir des applications efficaces et économiques dans les ponts et les quais. Ils sont de plus en plus utilisés en raison de leur temps de nombreux avantages par rapport aux matériaux traditionnels, à savoir légèreté, de résistance, de bonnes propriétés d'isolation, une maintenance réduite et des performances améliorées lorsqu'ils sont soumis à des environnements agressifs. Cependant, le comportement du feu a été récemment identifié par plusieurs auteurs comme le point le plus critique pour ces matériaux est maximisé.

Dans la construction de ponts, les panneaux sont les plus vulnérables dans le système en raison de leur exposition aux actions directes de l'élément de charge de roue, les attaques chimiques, les effets de la température / humidité, la fatigue et le feu. En outre, les matériaux composites utilisés dans les infrastructures civiles représentent un risque exceptionnellement élevé parce que les polymères sont très inflammables et libèrent de grandes quantités de chaleur, de la fumée et des vapeurs quand ils brûlent et brûlent. En outre, lorsqu'il est exposé à des températures élevées (généralement supérieures à 100 ° C), la matrice polymère est ramollie, ce qui peut provoquer une déformation, de gauchissement et de l'effondrement.

Dans ce contexte général, cette thèse de mastère utilise le nouveau pont Avançon à Bex (Suisse) comme une étude de cas pour analyser la réponse thermique, mécanique et thermomécanique du tablier de pont, construit en utilisant un sandwich balsa-GFRP, panneau des températures élevées. Elle a développé un modèle numérique en utilisant le programme d'éléments finis (FE), ABAQUS, qui étudie la réponse thermomécanique en tenant compte de la réponse non linéaire de la structure et les propriétés du matériau dépendant de la température.

RESUMEN

Las estructuras realizadas con compuestos de FRP han demostrado que aportan aplicaciones eficientes y económicas en puentes y muelles. Están siendo cada vez más utilizados debido a sus muchas ventajas en comparación con los materiales tradicionales, a saber, ligereza, resistencia, buenas propiedades de aislamiento, bajo mantenimiento y un rendimiento mejorado cuando se somete a ambientes agresivos. Sin embargo, el comportamiento frente fuego se ha identificado recientemente por varios autores como el punto más crítico para que estos materiales se aprovechen al máximo.

En la construcción de puentes, los tableros son el elemento más vulnerable en el sistema debido a su exposición a las acciones directas de carga de las ruedas, los ataques químicos, los efectos de temperatura/humedad, la fatiga y el fuego. Además, los materiales compuestos utilizados en infraestructuras civiles representan un peligro excepcionalmente alto ya que los polímeros son altamente inflamables y liberan grandes cantidades de calor, humo y gases cuando arden y queman. Por otra parte, cuando se exponen a altas temperaturas (por lo general más de 100ºC) la matriz de polímero se ablanda, y esto puede causar distorsión, alabeo y colapso.

Dentro de este contexto general, esta tesis de Master utiliza el nuevo puente Avançon en Bex (Suiza) como estudio de caso, para analizar la respuesta térmica, mecánica y termomecánica del tablero del puente, construido mediante un panel sándwich de balsa-GFRP, a temperaturas elevadas. Se ha desarrollado un modelo numérico, utilizando el programa de elementos finitos (FE) Abaqus, que estudia la respuesta termomecánica teniendo en cuenta, la respuesta no lineal de la estructura y las propiedades del material dependientes de la temperatura.

AKNOLEDGEMENTS

First, I would like to express my sincere gratitude to my main supervisor, Dr. Chao Wu, for his patience and motivation. I would also like to extend my appreciation to my co-supervisors, Dr. Anastasios P. Vassilopoulos and Porf. Dr. Thomas Keller.

I would like to express my deepest thanks to Vicente Albero for his unconditional support and patient, even on Sundays. I will also not forget José Alós, Antonio Hospitaler, Pedro Serna and Guillem Peris for their help and for introducing me in the world of structures on fire.

I also appreciate the sound support from the incredible team working in the laboratory (CCLab-EPFL), for their support and help. Especially for my office mates, always willing to listen.

I would also like to thank my family and friends all over the world for their amazing support and care, Thanks in particular for the people that I have met in Lausanne, specially to my girls, they have made me feel at home and have treated me like their family, they will always have a special place in my heart.

And, last but not the least, my gratitude goes to my own family for their tireless support, particularly my mother for the extraordinary sacrifices throughout life and unconditional love, my father whom I hope I have made proud and for his patience, support and advices, and my brother, always a model to follow.

TABLE OF CONTENTS

ABSTRACT

RÈSUMÈ

RESUMEN

AKNOLEDGEMENTS

LISTE OF TABLES viii

LISTE OF FIGURES ix

1. INTRODUCTION 1

1.1 Context and motivations 1
1.2 Objectives 3
1.3 Methodology 3
1.4 Thesis organization 4

2. STATE OF THE ART 5

2.1 Composite sandwich panels in civil construction 5
2.2 Sandwich panels in bridge deck construction 7
2.3 Performance in service of sandwich panels 9
2.3.1 Durability 9
2.3.2 Sustainability 10
2.3.3 Corrosion 11
2.3.4 Fire resistance behaviour 11
2.4 Fire hazard in bridges 12
2.4.1 Sources of fire 15
2.4.2 Fire localization 16
2.5 Fire action 17
2.5.1 Phases and spread of fire 17
2.5.2 Fire analysis 19
2.5.3 Human risk 23
2.6 Modelization: Fire engineering 24
2.6.1 Field of application of different design models 31
2.7 Fire protection 31

3. MATERIALS CHARACTERIZATION 33

3.1 Balsa-GFRP Sandwich Panel 33
3.2 Balsa wood 35
3.2.1 Macro and micro structure 36
3.2.2 Physical and mechanical properties 37
3.2.3 Thermal properties 40

3.2.4 Properties function of temperature 42
3.2.5 Fire behaviour 47
3.2.6 Degradation, decomposition and deterioration 49
3.3 Glass Fibber Reinforced Polymer 50
3.3.1 Glass fibres 50
3.3.2 Vinyl ester 51
3.3.3 Physical and mechanical properties 52
3.3.4 Thermal properties 54
3.3.5 Properties function of temperature 55
3.3.6 Fire behaviour 60
3.3.6.1 Fire reaction 61
3.3.6.2 Fire resistance 64
3.3.7 Degradation, decomposition and deterioration 65
4. FE MODELIZATION AND CASE STUDY 68
4.1 Background 68
4.1.1 Heat transfer model 68
4.1.2 Structural model 69
4.2 Case study: Avançon Bridge 70
4.2.1 Situation and context 70
4.2.2 Structure and composition 71
4.2.2.1 Core 72
4.2.2.2 Skin 72
4.2.3 Structural design 73
4.2.4 Fire protection 73
4.3 Finite Element Model 74
4.3.1 Structural model 74
4.3.1.1 Mesh 74
4.3.1.2 Mechanical properties 76
4.3.1.3 Boundary conditions 77
4.3.1.4 Gravity loads 78
4.3.2 Heat transfer model 78
4.3.2.1 Mesh 79
4.3.2.2 Thermal properties 79
4.3.2.3 Thermal loads 80
4.3.3 Thermomechanical model 82
4.3.3.1 Failure Criteria 83
5. RESULTS AND DISCUSSION 85
5.1 Mechanical behaviour 85

5.1.1 Deflection.....85
5.1.2 Stresses.....88
5.2 Thermal behaviour.....90
5.3 Thermomechanical behaviour.....95
6. CONCLUSIONS AND FURUTE WORK.....101
6.1 Conclusions.....101
6.2 Future work.....102
BIBLIOGRAPHY.....103

LISTE OF TABLES

Table 1. Some of the major fires in the last 15 years 13
Table 2. Fire classification..... 19
Table 3. Fire reaction classes EN 13501-1 20
Table 4. Lack of oxygen effects 24
Table 5. Summary of the modelling approaches used in previous fire bridge studies... 28
Table 6. Mean characteristics of thermal approaches..... 29
Table 7. Mean characteristics of advanced structural models 30
Table 8. Field of application of different design methods..... 31
Table 9. Elastic and Poisson's ratios at approx. 12% moisture content 39
Table 10. Balsa mechanical properties per density class..... 40
Table 11. Thermally induced changes in wood 49
Table 12. E-glass compositions 51
Table 13. Typical fibre properties 51
Table 14. Typical properties of matrix materials. 52
Table 15. Typical values for unidirectional FRP composites..... 52
Table 16. Mechanical properties of GFRP profiles 53
Table 17. Thermal properties of GFRP 54
Table 18. Main processes when a composite is exposed to fire 60
Table 19. Mesh features..... 76
Table 20. Mechanical properties of the materials..... 77
Table 21. Thermal properties of the materials..... 79
Table 22. Temperature distribution along the structure 81
Table 23. Deflection values 88
Table 24. Stress values 89
Table 25. Deflection thermo-mechanical values 95
Table 26. Deflection values at failure time..... 96

LISTE OF FIGURES

Figure 1. FRP Hybrid box beam concept 5
Figure 2. Monocoque Fibre Composite truss concept 6
Figure 3. Novartis Campus with GFRP sandwich roof. 6
Figure 4. Various FRP deck systems. 8
Figure 5. Fire tetrahedron 17
Figure 6. Time-temperature curve for a real fire 18
Figure 7. Fire curves scheme 20
Figure 8. The three nominal curves defined in the Eurocodes 21
Figure 9. Standard and parametric curve 22
Figure 10. Different existing fire curves 23
Figure 11. Steps of structural fire engineering 25
Figure 14. Temperature-time profiles at the front (heated) skin, middle of balsa core and back skin exposed to the heat flux 50 kW/m2. 34
Figure 15. Effect of heat flux on the ignition times of 2 sandwich composites 34
Figure 16. GRP/Balsa- core HRR curves for different irradiances. 35
Figure 17. Micrograph and sketch of the cellular nature of balsa wood 36
Figure 18. Simplified microstructure of balsa wood 37
Figure 19. Principal anisotropy direction of the material 37
Figure 20. Variation of compressive strength (longitudinal direction) 39
Figure 21. Shear modulus and shear strength vs. density for all shear planes 40
Figure 22. TC graphed against density 41
Figure 23. Transverse elastic modulus for tension and compression and in-plane elastic modulus 43
Figure 24. In-plane and transverse shear moduli. 43
Figure 25. Effect of temperature on compression strength 44
Figure 26. Normalized high-temperature strength 44
Figure 27. Transverse (axial) and in plane (radial) compressive strengths 44
Figure 28. Effect of increasing temperature on the tensile strength and modulus of balsa 45
Figure 29. Tensile stress vs strain curves at different temperatures 45
Figure 30. Specific heat and TGA data for balsa wood (20°C/min) 46
Figure 31. Schematic of a burning wood 48

Figure 32. Mass loss-temperature curve 48
Figure 33. Microstructure of the balsa before and after thermal decomposition 50
Figure 34. Structure of vinyl ester pre-polymer. 52
Figure 35. Longitudinal and transverse modulus as a function of angle inclination of the fibres 53
Figure 36. Poisson's ratio as a function of angle of inclination of the fibres 53
Figure 37. Schematic of the effect of iso-thermal heating on the mechanical property of a laminate. 55
Figure 38. Degradation of elastic constants with temperature 56
Figure 39. Temperature degradation curves for elastic properties 57
Figure 40. Comparative effect of temperature on the tensile strength of different types of laminates 57
Figure 41. Effect of temperature on tensile strength of E-glass/vinyl ester composite.. 57
Figure 42. Comparison of the failure times for a glass/vinylester under tension or compression 58
Figure 43. Effect of the temperature on the compressive strength of a glass-vinyl ester laminate (a) & (b) 58
Figure 44. Specific heat capacity of char and virgin composite (E/glass/vinylester) as a function of temperature 59
Figure 45. Thermal conductivity of char and virgin composite (E/glass/vinylester) as a function of temperature 59
Figure 46. Effect of temperature on the various responses of a fiberglass composite ... 61
Figure 47. Heat flux against time-to-ignition for 4 composite materials 62
Figure 48. LOI values for several thermoset and thermoplastic composite materials ... 62
Figure 49. HRR profile for a glass/vinyl ester composite 63
Figure 50. Effect of incident heat flux on the smoke yield and smoke generation verses time 63
Figure 51. Mass loss curves for glass/vinylester and glass/phenolic 64
Figure 52. Retained Post-fire flexural strength (%). 65
Figure 53. Tensile, compressive and flexural strength for glass/vinylester 65
Figure 54. Mechanisms involved in the thermal decomposition 66
Figure 55. Imagen of E-glass/VE virgin sample and the same sample heated up to 548 ºC at 20º C/min 67
Figure 56. Microstructure of the laminate after thermal decomposition of the polymer matrix 67
Figure 57. Images taken during the construction of the bridge 70

Figure 58. Image of Avançon Bridge 71
Figure 59. Cross section (mm) 72
Figure 60. Longitudinal section (mm) 72
Figure 61. Mesh used in the FE model 75
Figure 62. Detail of the division of the mesh 75
Figure 63. Temperature dependent modulus of elasticity and Yield strength of S355 .. 76
Figure 64. Temperature dependent coefficient of thermal expansion and Poisson's Ratio of S355 77
Figure 65. Critical load position according to SIA261 78
Figure 66. Eurocode 3 values for thermal conductivity and specific heat 80
Figure 67. Images of FDS simulation 80
Figure 68. Graphic representation of temperature 1 input 81
Figure 69. Graphic representation of temperature 2 input 82
Figure 70. Deflection contour of the composite bridge 85
Figure 71. Longitudinal deflection of the deck 86
Figure 72. Transversal deflection of the deck 86
Figure 73. Longitudinal deflection of the girders 87
Figure 74. Illustration of the maximum deflection u_{max} at the deck and maximum deflection in girder 1, u_g 88
Figure 75. Normal stresses in the girders 89
Figure 76. Normal stress contour 89
Figure 77. Temperature contour of the bridge 90
Figure 78. Temperatures evolution along the transversal span 91
Figure 79. Detail of the temperature contour of the deck 91
Figure 80. Temperatures evolution through-the-thickness of the deck (middle span) ... 92
Figure 81. Temperatures evolution through-the-thickness of the deck (interface GFRP-deck) 92
Figure 82. Temperatures evolution along the girders 93
Figure 83. Temperature evolution in the cross section of the girder 94
Figure 84. Temperature evolution of the deck and the girder 94
Figure 85. Global deformation contour 95
Figure 86. Deflection evolution in time for girder 1 96
Figure 87. Von Mises stress in temperature for Girder 1 97
Figure 88. Normal stress evolution in time for Girder 1 97

Figure 89. Temperatures distribution through-the-thickness of the deck..... 98
Figure 90. Deflection evolution in time for the girder 98
Figure 91. Deflection evolution in time for the deck 99
Figure 92. Von Mises stresses for Girder 1 99
Figure 93. Temperatures distribution through-the-thickness of the deck at failure time 100

1. INTRODUCTION

1.1 Context and motivations

Throughout history, the major breakthroughs in civil engineering have usually stemmed from the use of new materials (Correia, 2015). The durability problems associated with traditional materials and the needs of higher speeds of construction, have had a stimulating effect in the development of innovative structural solutions (Hollaway, 2010; Davalos, et al., 2006).

These demands have coincided with the arrival of new materials in the field of construction such as fibre reinforced polymer (FRP) composites (Keller & Bai, 2014) that are presently assuming a particular relevance, being considered as an enhancement or substitute for infrastructure components that are constructed of traditional civil engineering materials, namely concrete and steel (Jain, et al., 2011). However the lack of ductility of this material is a significant disadvantage with regard to the acceptance of FRP structures by structural engineers (Keller, 2010).

Structures made of FRP composites have been shown to provide efficient and economical applications in bridges and piers. They are being increasingly used due to their several advantages when compared to traditional materials, namely, the lightness, strength, good insulation properties, low maintenance and improved performance when submitted to aggressive environments. At the same time, new design issues and challenges are inevitably encountered as the range of applications for these composite materials in civil engineering constantly increases.

Within the literature survey, some critical issues related with FRP materials such as their durability, sustainability and fire behaviour has been recently identified by several authors as the most critical gap for these materials to be fully exploited for applications in engineering structures. (Correia, 2015; Keller & Bai, 2014; Battles, et al., 2000; Hollaway, 2010; Karbhari & Chin, 2001). Furthermore, Davalos et al., (2006) highlighted that a critical obstacle to the widespread use and application of FRP structures in construction was the lack of design guidelines along with the lack of performance data and accepted engineering standards (Hollaway, 2003). However, several groups are currently working to create a design code including the National Institute of Standards and Technology (NIST), the American Association of State Highway Officials (AASHTO) and the European Structural Polymeric Composites Group. They are using the existing material and bridge codes as guidelines to shape their research and analysis (Kontopanos, 2001).

In bridge construction, these structural applications correspond essentially to the decks, since piers and abutments are still being constructed using traditional materials (Correia, 2015). The modular panel construction of bridge deck systems enables quick project delivery, it can be constructed and

put into service in a relatively short time and at a competitive cost. Additionally, its light-weight materials and ease of construction provide labour cost and traffic control cost savings to offset a higher first cost (Hollaway, 2010). However, decks are the most vulnerable element in the bridge system due to its exposition to the direct actions of wheel loads, chemical attack, temperature/moisture effects (Hollaway, 2010), fatigue and fire (Correia, 2015). Among all this concerns, fire hazard is the one that is still not accounted in conventional bridge design. Currently it is being developed some recommendations at European level (CIB Report, 2000) related to fire test procedures, although the final document is not expected to be available in a short term.

In addition, the composites used in civil infrastructure pose an unusually high hazard because the polymers often used are highly flammables and release copious amounts of heat, smoke and fumes when they smoulder and burn. When composites are exposed to high temperature (typically over 100ºC) the polymer matrix will soften, and this can cause distortion, buckling and failure of load-bearing structures since the stiffness and strength properties are reduced (Mouritz, 2007).

Furthermore, although the probability of fire breaking out in bridges is low, in the last two decades there has been an increase of fire incidents mainly related with vehicle accidents (Garlock, et al., 2012). These fires, also referred to as hydrocarbon fires or fuel fires, are much more severe than building fires and are characterized by a fast heating rate and a higher peak temperature, reaching as high as 1000 °C within first few minutes of fire.

Due to this concern, the scientific community is developing several studies in this field. In Composite Construction Laboratory of EPFL a line of research focuses on the long-term performance of composite materials and engineering structures. Inside this research axe, it is being studied the behaviour against high temperatures of composite sandwich decks.

Thus, within this general context, and using as a case study the new Avançon Bridge in Bex (Switzerland), this Master thesis delves into the thermal, mechanical and thermomechanical response of a GFRP-balsa sandwich bridge deck at elevated temperatures. More specifically, bridge deck fire response will be analysed under real fire conditions corresponding to a tanker truck accident carrying 35 m^3 of gasoline situated below the bridge, with a heat release rate (HRR) of 2400 kW/m^2. By the development of a numerical model using the finite element (FE) program Abaqus, the thermomechanical response will be studied considering the non-linear response of the structure with temperature dependent material properties.

It has been considered a relevant subject of study due to FRP decks offer a sustainable solution for the rehabilitation of functionally obsolete bridges plus they offer the possibility of immediate repair and

replacement saving the economic consequences due to interruptions to traffic flow. In addition, in recent years bridge fires are becoming a growing concern due to rapid development of urban ground transportation and increased shipping of hazardous materials (flammable materials, spontaneously combustible materials, dangerous materials, etc.) (Alos-Moya, et al., 2014; Kodur & Naser, 2013).

1.2 Objectives

All the recent interest in utilizing fibre reinforced plastic composites as structural members in infrastructure applications has brought the issue of composite durability to the forefront. In order to shed some light on this topic, the main purpose of this research is to describe and characterize the thermostructural behaviour of a sandwich composite bridge (Avançon Bridge) under elevated and high temperatures. Thereby, the following specific objectives have been defined:

- To investigate analytically the behaviour of the sandwich structure composed of two GFRP face sheets and balsa wood under elevated and high temperatures.
- To assess the distribution of temperatures in time through the thickness of the sandwich deck in order to evaluate its thermal behaviour.
- To expose the outstanding mechanical behaviour of sandwich panels used as bridges decks.
- To develop a thermo-structural model with the software ABAQUS in order to be able to accurately predict the behaviour of the bridge.
- To understand and model the progressive changes in states of GFRP-balsa material within temperature increment.
- To predict the time-to-failure of the composite deck in fire and to establish its structural limits.

1.3 Methodology

For the development of this work and for attainment of these objectives, first of all a literature study on the historical and current projects related to the structural use of GFRP in bridges will be made. The research will include a general overview of the fire action focusing in fire hazard on bridges, its localization and possible sources. Furthermore, the characteristics of the GFRP-Balsa sandwich deck (thermal and fire behaviour) will be exposed including, its performance in service (sustainability, long-

term durability and corrosion) and the development of the behaviour of the two materials composing the sandwich deck panel separately. In addition, the study of analytical models and experimental investigations used to assess the failure of load-bearing structures under elevated temperatures will be exposed.

In this line, it is seek to assess the time to failure of the bridge deck. For that purpose, a finite element analysis will be implemented in which will be incorporated the characteristics of each material in time. The purpose of this numerical study will be the development of a model that could simulate the thermo-mechanical behaviour of the sandwich panels until failure, creating a calculation tool calibrated with the experimental characteristics obtained in literature.

1.4 Thesis organization

This thesis is organized in six chapters.

In this chapter, it is intend to make a brief introduction to the topic covered in this work, placing it in the context of civil engineering, and present their objectives and methodology.

In the second chapter, the state of the art, describes and introduces the general principles of sandwich structures, the use and applications of GFRP sandwiches in civil constructions and its behaviour at high temperatures. In addition, it is presented a general review of the fire action and its medialization as well as the position of bridges against fire hazard and a general view of fire protection systems.

In the third chapter, the thermal characteristics and fire behaviour of GFRP/ balsa sandwich panels are developed along with the independent study of the behaviour of both materials. Physical, mechanical and thermal properties, fire resistance and reaction, and degradation of the materials are presented in this chapter.

In the fourth chapter, a review of existing models for the thermo-mechanical simulation and the detailed explanation of finite element model is exposed.

In the fifth chapter, the results of the mechanical, thermal and thermo-mechanical analysis are presented and discussed.

Finally, on the fifth chapter, a summary of the most significant findings of this thesis and aspects that are likely considered to be developed in future studies are presented.

2. STATE OF THE ART

2.1 Composite sandwich panels in civil construction

The use of composite sandwich structures in aeronautical, automotive, aerospace, marine and civil engineering applications is getting wider as these structures have excellent stiffness to weight ratios that leads to weight reduction and fuel consumption (Mouritz & Gibson, 2006; Hollaway, 2010).

In the last decade, sandwich constructions are been commonly used in civil engineering projects both, in volumes as well as in applications, becoming the new generation of materials (Manalo, 2013). Furthermore, the evolution of sandwich structures with enhanced material systems provided an opportunity to expand the application of this material in civil infrastructure. In fact, research efforts throughout the world are continuously aiming toward the development of new and innovative sandwich structures utilising fibre composites to address the need of the construction industry for more durable and cost-effective infrastructure.

One important application of sandwich construction in civil engineering is the sandwich bridge deck. The inherent advantages in strength and stiffness per unit weight as compared to steel reinforced concrete decks make the composite sandwich bridge decks a good alternative. Moreover, over the past 15 years, a significant amount of research has been carried out to investigate its use for replacement of existing deteriorated bridge decks and for new bridge constructions (Dehghan-Manshadi, 2011; Manalo, 2013). Several bridges have been constructed in various parts of the world using lightweight FRP sandwich decks which will be briefly detailed in following sections.

Another use that is now gaining interest is the development of structural beams. The idea of using sandwich structure for beam application was pioneered by Canning et al. (1999) who proposed the use of composite sandwich shear web in an innovative hybrid box section (Figure 1).

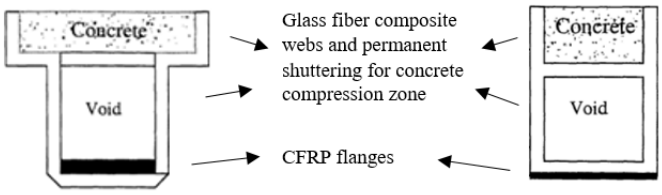

Figure 1. FRP Hybrid box beam concept (cited by (Manalo, 2013))

A similar structural concept was used by Primi et al. (2012) in the construction of a new FRP bridge in Spain. The webs of this hybrid fibre composite bridge beam are sandwich panels with polyurethane core and glass-fibre skins (Potyrała, 2011). Similarly, Lopez-Anido and Xu (2002) developed a structural system based on the concept of sandwich construction with strong and stiff fibre composite

skins bonded to an inner glulam panel. These studies show that is highly practical, however, very limited attempts have been done so far to use composite sandwich materials for this type of structural application, even if engineers have access to a wide range of composite sandwich panels. The main reason could be that most of the currently used core material systems are not appropriate for this type of structural application (Manalo, et al., 2013).

On the other hand, the development and use of fibre composite truss systems in recent applications have demonstrated that composite sandwich construction can be effective and economic. One example is the deployable structure constructed by Omar (2008) where the main frames are formed from modular fibre composite panels that are connected and stressed into position by prestressing cables (Omar, et al., 2007). Other example is the Monocoque Fibre Composite (MFC) truss concept proposed by Humphreys et al (1999) and shown in Figure 2, which uses two planer skins that contain the fibre separated by a core material.

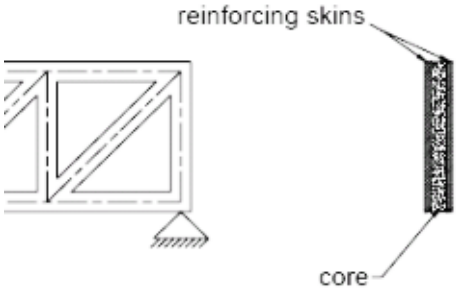

Figure 2. Monocoque Fibre Composite truss concept (Humphreys, et al, 1999)

In building construction, despite the numerous advantages in housing and construction as the reduction of installation and transportation costs and the speed up construction, FRP composites have not yet had the same success (Dehghan-Manshadi, 2011). They have been used in non-structural architectural or aesthetic applications such as cladding, roofing, flooring and partitions. For example, the integrated GFRP sandwich roof structure (Figure 3), constructed for a main gate building in Switzerland by Keller et al., or the development of pultruded FRP composite panels with polyethylene foam core for use in walls and floors in a two-storey building structure designed by The Advanced Composite Construction System (ACCS).

Figure 3. Novartis Campus with GFRP sandwich roof. (Keller & Haas, 2008)

In Australia, the Centre of Excellence in Engineered Fibre Composites (CEEFC) at University of south Queensland in collaboration with the different railway industries, has conducted a wide number of research and development projects, involving innovative fibre composite railway sleepers. These composite sandwich structure are made up of glass fibre composite skins and modified phenolic core material. It has been proven that it has better mechanical properties than most of the commercially available sleepers and has showed comparable properties with the existing timber turnout sleepers.

The sandwich panels can also be used for offshore oil and gas structures platform. The use of composite panels has been increasing in the offshore industry as steel substitutes due to their weight and stiffness (Avó de Almeida, 2009). Furthermore, on the coastline, on boardwalks, jetties, pontoons, etc., the structures also operate in a very corrosive environment resulting in serious durability problems for steel and reinforced concrete. Even hardwood, traditionally been used to overcome some of these problems, would require replacement every 10 to 15 years. However, the composite waler made from glue-laminated sandwich structure is a viable substitute for this application because of its excellent corrosion resistance and durability properties (Manalo, 2013).

The sum of all this applications demonstrate the wide possibility of using fibre composites sandwich as an innovative and effective material system in civil engineering and construction. However, the diverse range of uses for composite materials means they can be exposed to a variety of threats, e.g. their increasing use in high fire risk applications raises the likelihood of severe fire incidents involving this material (Mouritz & Gibson, 2006).

2.2 Sandwich panels in bridge deck construction

The development of bridge decks fabricated entirely from polymer matrix composites, has been largely motivated by the modular concept for rapid construction and durability considerations. The technologies developed to date have moved rapidly from their initial stage of concept validation, into full-scale prototype construction and field implementations. (Chen & Zhao, 2014; Cheng & Karbhari, 2006).

All-composite panels have shown good potential in bridge deck replacements as well as in new bridge constructions in fact many all-composite deck systems are currently available. National Cooperative Highway Research Program (NCHRP) (Transportation research board of the national acedemies, 2006) classifies FRP decks in three categories based on their composition: honeycomb sandwich, solid core sandwich and hollow core sandwich.

Some of the FRP bridge decks systems available on the market are shown in Figure 4: Hardcore (solid core), Kansas (honeycomb), Superdeck (hollow core), EZ-Span (hollow core), DuraSpan (hollow core), ASSET (hollow core), ZellComp (hollow core), ACCS (hollow core), X-shaped filament wound, cell core truss, and corrugated-core sandwich systems

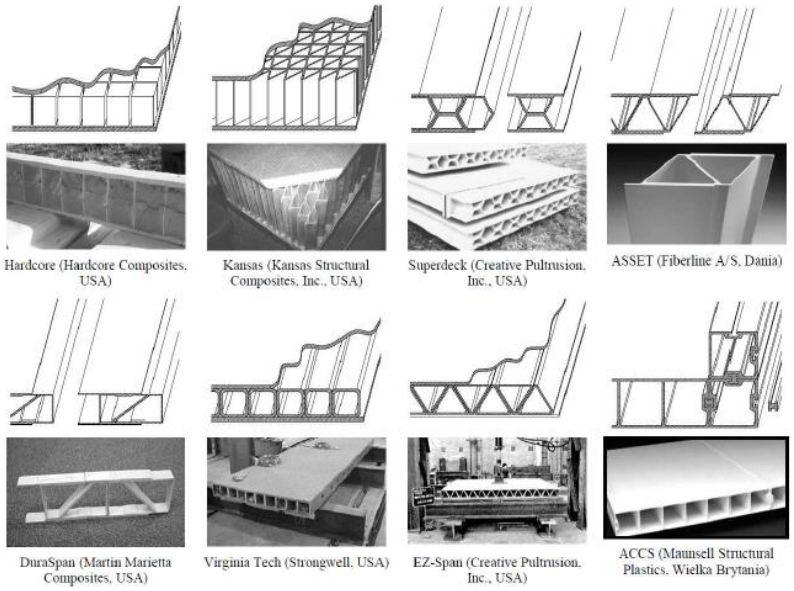

Figure 4. Various FRP deck systems (Cheng & Karbhari, 2006).

Focussing in sandwich panel systems, the best known and most used in bridge construction are the Kansas and Hardcore decks (Schollmayer, 2009).

Kansas Structural Composites, Inc. manufactures an FRP deck composed of top and bottom face sheets with a sinusoidal honeycomb FRP core which is manufactured using hand lay-up techniques (Kontopanos, 2001; Schollmayer, 2009). For this system, glass fibres, polyester as well as honeycomb cores and pultruded edge stiffening members are used (Keller, 2001). The first all-composite bridge in the U. S. (No-Name Creek near Russel/Kansas in 1996) was built using the Kansas deck. After installation, the bridge deck has been continually monitored and has proved its efficacy since the deflections are within acceptable limits (Kontopanos, 2001).

On the other hand, Hardcore deck system is fabricated using a mainly automated technology known as VARTM. The slab elements consist of outer deck layers, generally made of glass fibres and vinylester, as well as an orthotropic honeycomb core made of foam blocks of variable thickness. Moreover, this system has the capability to utilize alternative matrix materials including polyester, epoxy and phenolic if is needed by the design (Keller, 2001; Kontopanos, 2001). The first bridge using the hardcore bridge deck was built in 1997 in Delaware, U. S. with a total span of 23m supported by concrete girders.

In addition to its use in new structures, these types of decks has also been used to replace old concrete bridge decks in renovations and to improve the load rate of bridges.

2.3 Performance in service of sandwich panels

2.3.1 Durability

All materials have a finite life: metals can corrode and can suffer from fatigue; wood can rot; concrete can crack or suffer from various chemical degradation processes; plastics can perish, etc. Composite structures are no exception to deterioration, however, all other materials have been around for long enough to know and make allowance for their weaknesses (Halliwell, 2004).

FRP are now being specified for applications designed to last for 30, 40 or even 60 years without loss of functional effectiveness. Moreover, the accelerating trend towards using FRPs in bridges and buildings means a further extension of the required lifetime, possibly to almost a century.

All construction materials are subject to deterioration in service due to exposure to certain environmental elements. Nevertheless practical applications and scientific studies conducted so far, have attested the overall good performance of FRP materials when subjected to aggressive environments, particularly when compared with traditional materials (Correia, 2015).

Kharbari et al. identified the following environmental conditions as those that influence the most the durability of FRP materials used in civil engineering applications: moisture/solution, thermal effects, ultraviolet radiation, alkalinity, creep/relaxation, fatigue and fire.

Focusing on sandwich panels, some of these actions may cause deformation, loss of carrying capacity and degradation of material properties. Variations in temperature and humidity may cause condensation on the inner faces of the layers (or internal corrosion may cause loss of adhesion between the core and the blades), the core material degradation and/or loss of insulating properties. Solar radiation can cause discoloration of the blades, which cannot be acceptable from an aesthetic point of view. High temperatures may also cause an increase of pressure in the gas expanding agent present in the cells of some core materials, causing local delamination of the panel in the weakest areas (Avó de Almeida, 2009).

The choice of material is hence an important issue as regards the durability of the sandwich panels, the layers must be adequately protected by suitable coatings and the durability of the adhesive material

is important to ensure good adhesion between the layers and the core and thereby its strength. Therefore, in order to guarantee a good performance, the key element seems to be the adequacy of the polymeric matrix to the environmental aggressiveness in harsher environments. As an alternative to the most conventional polyester resin, Correia notes that it is generally preferable to adopt resins with improved behaviour, such as vinylester or even epoxy.

It should be kept in mind that composites have only been used, even in the aerospace world, for structural components for about 60 years, and therefore there is no substantial evidence of their behaviour in time (Avó de Almeida, 2009; Correia, 2015). Further studies should be made in order to assess their long-term durability.

2.3.2 Sustainability

Sustainable development has become an increasingly important theme in many different engineering fields. The most widely used and accepted definition of sustainable development is given in the Common Future (World Commission on Environment and Development, 1987) as 'the ability to make sustainable development to ensure that it meets the needs of the present without compromising the ability of the future generations to meet their needs'. The sustainability of all construction materials has to be assessed taking into account the various phases of their life cycle, namely the following: the manufacturing phase, the service life and the end of the life cycle (Correia, 2015; Valbona, et al., 2014).

The most important limitation of FRP materials in terms of sustainability takes place at the end of the life cycle (Correia, 2015). Due to non-reprocessability of thermosetting resins (most common resin used for civil engineering structural applications) such as polyester or epoxy, the waste management alternatives are very limited. As a consequence, the most frequent waste management option involves processing the FRP materials to granulate and using them as landfill material, which has limited intrinsic value (Potyrała, 2011; Correia, 2015).

However, nowadays, several options for recycling these materials are been studied, e.g., chemical recycling, applied to dissolve the resin and fibres which allows the former components to be reused in other composite products; thermal recycling, for separating matrix from fibres; incineration with energy recovery, using the energy released in controlled incineration for heating or electricity (Valbona, et al., 2014).

Some authors, Correia (2015), Valbona et al., (2014), highlight the future possibility that FRP materials become at least as sustainable as the traditional construction materials they compete with. And this largely depends on the success of the development of thermoplastic resins since after recycling these resins they keep the vast majority of their original mechanical properties (Correia, 2015).

2.3.3 Corrosion

Composite materials as compared to traditional materials (named reinforced concrete, steel, wood, etc.…) possess a substantially higher resistance to corrosion, aggressive media and chemical reagents (Avó de Almeida, 2009; Correia, 2015; Hollaway, 2010). This make them attractive in application where corrosion is a concern. Furthermore, this characteristic allows composites structures to have a long service life without additional maintenance costs.

2.3.4 Fire resistance behaviour

Construction materials are required to have adequate fire reaction behaviour, avoiding fire deflagration, flame spread and excessive smoke production and spreading. Additionally, structural elements are required to have both, sufficient fire resistance, in order to prevent structural collapse under fire during a sufficient period of time, and suitable thermal insulation and tightness so as not to contribute to fire growth.

The decision to apply sandwich panels in construction may be limited by the general safety in fire situation. This is due to the characteristic of the materials used since some of them are susceptible to ignition and later to the contribution to fire. Some organic matrix can decompose at temperatures around 300°C/400°C, releasing heat, smoke, soot and toxic volatiles. Besides, when they are heated to moderate temperatures (100°C/200°C), these materials soften, creep and distort; therefore, their mechanical properties suffer remarkable reductions, particularly those that are more matrix dependent.

In this context, there are legitimate concerns with the fire behaviour of composite materials. However, in spite of these unfavourable properties, FRP materials present other attributes that are useful in a fire situation. In opposition to other traditional materials, such as steel, composites are very good heat insulators, and this feature is important for slowing the spread of fire. Also when compared to steel, composites present better burn-through resistance, providing an effective barrier against flame, heat, smoke and toxic fumes.

Furthermore, several measures, can be applied to improve the fire performance of panels such as superficial protections of the layers, the use of phenolic resins or retardant additives flame and smoke.

The fire behaviour of sandwich panels is further studied in next chapters.

2.4 Fire hazard in bridges

Throughout history, many bridges collapsed due to reasons that can be classified into two broad categories, namely, natural factors and human factors. Natural hazards encompass cases where failures have taken place due to flooding, storms, earthquake or debris flow. These are often unavoidable and can cause serious damages to bridges. In addition to the natural factors, human factors, are distinguished from design errors and construction method, collision, vehicle overloading, fire, terrorist attack, negligence, lack of inspection and maintenance, etc., and may also result in bridge collapses (Deng, et al., 2015; Imam & Chryssanthopoulos, 2012).

Bridge collapse usually associates with serious economic losses since traffic is usually hard to divert and affects the traffic quality in the area (Garlock, et al., 2012; Alos-Moya, et al., 2014). Therefore, the causes and mechanisms of bridge collapse have been studied by researchers and engineers. In fact, from the application of lessons learned from bridge failures, there has been many advances in bridge design and engineering during the latter half of the past century.

On the other hand, bridge collapse is usually a very complex process that results not only from a single factor but from a combined effect of many. Hence, it is sometimes difficult to identify the leading factor that has directly resulted in the collapse (Gibson, et al., 2011). In this research, a review of fire hazard in bridges is presented.

The probability of fire breaking out in bridges is thirteen times lower than that in buildings (Kodur, et al., 2015), however, the impact of such fire on bridges can be much more devastating due to lack of adequate fire protection features and firefighting measures. The primary adverse consequence is loss of service of the bridge, either temporarily or permanently (Garlock, et al., 2012; Wright, et al., 2013). The literature review show that there are no known cases where bridge failure during a fire event has caused human loss-of-life. This makes a clear difference between bridge fires and fires occurring in buildings and tunnel structures where structural performance has a more direct impact on human safety during the fire event.

The vulnerability of a bridge to fire hazard is mainly a function of the performance of its structural members under fire conditions, named super-structural members (slabs and decks) and sub-structural members (girders, piers and abutments). Thus, the overall fire resistance of a structure is a function of fire performance of both members (Naser & Kodur, 2015). Some factors influencing this response include geometrical features, materials used in construction, loading and restraint conditions, fire intensity, among others.

Each year there are many fire events that involve bridges but only a very small subset of events can cause serious bridge damages. The risk of bridge fire is strongly related to the probability of vehicle accidents on or under the. In the last two decades, there has been an increase of fire related accidents in bridges, and some of these fire incidents have led to collapse. Figure 1 show some of the major fire accidents of these decades.

Table 1. Some of the major fires in the last 15 years (Garlock, et al., 2012)

Bridge/ Location	Date	Cause of fire	Bridge material
Bridge over I-75 near Hazel Park, MI, USA	July 15, 2009	A gasoline tanker struck an overpass on I-75	Composite deck (steel girders + reinforced concrete slab)
Big Four Bridge, Louisville, KY, USA	May 7, 2008	Electrical problem of the lighting system, took two and a half hours to control the fire	Steel truss bridge
Stop Thirty Road, State Route 386 Nashville, TN, USA	June 20, 2007	A fuel tanker truck rear-ended a loaded dump truck. The tanker erupted into flames beneath the bridge	Concrete hollow box-beam bridge
I-80/880 interchange in Oakland, CA, USA	April 29, 2007	A gasoline tanker crashed	Composite deck (steel girders + reinforced concrete slab) supported by reinforced concrete columns
Bill Williams River Bridge, AZ, USA	June 20, 2007	A gasoline tanker over-turned Concrete	Concrete deck (precast prestressed I girders + cast in place reinforced concrete slab)
Belle Isle Bridge in NW Expressway, Oklahoma City, OK, USA	Jan 28, 2006	ıck crashed into the bridge	Concrete deck (precast prestressed I girders + cast in place reinforced concrete slab)
Wiehltalbridge in motorway A4, Cologne-Olpe, Germany	Aug 26,2004	Following an accident, a gasoline tanker fell down and started a fire under the first bridge span	Orthotropic steel deck supported in concrete piers and abutments
Bridge over the Norwalk River near Ridgefield, CT, USA	July 12,2005	A tanker truck carrying 30.3 m3 of gasoline overturned, caught fire, and burned out on the bridge	Concrete deck (precast prestressed box girders + cast in place reinforced concrete slab)
I-95 Howard Avenue Overpass in Bridgeport, CT, USA	March 26,2003	A car struck a truck carrying 30.3 m3 of heating oil	Composite deck (steel girders + reinforced concrete slab)
I-20/I-59/I-65 interchange in Birmingham, AL, USA	Jan 5, 2002	A loaded gasoline tanker crashed	Steel girders
I-80W/I-580E ramp in Emeryville, CA, USA	Feb 5, 1995	A gasoline tanker crashed	Composite deck (steel girders + reinforced concrete slab)

Besides, in recent years, due to urbanization, ground shipping have increased demand on transportation (transit of flammable and combustible materials) (Naser & Kodur, 2015). This should

not present a problem if it were not for the fact that the primary cause of damaging fire events for bridges is fuel tanker vehicle crashes (Wright, et al., 2013). Furthermore, significant recent research have highlighted some critical fire safety deficiencies of the materials used in vehicles (National Fire Protection Association, 2007) which may help to combustion and fire spread due to their poor fire performance and fire resistance properties (Mhirschler & GBH International, 2008).

Fires that fully involve the cargo of tanker or flammable goods in trucks, are the subset of crash events that cause serious damage or bridge collapse (Naser & Kodur, 2015; Garlock, et al., 2012; Wright, et al., 2013). Events involving other vehicle types, as busses, empty trucks or cars, can also cause bridge damage but there is a lower potential for them to become fully involved as fuel sources in fire events (Wright, et al., 2013). They may cause lesser forms of repairable damage that may result in temporary loss of service.

These fires, also referred to as fuel or hydrocarbon fires, are much more severe than building fires and are characterized by a fast heating rate and a higher peak temperature, reaching as high as 1000 °C within first few minutes of fire (Garlock, et al., 2012; Alos-Moya, et al., 2014; Mouritz, 2007; Kodur, et al., 2015). Also, collapses typically occur in less than one-half hour (Naser & Kodur, 2015), which does not leave much time for firefighting response.

Non-vehicle related fire events, such as construction fires, trash fires, and wildfires have also involved bridge structures and can cause damage in some cases, but these are less common than crash events (Wright, et al., 2013). However, Simeini (2015) exposes that the impact of wildfires is expected to increase dramatically in the future because of the combined effects of the spreading of the Wildland Urban Interface (WUI) and climate changes (Simeoni, 2015). On the other hand, further bridges are open to general population and are easily accessible to public with minimum or no security at all, thus, are susceptible to vandalism which can often lead to fires (Kodur & Naser, 2013).

So the vulnerability of bridges vary widely depending on local and specific factors, therefore its exposure is difficult to quantify in a general sense. However, various bridge features can be identified that affect the probability of accidents and conditions that increase fire risk (Wright, et al., 2013).

For non-vehicle sources, bridge location, site conditions, and site activities are contributing factors (Garlock, et al., 2012): bridges located in areas where there is an elevated wildfire risk are more susceptible, thus, situation is a first factor; wood structures are vulnerable to ignition from relatively small fire events while steel and concrete bridges require large external fire events to cause damage, thus, bridge materials is a second factor; the presence of flammable materials near a bridge elevates risk since they can be ignited by natural causes or arson, thus, site activities is a third factor.

For vehicle crash events, some of the risk factors that need to be considered are: firstly bridge features (roadway conditions), narrower shoulders or visibility increase the probability of crash events, collisions occur at different points and involve different elements of the bridge; next, road classification and mode, bridges on arterial roads, including interstates and expressways, are three times more likely to be exposed to a vehicle fire compared to collector roads (Wright, et al., 2013); traffic composition and volume, bridges on or over routes with high large truck volume in the traffic composition will be exposed to higher risk; vehicle size and type, parameter that determines the potential size of fire events since as previously appointed, the majority of damaging fire events are caused by large vehicle fires or their hazardous cargo.

This risk is difficult to evaluate in a general sense because each bridge will have specific risk factors. In general, fire resistance is achieved via proper design, selection of materials and detailing of the structural members (Kodur, et al., 2015). This is due to, at the moment, there are no specific requirements in codes and standards for fire resistance of structural members in bridges. Additionally, media reports highlight the difficulty in finding concise information about fire events, most news media reports focused on the public impact of the events, not on technical details which difficult to obtain detailed data about most fire incidents (Wright, et al., 2013).

2.4.1 Sources of fire

Bridges can be exposed to fire from a variety of sources. With the exception of timber and FRP structures, most bridges are constructed from non-combustible materials. The fuel source for bridge fires does not come from the bridge itself, it comes from materials and events occurring in proximity to the bridge.

For highway bridges as well as for railroad bridges, vehicles represent a major potential fuel source. Possible collisions between users, can cause automotive fluids to be spilled within the engine compartment, near fuel system components or on the ground underneath the vehicle. The latest suppose the major hazard for bridges spanning over the roads, the formation of so-called pool or spill fires. The danger posed by these fires depends, in large part, on the volume of the fluid spill and its area, and on the other hand, on the slope and other characteristics of the surface onto which the fuel is spilled (Gottuk & White, 2015; National Fire Protection Association, 2007).

Additionally, debris and other combustible materials can become fuel sources if they are present underneath or adjacent to the bridge. Natural forest and brush fires may represent a fuel source depending on the location of the bridge and the surrounding ground cover. Furthermore, bridges are

easily accessible to public thus being susceptible to vandalism which can often lead to arson fires (National Fire Protection Association, 2007; Garlock, et al., 2012; Kodur & Naser, 2013).

2.4.2 Fire localization

Bridge fire exposures are typically local type fire exposures that are not confined by walls like in a building or tunnel. The extent of damage is very dependent on the location of the fire relative to the bridge and has a negative effect on the structural resistance, from permanent deformations to collapse. The members will lose strength and stiffness as a function of temperature and their response can be determined through large-scale testing or computer simulations.

There is an approximately equal likelihood of fires starting above and below the bridge (National Fire Protection Association, 2007). Nevertheless, previous studies (see (Wright, et al., 2013; Garlock, et al., 2012; Alos-Moya, et al., 2014)), showed that an accident involving a tanker truck carrying gasoline under a bridge was the worst possible scenario when analysing the fire response of bridge decks. Therefore, fires occurring below bridges are much more damaging compared to fires confined to bridge decks since the structural members are protected by asphalt concrete cover (Pagani, et al., 2014). When a fire is developed on top of a bridge, most of the heat flux from fuel fires is directed upward. This, plus the insulating effect of the concrete cover, can be expected to keep the heat low enough to cause little damage. However, as is the case for large fuel spills, burning fuel can drain off the bridge deck and pool under the bridge, resulting in fire both above and below the bridge.

Another aspect to take into account is the height of a bridge deck, if it is not greater than 10 m, the vegetation cannot grow and thicken too much under it, whereas when dealing with a much higher bridge deck (not less than 20 m) the trees can grow under it and therefore make up a bushfire (Pagani, et al., 2014).

Other severe fires have been reported in close proximity to bridges, such as fires that migrated from beneath the bridge to locations outside the bridge. Based on some of the literature data, these types of incidents did in many cases cause significant damage but not as severe as fires beneath the bridge (Wright, et al., 2013).

One characteristic of fires below the bridge is that the fires do not heat the bridge uniformly, they cause localized regions of higher temperature. The open-air nature of the fire results in intermittent flame contact that varies the heat flux into the bridge members. This causes significant temperature gradients within the bridge components and significant temperature differences between different locations in the structure. Moreover, these temperature gradients induce differential thermal expansion

of the components that can result in very high internal stresses and distortion of components (Imam & Chryssanthopoulos, 2012; National Fire Protection Association, 2007). In addition, boundary conditions determined by the presence of expansion joints, bearings, substructure elements, and adjacent spans, have a large influence on the development of these internal forces (Alos-Moya, et al., 2014). On the other hand, these fire events that acts on a part of the bridge will experience lower overall deflection compared to fire events that evenly heat all members.

The most relevant bridge fire scenarios are fires that completely immerse the object, fires impinging onto a structural element located above the fire, and fires confined beneath the bridge flow between beams (Wright, et al., 2013). A better understanding of the sensitivity of fire type and location on the effects of potential damage to bridges is needed to quantify the risk of various fire scenarios.

2.5 Fire action

2.5.1 Phases and spread of fire

The fire can be described in a synthetic way, as a rapid oxidation process in which occurs an exothermic chemical reaction that releases energy in the form of heat and light. In order for any fire to occur, four critical elements must be present: energy activation, fuel, chemical reaction and oxidizer. This is commonly referred to as the fire tetrahedron (Figure 5), each side of the figure represents one of the four ingredients demonstrating the interdependence of these ingredients in creating and sustaining fire.

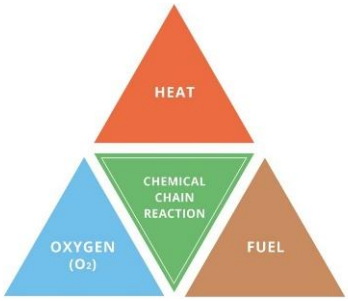

Figure 5. Fire tetrahedron (Spruce, 2016)

The activation energy (heat) works as an ignition source, in other words, is responsible for providing the energy required for the initiation of the oxidation reaction. Fuel, such as wood, is the component that is consumed by the reaction, leading to the production of heat. The third element is oxidising (oxygen) element responsible for the feeding response and sustaining combustion. And the last element is the chemical reaction between the other three elements. If any one of the components is

missing, a fire cannot occur (National Fire Protection Association, 2007; Chandler, 2009; Cote & Bugbee, 1988). A fire will extinct when there is no more fuel or oxidizer available.

The development of fire essentially comprises four phases. In a first phase, the ignition starts with the combustion of a material (ignition temperatures 300±400 °C), this is the instant at which all sides of the fire tetrahedron meet and combustion begins. Then, the fire is spread to other flammable materials which are around the material already in combustion, thereby initiating a second phase of a fire, the growth phase. As consequence of the combustion of materials, release of energy occurs in the form of heat and radiation, fumes and gases. This growth phase is achieved at ambient temperatures above the ignition temperatures, between 300 and 500 °C. With the evolution of the fire, volatile compounds are released which act as accelerators in the combustion reaction of the materials present in the scenario, which increase the temperature to a value of about 600 °C, leading to an overall inflammation called flash-over (generalized inflammation).

The penultimate stage of fire growth is reached when the fire is fully developed and the temperature is maintained approximately constant between 900 and 1200 °C, thence following a cooling phase. In the latter stage of the fire, there is a decrease in temperature. Figure 6, illustrates the phases constituting a fire.

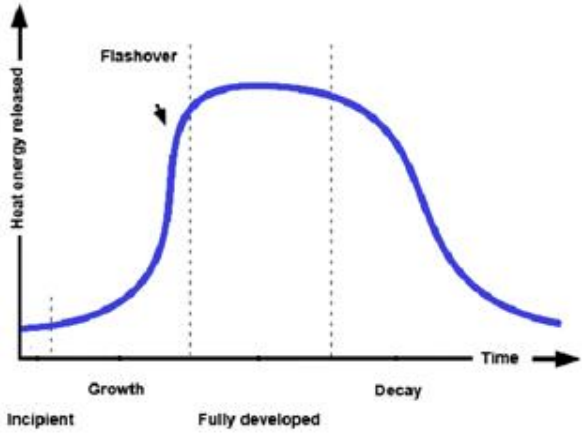

Figure 6. Time-temperature curve for a real fire (Hartin & MS, 2008)

The spread of the fire that takes place in the growth phase is the result of the transference of heat energy from the flames. In accordance with this phenomenon, fire spreads in three different ways: convection, conduction and radiation.

Conduction is the passage of heat energy through or within a material because of direct contact. Convection is defined as the transmission of heat within a liquid or gas due to their difference in density, is the flow of fluid or gas from hot areas to cooler areas. The heated air is less dense, and rises,

while cooler air descends. And finally, radiation is the transmission of heat traveling via electromagnetic waves, without objects or gases carrying it along. Radiated heat goes out in all directions, unnoticed until it strikes an object. (National Fire Protection Association, 2007; Swan, 2014).

2.5.2 Fire analysis

Not all fires are the same thus, different fuels create different fires and require different types of fire extinguishing agents. Exists the possibility that using particular types of fire extinguishers on ignited materials or liquids, may make the fire considerably worse and elevate the risk (Fire Safety Technical Guide, 2015). For this reason, categorising fires makes easier to choose the most appropriate method of fighting the fire. Fires are classified in relation to the combustion materials which have (or could be) ignited:

Table 2. Fire classification

Class	Description
Class A	Fires in ordinary combustibles such as wood, paper, cloth, trash, and plastics
Class B	Fires in flammable liquids such as gasoline, petroleum oil and paint, also including flammable gases such as propane and butane
Class C	Fires involving energized electrical equipment such as motors, transformers, and appliances.
Class D	Fires in combustible metals such as potassium, sodium, aluminium, and magnesium
Class K	Fires in cooking oils and greases such as animal's fats and vegetable fats.

Once the type of fire is classified according to the agent that fuels the fire, it is necessary to classify the materials according to their reaction. Reaction to fire classification is performed according to the so called Euroclass system specified in the standard EN 13501-1 "Fire classification of construction products and building elements". The aim is to define a harmonized procedure for the classification of construction products according to fire separation performance and smoke tightness. This standard affects mainly surface covering materials, insulation materials, floor coverings, pipe insulation materials and cables.

Fire reaction are divided into seven main classes. According to this system, the properties are indicated by a letter (A1, A2, B, C, D, E and F) and the time for which the property is maintained is indicated by an index (10, 15, 20, 30, 45, 60, 90, 120, 180, 240 o 360). Table 3 (European Committee for Standardization (CEN), 2002), show the description of each fire reaction class:

Table 3. Fire reaction classes EN 13501-1 (CEN 2002)

Class	Description
F	Products for which no reaction to fire performances are determined or which cannot be classified in one of the classes A1, A2 , B , C , D , E.
E	Products capable of resisting, for a short period, a small flame attack without substantial flame spread.
D	Products satisfying criteria for class E and capable of resisting, for a longer period, a small flame attack without substantial flame spread. In addition, they are also capable of undergoing thermal attack by a single burning item with sufficiently delayed and limited heat release.
C	As class D but satisfying more stringent requirements. Additionally under the thermal attack by a single burning item they have limited lateral spread of flame.
B	As class C but satisfying more stringent requirements
A2	Satisfying the same criteria as class B for the SBI-test according to EN 13823. In addition, under conditions of a fully developed fire these products will not significantly contribute to the fire load and fire growth.
A1	Class A1 products will not contribute in any stage of the fire including the fully developed fire. Be capable of satisfying automatically all requirements of all lower classes.

There are two additional classifications for smoke production (s1, s2, s3) and for flaming droplets/particles (d0, d1, d2).

So, in order to analyse the behaviour of these constructive elements in case of fire, it is necessary, first, to establish a mathematical model that simplifies the real action of the fire. Using mathematical expressions it has been possible to estimate the temperatures along the evolution of a fire, obtaining a fire curve to simulate fire action. EN 1991-1-2 (Eurocode 1, part 1-2) allows for the use of two different approaches; nominal time-temperature curves and natural fire models.

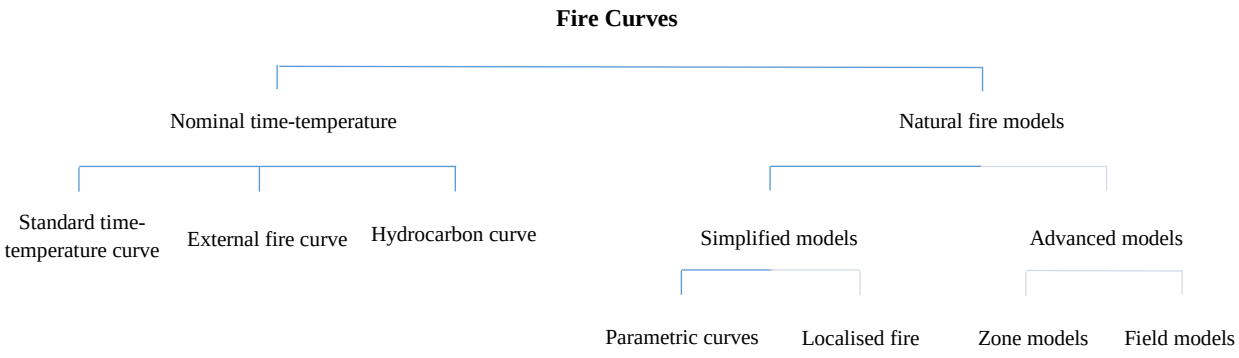

Figure 7. Fire curves scheme

As described by Lennon et al., (2006), the nominal fire curves provide a simple means of assessing building materials and components against a common set of performance criteria subject to a closely defined thermal and mechanical loading under prescribed loading and support conditions. They are classified into: standard time-temperature curve, external fire curve and hydrocarbon curve.

The standard time-temperature curve, also referred as ISO 834, can be used for all fire design scenarios. The standard fire curve is used internationally for fire resistance testing of components and is given by the following equation:

$$\theta_g = 20 + 345 \log_{10}(8 * t + 1) \quad [1]$$

Where

θ_g: Is the gas temperature in the fire compartment [°C]

t: is the time [min]

On the other hand, the application of the external fire curve, is for the outside of external walls which can be exposed to fire from different parts of the façade.

$$\theta_g = 20 + 660\,(1 - 0{,}687 * e^{-0{,}32*t} - 0{,}313 * e^{-3{,}8*t}) \quad [2]$$

Where

θ_g: Is the gas temperatures in the fire compartment [ºC]

t: is the time [min]

The hydrocarbon curve is applicable where small petroleum fires might occur, i.e. car fuel tanks, petrol or oil tankers, certain chemical tankers etc. Therefore, for such situations, an alternative temperature-time curve has been developed:

$$\theta_g = 20 + 1080\,(1 - 0{,}325 * e^{-0{,}167*t} - 0{,}675 * e^{-2{,}5*t}) \quad [3]$$

Where

θ_g: Is the gas temperatures in the fire compartment [ºC]

t: is the time [min]

In Figure 8 is shown the representation of the three nominal fire curves:

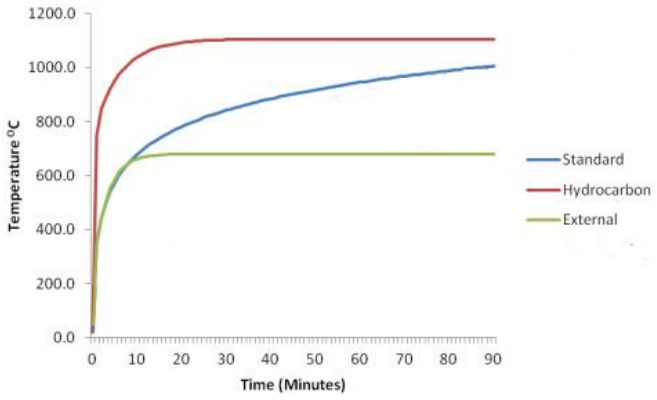

Figure 8. The three nominal curves defined in the Eurocodes (SteelConstruction, 2012)

However, the evolution of the temperature in an actual fire is not same in all cases, it depends on many factors and the temperature is not always growing over time. Unlike a nominal fire curve, a natural fire model takes into account how the environment, density of combustible materials and ventilation

will affect the development of the fire (European Committee for Standardization, 2008). This fire models allow for a more realistic fire scenario to be considered in design and are classified as: simplified models and advanced models.

Inside simplified models it is differentiated between parametric curves and localised fires (Figure 9). The first ones are closer to the behaviour of a real fire compared to the standard curves and they take into account the three main parameters influence the development of a fire: fire load density, ventilation conditions and thermal properties of the envelope of the sector. Localised fires are used when the possibility that the entire sector remains engulfed in flames is very low.

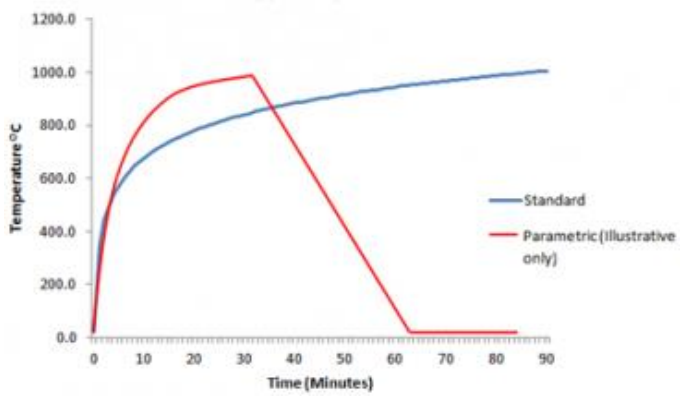

Figure 9. Standard and parametric curve (SteelConstruction, 2012)

Though efficient, those functions cannot represent accurately the fire development and it does not account the three-dimensional fuel distribution (Quiel, et al., 2015). However, in advanced models -zone and field models-, the sequence of events are studied with sophisticated numerical tools based on computational fluid dynamics (CFD) that take into account the main parameters that control the evolution of the fire (Código Técnico de la Edificación de España (CTE), 2010). This type of models are further explained in section 2.6 Modelling: fire engineering.

In addition to Eurocode 1, other curves have been developed in order to fulfil different needs and are mainly applicate in the studies of tunnel fires. Derived from the above-mentioned hydrocarbon curve, the French regulation developed the so called HydroCarbon Modified curve (HCM), an increased version of the initial hydrocarbon curve. The maximum temperature of the HCM curve is 1300ºC instead of the 1100ºC (Figure 10). The temperature development is described by the following equation:

$$\theta_g = 20 + 1280\,(1 - 0{,}325 * e^{-0{,}167*t} - 0{,}675 * e^{-2{,}5*t}) \qquad [4]$$

Where

θ_g: Is the gas temperatures in the fire compartment [ºC]

t: is the time [min]

On the other hand, the RABT curve was developed in Germany as a result of a series of test programmes such as the Eureka project. In the RABT curve, the temperature rise is very rapid up to 1200°C within 5 minutes. The duration of the 1200°C exposure is shorter than other curves with the temperature drop off starting to occur at 30 minutes for car fires and 60 minutes for train fires.

The RWS curve was developed by the Rijkswaterstaat (Ministry of Transport in the Netherlands). This curve is based on the assumption that in a worst case scenario, a 50 m³ fuel, oil or petrol tanker fire with a fire load of 300MW could occur, lasting up to 120 minutes. The difference between the RWS and the Hydrocarbon curve, is that the latter is based on the temperatures that would be expected from a fire occurring within a relatively open space, where some dissipation of the heat would occur. The RWS curve is based on the sort of temperature you would find when a fire occurs in an enclosed area, such as a tunnel, where there is little or no chance of heat dissipating into the surrounding atmosphere. It simulates the initial rapid growth of a fire using a petroleum tanker as the source, and the gradual drop in temperatures to be expected as the fuel load is burnt off.

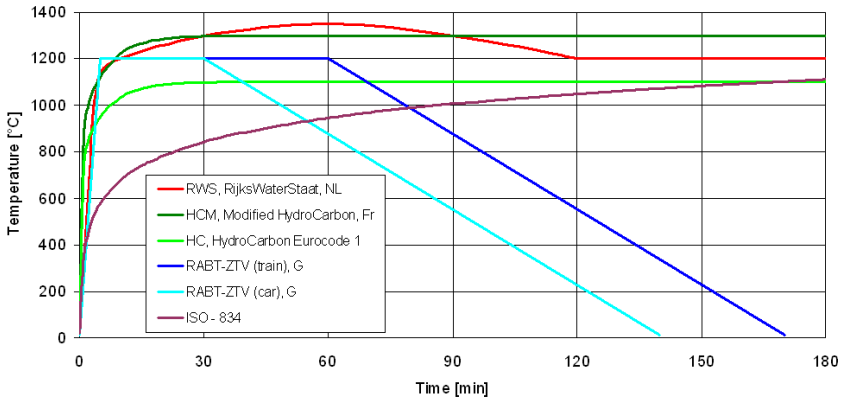

Figure 10. Different existing fire curves (Promat Internacional , 2013)

2.5.3 Human risk

The occurrence of a fire is something that puts human lives at risk and that is detrimental the equity level of real estate. Here is presented some of the main consequences of the occurrence of a fire can cause the level of human life (National Fire Protection Association, 2007; Rodrigues-Morgado, 2012)

- Oxygen level - the consumed oxygen can cause death by suffocation;

Table 4. Lack of oxygen effects

Oxygen levels	Person experiences:
21 percent	Normal outside air
17 percent	Impaired judgment and coordination
12 percent	Headache, dizziness, nausea, fatigue
9 percent	Unconsciousness
6 percent	Respiratory arrest, cardiac arrest, death

- Flames and heat - flames produced and the released heat can cause severe burns and even death of the occupants/users; Heat is also a respiratory hazard, as superheated gases burn the respiratory tract.
- Smoke - the smoke released influences the vision and guidance, conditioning evacuation building and increasing exposure to potential noxious gases produced during fire; most fire deaths are not caused by burns, but by smoke inhalation.
- Toxic gases and vapours- the production of gases, such as carbon monoxide (CO) and Carbon dioxide (CO_2), can cause serious damage or be deadly, even in small quantities, as it replaced oxygen in the bloodstream; Foglike droplets of liquid can poison if inhaled or absorbed through the skin.
- Structural collapse - any partial or total collapse of the building can cause death people, either by direct impact due to the collapse, or by way of obstruction evacuation.

2.6 Modelization: Fire engineering

Traditionally, the behaviour of structures under fire conditions have been achieved by prescriptive simplified procedures (Silva, et al., 2014), the fire parts of Eurocodes provide at present a wide range of calculation methods. They allow engineers to follow either a prescriptive approach or to use sophisticated computer models. The prescriptive approaches are generally focused on checking if structure members meet the fire safety requirements prescribed in national fire regulations, they propose a safety level that is relatively easy to achieve and implement, however it may be conservative especially for structures in which significant moment redistribution capability exists (Palm, 1994; European Committee for Standardization, 2008). Computer-based analysis provides more accurate answers to fire safety objectives but always been on the basis of performance-based rules.

Using structural fire engineering, engineers can assess the necessary fire resistance to structure in order to avoid the spread of fire and/or to prevent a premature structural collapse. The fire performance of a

whole structure, or a part of it, is carried out by following, for a given design fire scenario, three successive steps of structural fire engineering (Sokol & Wald, 2010; European Committee for Standardization, 2008): Fire Analysis, Thermal analysis and Structural analysis. The overall complexity of the fire safety design will depend on the assumptions and methods adopted to predict each of the three design steps.

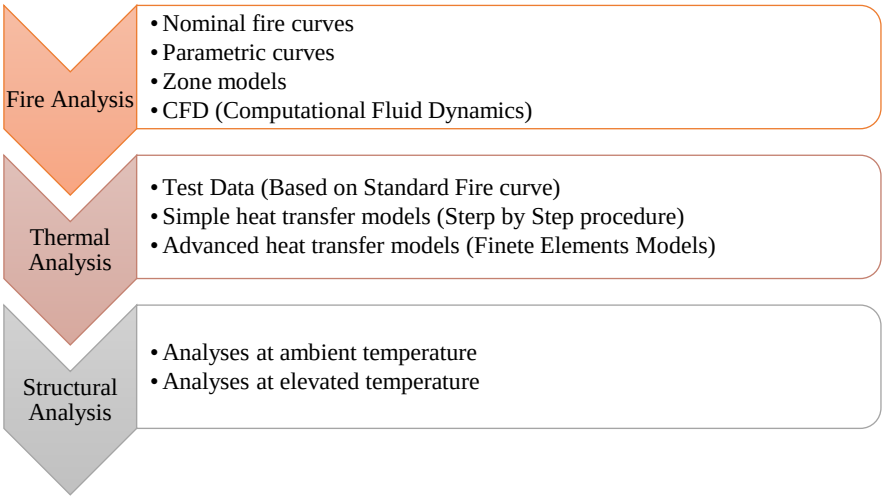

Figure 11. Steps of structural fire engineering

In the first step, fire analysis, is it calculated the thermal actions/exposure with the fire models. The main objective of the fire modelling is the simulation of the fire development and the prediction of thermal actions (gas temperature, heat flux) on the structural members (in order to determinate, in a following step, the temperature in the structural members). The spectrum for fire and heat transfer modelling varies in complexity from very simple models (i.e. standard fire curves) or very complex ones (i.e. Computational fluid dynamics).

The simplified models as presented in the previous section, are generally empirical models based on conventional assumptions predicated on the statement that the surface temperature of the structural elements is the same as the fire's temperature time history. This procedure avoids the need for a heat transfer and fire's characteristics calculation that accounts for the stand of for orientation of the structure to the fire. The locations at which the standard fire temperatures are applied must be determined by the user based on the assumed spatial extent of fire exposure (Quiel, et al., 2015; European Committee for Standardization, 2008; Silva, et al., 2014).

More advanced models, zone and fire models, allow temperatures, smoke descent, flame spread, time to flashover and many other effects to be calculated.

Zone models take into account the main parameters controlling the fire, but introduce simplified assumptions that limit the domain of application. The simplest model is a one-zone model for fully developed fires (post flashover fires), in which the conditions within the compartment are assumed to be uniform and represented by a single temperature. Two-zone models may be used for pre-flashover situations, mainly in the growth phase of a fire. The model is based on the hypothesis of smoke stratification, separating the fire compartment into two distinct layers: a hot upper layer (containing most of the fire's heat and smoke), and a cool lower layer (which remains relatively uncontaminated by smoke) (European Committee for Standardization, 2008).

On the other hand, at the end of the model complexity spectrum, it is found that fire analysis has been performed using numerical models based on the Computational Fluid Dynamics (CFD) software packages, also named field models. These tools are capable to calculate the heat transfer to the structural elements from the defined fire hazard as well as to provide a reliable description of fire evolution, making it more accessible to simulate the actual fire dynamics for different scenarios (Silva, et al., 2014; Quiel, et al., 2015). It is difference between three cases of field models, according to the turbulence method implemented in model: Direct numerical simulations (DNS), Large Eddy Simulation (LES) and Reynolds-averaged Navier Stokes (RANS).

They are characterized for been robust and generate significant levels of numerical resolution; they incorporate submodels for turbulence, heat transfer and combustion and are based on a complete, time-dependent, three-dimensional solution of the fundamental conservation laws (conservation of mass, momentum, and energy). However, they are also computationally expensive and may not be practical in many applications due to budgetary and scheduling constraints. Furthermore, they require a large amount of input, much of which must be assumed if relevant data, observations, or design guidance is not available (European Committee for Standardization, 2008; Quiel, et al., 2015).

Other researchers have pursued an "intermediate" approach that accounted for the duration and geometry of the fire to calculate heat transfer to the structural elements based on idealized and semi empirical combustion models. The simplest approach is to represent the fire using a point source radiation model (Figure 12a), in which the fire geometry is neglected when calculating radiation heat transfer with the exception of using the fire height to determine its vertical position. A more detailed method is the solid flame model (Figure 12b), in which the fire is represented as a solid vertical object (typically a cylinder) that emits radiation from all sides. Variations to the solid flame model have been made dividing the vertical fire structure with two zones (Figure 12c): the luminous zone (i.e. the unobscured flame region) and the smoke-obscured upper region (Quiel, et al., 2015; Mc Grattan, et al., 2000).

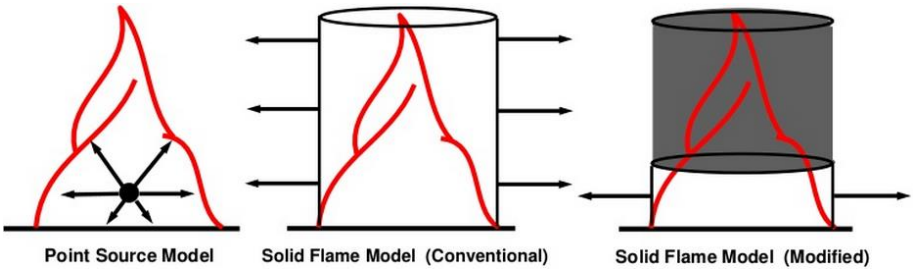

Figure 12. Schematic diagram of thermal radiation models (Mc Grattan, et al., 2000)

The results of these models can then be used to calculate or estimate radiation heat transfer from the fire to the structural elements. By obtaining the fire's geometry and intensity for its given location, the distribution of fire effects over the bridge structure can be calculated.

These approaches are less computationally intensive and detailed than CFD solutions but anyway they allow for a scenario specific calculation of the fire characteristics and provide a conservative model of the fire hazard with greater efficiency.

To date, solid flame models have not been commonly used for the analysis of bridges subject to fire but are often used in the energy industry to calculate the safe distance separation needed between potential pool fire hazards and nearby storage locations of fuel or other hazardous materials.

Table 5 provides a summary of representative studies for the three groups. The modelling approach used to represent the fire, calculate heat transfer, and calculate the resulting structural response of the bridge is shown for each study.

Once the thermal actions are calculated, the thermal transfer to the structural elements has to be calculated in order to determinate the heating rate and temperatures on structural members. Thermal models, which will be used, should be based on the acknowledged principles and assumptions of the theory of heat transfer.

The thermal analysis in structural members can be extremely complex, especially for materials that retain moisture and have a low thermal conductivity. Different modelling can be used according to the assumptions and needs. The simplest method of defining the temperature profile through the cross-section is to use test data presented in tables or charts which are published in codes or design guides. These test data are generally based on standard fire conditions (Pintea, 2016).

Going a little more in depth, in codes and design guides simple design equations are presented to predict the temperature development. The approach considers both radiative and convective heat transfer and, although a spreadsheet is required to solve the equations over the fire duration, it is simple to use.

Table 5. Summary of the modelling approaches used in previous fire bridge studies (Quiel, et al., 2015)

Section	Authors	Location	Bridge type	Fire model	Heat transfer model	Structural model
Standard fire and other simplified methods	Dotreppe et al.	Vivegnis Bridge, Liege, Belgium	Tied steel arch plus concrete deck	Standard hydrocarbon fire curve	Applied temperature time history to "exposed" surfaces of 2-D solid element thermal FE cross-section	Beam and shell elements for structural FE model of the bridge
	Liu et al.	MacArthur Maze, Oakland, CA, USA	Steel girders with concrete deck	Standard hydrocarbon fire curve	Applied temperature time history to "exposed" surfaces of 3-D solid element thermal FE model	Solid and shell elements for structural FE model of a single girder and slab
	Kodur et al.	Hypothetical	Steel girders with concrete deck	Standard hydrocarbon fire curve	Applied temperature time history to "exposed" surfaces of 3-D solid element thermal FE model	Solid and shell elements for structural FE model of a single girder and slab
	Paya-Zaforteza and Garlock	Hypothetical	Steel girders with concrete deck	Standard hydrocarbon fire curve and a design fire	Applied temperature time history to "exposed" surfaces of 3-D solid element thermal FE model	Solid elements for structural FE model of a single girder and slab
	Aziz and Kodur	Hypothetical	Steel girders with concrete deck	Standard hydrocarbon fire curve and two design fires	Applied temperature time history to "exposed" surfaces of 3-D solid element thermal FE model	Solid elements for structural FE model of a single girder and slab
Computational fluid dynamics (CFD) modelling	Choi	MacArthur Maze, Oakland, CA, USA	Steel girders with concrete deck	Constant heat release rate per unit area of 2500kW/m2	Applied temperature time histories based on CFD modelling to 3-D solid FE model	Solid elements for structural FE model of the overpass bridge
	Bajwa et al.	MacArthur Maze, Oakland, CA, USA	Steel girders with concrete deck	Constant fire temperature of 1100°C	Applied temperature time histories based on CFD modelling to 2-D solid FE model	Solid elements for structural FE model of the overpass bridge
	Wright et al.	I-65 Overpass, Birmingham, AL, USA	Steel girders with concrete deck	Heat release rate time histories for a fuel tanker and other burning vehicles from published sources	Applied temperature time histories based on CFD modelling to 3-D solid FE model	Solid elements for structural FE model of the overpass bridge
	Alos-Moya et al.	I-65 Overpass, Birmingham, AL, USA	Steel girders with concrete deck	Several constant heat release rates per unit area that are representative of a burning tanker truck	Applied temperature time histories based on CFD modelling to 3-D solid FE model	Solid elements for structural FE model of the overpass bridge
	Tonicello et al.	Hans-Wilsdorf Bridge, Geneva, Switzerland	Helical steel arch bridge	Heat release rate time histories for burning vehicles from published sources	Assigned isotherm temperature time histories to finite elements based on CFD modelling´	Beam and shell elements for structural FE model of the bridge
Intermediate models	Bennetts and Moinuddin	Hypothetical	Cable-stayed bridge	Calculated max.radiation heat flux to targets based on size of tanker truck for an assumed duration	Applied heat flux as an equivalent max. temp. to multi-layered lumped thermal mass elements	Lumped mass material weakening relative to applied load
	Astaneh et al., Noble et al.	MacArthur Maze, Oakland, CA, USA	Steel girders with concrete deck	Constant fire temperature of 1200°C	Analytically calculated heat flux from a "firebath"solid flame model, applied to 3-D solid element thermal FE model	Solid element structural FE model of the overpass bridge

By last, advanced heat transfer models based on either finite elements or the finite difference method allow the determination of the 2D or 3D temperature distribution in structural members (through the cross-section and along the length) in a fire (McGrattan & Miles, 22016). They are often used to estimate temperature gradients through structural members. Moreover, they can be applied to structural members under nominal fire conditions or natural fire conditions (European Committee for

Standardization, 2008). Such methods have to take into account non-linearity due to temperature dependence of material properties and boundary conditions. The three processes: conduction, convection and radiation can occur together, to which may be added mass exchange.

In principle, where the effects of a fire remain localised to a part of the structure, temperature distributions along structural members can be strongly non-uniform. So a precise calculation of temperatures should be determined by a full 3D thermal analysis. However, due to the prohibitive computing time of such analysis, it is often considered an acceptable simplification to perform a succession of 2D thermal analyses through the cross-sections of the structural members (European Committee for Standardization, 2008).

Likewise in simple models, the use of advanced models require knowledge of the geometry of structural members, thermal properties of the materials (thermal conductivity, specific heat, density, moisture...) and heat transfer coefficients at the member's boundaries (emissivity, coefficient of heat transfer by convection).

In Table 6 is exposed the main characteristics of the different thermal approaches named above. In a following chapter, the evolution and brief description of advanced thermal models will be discussed.

Table 6. Mean characteristics of thermal approaches

Model	Design charts/ Test data	Simple formulae	Advanced models
Complexity	Simple	Intermediate	Advanced
Heat transfers models	Conduction	Conduction	Convection Radiation Conduction
Analysis ability	Test results Standard fire conditions	Empirical solutions Standard fire conditions	Accurate solutions Any fire conditions
Member types	Dependent on available test data	Mainly steel members	Any material & construction methods
Input parameters	Construction type Member geometry	Heat flux or fire curves Boundary conditions Member geometry Material thermal properties	Heat flux or fire curves Boundary conditions Member geometry Material thermal properties
Solutions	Cross-sectional temperature charts Tabulated thermal data	Simple cross-sectional temperature profile	One to three-dimensional time & space dependent temperature profile
Design tools	Fire part of Eurocodes Test/Research reports	Fire part of Eurocodes Design guides	Finite element package
	Design charts/tables	Spreadsheet	Computer models

The last step in Structural Fire Engineering is the structural analysis in which it is calculated the mechanical response of structural members. From the temperature fields obtained for the structural members in the thermal analysis step and from the combination of the mechanical actions loads in case of fire, the structural behaviour can be assessed following one of the three possible approaches: member analysis, in which each member of the structure will be assessed by considering it fully

separated from other members, analysis of parts of the structure or global structural analysis that provides a much better understanding of overall behaviour of structure under fire condition.

According to the Eurocodes, three types of design methods can be used to assess the mechanical behaviour of structures: a simple calculation method, based on predefined tabulated data as given in EN 1994-1-2, simple calculation models and advanced calculation models. Two first approaches can been only applicable to steel and concrete composite structures however the advanced models can be applied to all types of structures.

Advanced numerical models are usually finite element models. They can simulate a partial or a whole structure in static or dynamic modes, providing information on displacements, stress and strain states in structural members and the collapse time of whole building if collapse occurs within the period of the fire. In Table 7 are named some of the characteristics that the user can define when utilizing this type of models

Table 7. Mean characteristics of advanced structural models

Boundary Conditions	Heat sources can be represented by either temperature-time functions or heat flux in boundary elements. Convection and/or radiation at boundaries of the structural model can be modelled by the heat transfer coefficient of boundary elements.
Meshing	The shape of the structural model are modelled by a finite element mesh of general flow continuum elements. The boundary elements or interface elements can be line shaped elements, triangular or quadrilateral elements.
Material Properties	The material can be isotropic, orthotropic or anisotropic.
Special Features	The thermal properties of conductivity, specific heat and emissivity can be temperature-dependent. Hydration heat, moisture evaporation and movement, change in contact conditions may be modelled.

In general, the structural analysis in the fire situation is based on ultimate limit state analysis, at which there is equilibrium of the structure between its resistance and its applied loading. However, significant displacement of the structure will inevitably occur, due to both material softening and thermal expansion, leading to large material plasticisation. Therefore, advanced fire analysis is a non-linear elastic-plastic calculation in which both strength and stiffness vary non-linearly.

These models can be used in association with any heating curve since in fire situation, the temperature field of structural members varies with time. As stress-strain relationships of materials are non-linear and temperature dependant, an appropriate material model has to be adopted in advanced numerical modelling to allow the shift from one behaviour curve to another, at each step of time (and thus of temperature).

Another aspect to be noted in the application of advanced calculation models is the material behaviour during cooling phase. Mechanical properties varies with temperature and material composition might

be totally modified when heated to an elevated temperature, even its strength might even be less after cooling than at maximum temperature (European Committee for Standardization, 2008).

These three processes are divided for convenience but for modelling the processes are interdependent and do not occur in isolation from each other. Therefore, the complete approach to modelling involves the concurrent analysis of all the processes until final failure of the composite structure in fire (Mouritz, et al., 2009).

2.6.1 Field of application of different design models

The following table shows the field of application of the available fire design methods. It is shown an overview of advanced calculation models available for fire modelling, thermal modelling, and structural modelling that can be used in fire engineering design.

Table 8. Field of application of different design methods (European Committee for Standardization, 2008).

Approach	Tools	Thermal actions	Thermal modelling	Structural modelling
Prescriptive approach (Standard fire design)	Pre-engineered data from standard fire tests (Data from manufacturers)	Standard ISO curve EN 1991-1-2	-	
	Tabulated data from EN 1994-1-2		EN 1994-1-2, §4.2	
	Simplified calculation models given in Eurocodes		Steel EN 1993 1-2 §4.2.5	Steel EN 1993-1 2 §4.2.3 §4.2.4
			Composite EN 1994-1-2 §4.3	
	Advanced calculation models		Steel and composite	
			FEA or FDA	FEA
Performance based approach (natural fire design)	Simplified calculation models	Fully engulfed fire (Parametric fire, standard ISO curve)	Steel EN 1993-1-2 §4.2.5	Steel EN 1993-1-2 §4.2.3 §4.2.4
		Localized fire		Specific rules based on fully engulfed fire §5.4
	Advanced calculation models	Zone models	Steel and composite	
		Field models	FEA or FDA	FEA

2.7 Fire protection

The behaviour of fibre reinforced polymers has been studied by many authors, among others researchers, Williams et al., concluded that is possible to achieve satisfactory fire performance if they are appropriately designed and adequately insulated.

Protection systems can be classified into two categories: passive fire protection (prevention of ignition and reduction of the impact of fires achieve without human intervention) and active fire protection (manual and automatic detection and suppression of fires).

In the case of bridge structures, the use of automated systems usually presents difficulties therefore, fire protection is mainly based in the use of passive protection systems that reduce the thermal exposure onto the bridge. It can be classified into flame-retardant filled composites and flame-retardant polymer composites.

Flame-retardant filled composites is a diverse group of chemicals which are added to manufacture materials in their final stages of processing. They inhibit or delay the spread of fire by suppressing the chemical reactions in the flame or by the formation of a protective layer on the surface of a material. There are two classes of fillers, inert and active, that are distinguished by their mode of action being the first group more effective (Mouritz, 2007). Moreover, there are other methods been developed to further improve the flame-retardant properties of composites such as nanocomposites.

In flame-retardant polymer composites the matrix is modified by polymerising the resin with an organ halogen compound. In fire event the flame temperature is lowered and thereby this effect slows the decomposition of the composite material.

3. MATERIALS CHARACTERIZATION

In this chapter will be summarized the present state of knowledge of fire behaviour of sandwich composite materials. After this introductory phase, the description and characterization of the materials involved in the case of study (Balsa core and Glass/vynilester skins) will be presented; physical, mechanical and thermal properties, real-time and residual strength and stiffness, fire behaviour and by last their degradation process under elevated temperatures.

3.1 Balsa-GFRP Sandwich Panel

The problems of durability, fire and post-fire strength and stiffness of sandwich structures represent a major interest for designers. When temperature change is significant, the mechanical properties may degrade significantly, and this may in turn change the load-response (Birman, et al., 2006; Grenier, 1998). Furthermore, the fire damage experienced by sandwich composite materials is different from the one occurring in composite laminates due to presence of the core material. The complexity of the problem is related to a number of coupled phenomena, including the dynamic problem of heat transfer, property degradation in temperature, resin decomposition, etc.

When the face skin is exposed to a heat flux, it experiences char formation, resin softening and degradation, delamination and matrix cracking (Mouritz & Gibson, 2006). Once the face skin has become severely degraded and is unable to provide significant thermal protection, the degradation of the core material takes place. Later, if the core material is decomposed it may separate from the charred face skin. Finally, if the exposure time continues, the decomposition and char zones can move towards the unexposed zones.

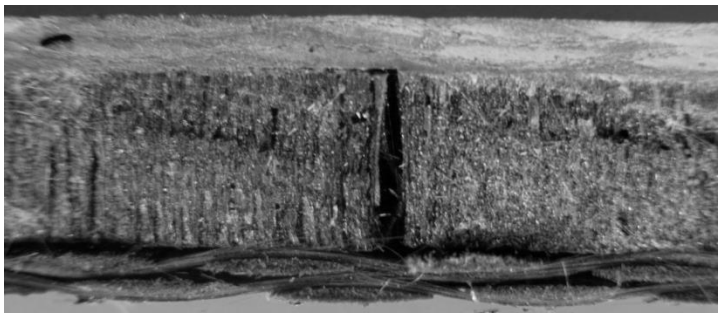

Figure 13. Image of a GFRP/Balsa sandwich panel exposed to a heat flux of 50 kW/m^2.

The formation of a char layer is an important process because it can promote significant flame retardation by limiting the access of oxygen from the atmosphere to the region of the composite that is decomposing (Mouritz & Gibson, 2006). Balsa wood yield a relatively large amount of char and

therefore provide good structural and dimensional stability in fire, however is mineral wool the most suitable core material for fire situations (Avó de Almeida, 2009).

One of the most important characteristics of sandwich panels is their good thermal insulation that is given by the thermal conductivity coefficient λ, the smaller the value, the greater the insulating capacity. Furthermore, the distribution of temperature through the thickness depends on the thermal conductivities of the constituent materials and whether are affected by temperature. In sandwich panels, when the heat flux affects only one face skin, the cold face is insulated to a very significant extent by the effect of the low thermal conductivity of the core material as can be observed in Figure 14. Moreover, this low thermal conductivity can also lower the ignition time.

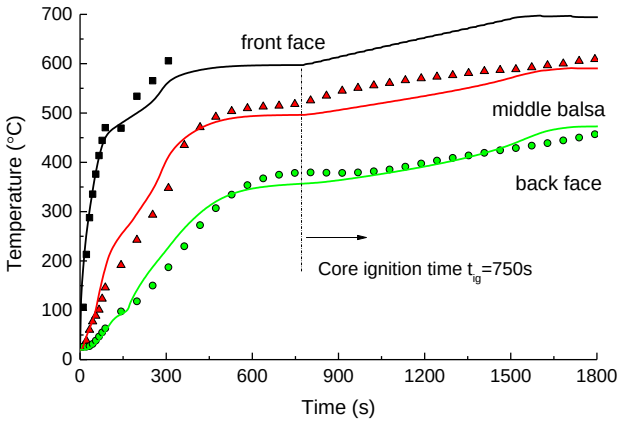

Figure 14. Temperature-time profiles at the front (heated) skin, middle of balsa core and back skin exposed to the heat flux 50 kW/m2. (Anjang, et al., 2014)

According to Mouritz and Gibson (2006) there is little published information on sandwich composite materials about ignition times maybe due to the complexity of the process because of the influence of the core material. Compeering ignition times for GRP skin-balsa and GRP skin-PVC core composite, the later one ignite more rapidly due to PVC core melts and decomposes faster.

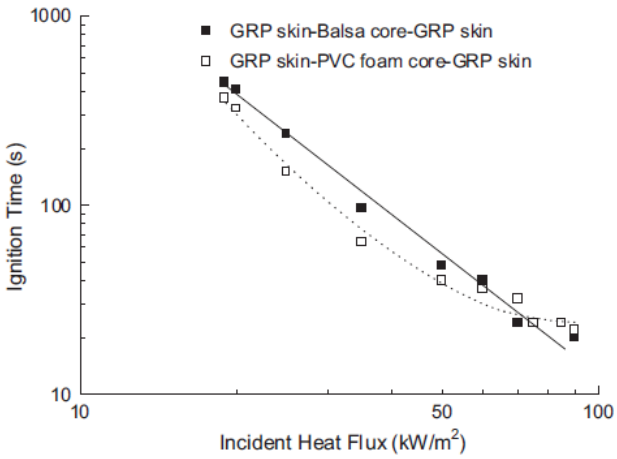

Figure 15. Effect of heat flux on the ignition times of 2 sandwich composites

As seen in the Figure 1Figure 16, the heat release rate generally increases with an increase in the incident heat flux. According to Grenier (1998) the initial peak in HRR may be attributed to surface pyrolysis with the subsequent decrease attributed to surface char formation.

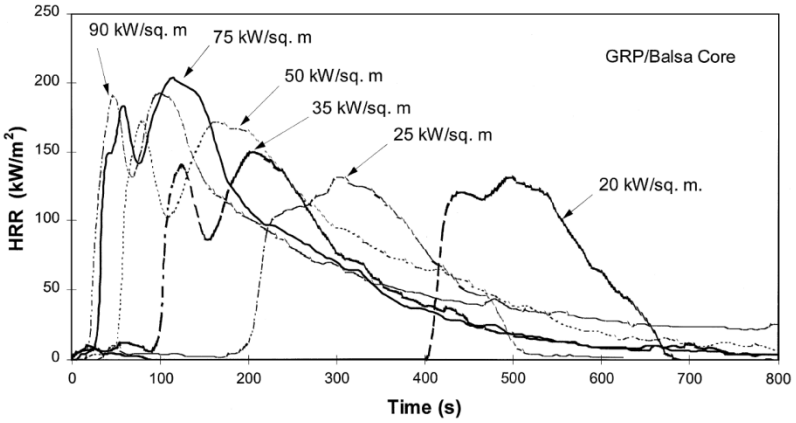

Figure 16. GRP/Balsa- core HRR curves for different irradiances (Grenier, 1998).

The residual properties of sandwich composites have not been thoroughly characterised (Mouritz & Gibson, 2006). However taking into account all of mentioned above, can be stablished that thicker face skins retain higher strength at longer times.

Studies performed on sandwich composites have shown that the fire resistance can be greatly improved by the use of a low density fire-resistant core material which allows slow the spread of fire (Avó de Almeida, 2009; Mouritz & Gibson, 2006). For this reason, sandwich composites are commonly preferred over single-skin laminates in applications requiring high fire resistance.

3.2 Balsa wood

Balsa (Ochroma Lagopus) is an equatorial tree that is mainly cultivated in the South American country of Ecuador and it is considered a diffuse-porous hardwood. Unlike balsa wood, which is obtained from the trunk of the tree, balsa panel production involves the adhesive joining of selected smaller cubic blocks or lamellas of balsa. In this way, end grain balsa panels of relatively uniform density can be produced (Osei-Antwi, 2014). Furthermore, the excellent strength-to-weight and stiffness-to-weight ratios as well as superior energy absorption characteristics make balsa wood a preferred material for cores of sandwich structures (Kepler, 2010; Osei-Antwi, 2014; Da Silva & Kyriakides, 2007).

Balsa wood cores first appeared in the 1940's in flying boat hulls. In bridge construction, the first applications were for military bridges such as the light weight 12.2-m-long deployable Composite

Army Bridge (CAB) (Kosmatka, 2008). A CFRP-balsa core sandwich has also been used as the deck of the 56-m span bascule footbridge in Arendal, Norway (Hollaway, 2010). More recently, a 12-m-long and 5-m-wide composite bicycle/pedestrian bridge in Utrecht (NL) was assembled from an upper GFRP-balsa sandwich deck or, other example, Coribm Bridge a FRP-wrapped Balsa Wood Bridge Deck on route LA 70 in Louisiana (Nair, et al., 2010). In all cases, as core material, balsa wood is subjected primarily to shear stresses.

3.2.1 Macro and micro structure

Like all woods, balsa wood has its own cellular microstructure shown in the micrograph in Figure 17. It is composed of different types of cells; tracheids (arranged longitudinally, 80-90% by vol.), parenchyma (arranged radially, 8-15% by vol.) and sap channels (Osei-Antwi, 2014; Vural & Ravichandran, 2003).

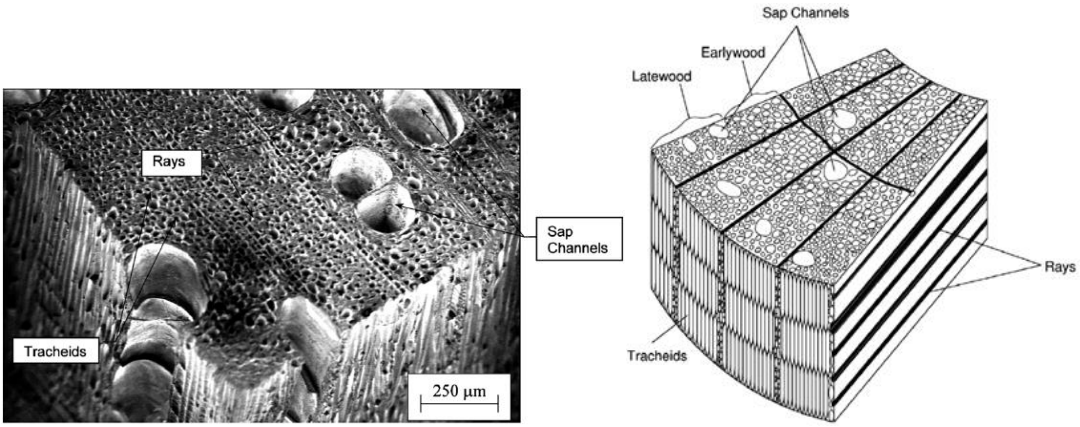

Figure 17. Micrograph and sketch of the cellular nature of balsa wood (Da Silva & Kyriakides, 2007)

Tracheids are the main cells, long bean pod shaped and aligned axially along the trunk of the tree. Their main function is structural support and they mainly consist of cellulose, hemicelluloses and lignin, which together form the elementary fibrils (Da Silva & Kyriakides, 2007). They are arranged in circumferential layers that constitute annual growth rings, which give the wood a polar symmetry (Figure 18). Trancheids consist of primary wall (P) and secondary wall (S) layers, been the secondary wall, further sub-divided into the S1, S2 and S3 layers. And these trancheids cells are interconnected by a middle lamella, which consists entirely of lignin, a relatively brittle phenolic polymer (Osei-Antwi, 2014; Vural & Ravichandran, 2003).

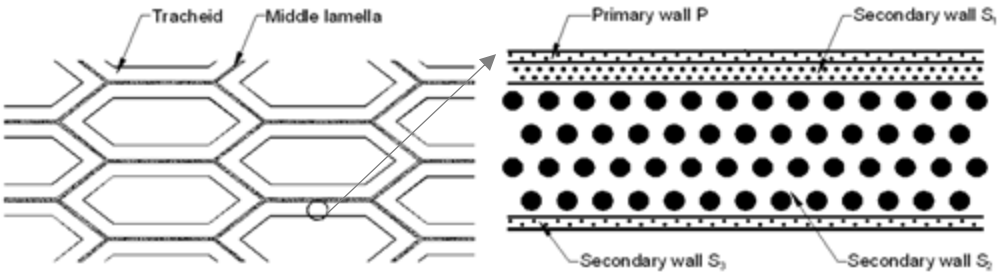

Figure 18. Simplified microstructure of balsa wood (Osei-Antwi, 2014)

Parenchyma are a second type of cell, shorter in length and with a more rectangular cross-sectional shape. They are arranged radially in groups (rays) that periodically penetrate the tracheids and are responsible for misalignments of the latter along the tree's natural axis (Osei-Antwi, 2014; Vural & Ravichandran, 2003)

A third type, sap channels, are responsible for fluid transport in the tree, have thinner cell walls and are relatively larger in diameter (150 to 250 μm compared to 30 to 40 μm for tracheids).

The complex microstructure described (periodic appearance of rays and sap channels and imperfections such as knots) results in a very significant anisotropy in mechanical properties.

3.2.2 Physical and mechanical properties

Physical and mechanical properties are derived from the microstructure. Wood is highly anisotropic with a high ratio of longitudinal to transverse properties. Balsa wood has three orthogonal axes in the longitudinal (L, along the grain), radial (R, across the grain and along the rays) and tangential (T, across the grain and transverse to rays) directions forming a heterogeneous porous composite.

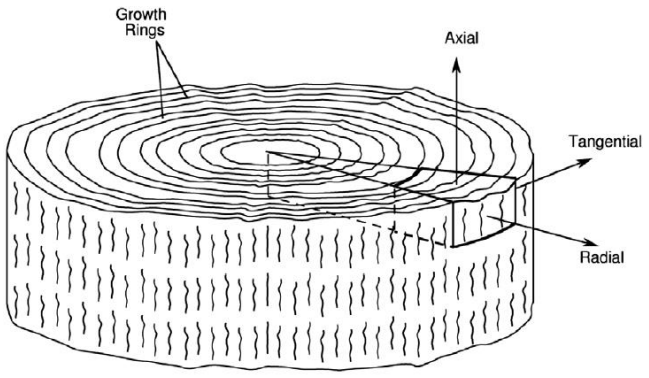

Figure 19. Principal anisotropy direction of the material (Da Silva & Kyriakides, 2007)

As a hygroscopic material, balsa wood can absorb water as a liquid, if is in contact with it, or in the form of vapour from the surrounding atmosphere. Because of its hygroscopicity wood always contains

moisture and this moisture affects all wood properties, but it should be noted that only moisture contained in cell walls is important (Britannica Academic, 2010). In addition, balsa wood, been a porous and very light wood, can hold up to four times its own weight in water; in the growing tree it can have a moisture content of up to 400% (Forestry Commission of New South Wales, 1991). However its absorptive capacity in perpendicular direction to the cell length or grain direction is lower (Pascoe, 2015).

Furthermore, since it has a biological in origin, balsa exhibits extremely variable properties, particularly density. The density of balsa wood can vary by an order of magnitude with the age and habitat of the tree. This variation occurs across the trunk due to the different growth of the early/spring wood and late/summer wood in each annual ring (Osei-Antwi, 2014). It covers densities from about 40–380 kg/m^3 making it one of the lightest woods available (Da Silva & Kyriakides, 2007; Goodrich, 2009). In relation with the degree of anisotropy, even though there is sufficient number of data showing that the degree for wood decreases with increasing density, there is not a well-established anisotropy–density relation for balsa wood (Vural & Ravichandran, 2003).

As for the hardness of the material Kotlarewski et al. (2016) conducted a series of tests to determine the load at maximum compressive extension of each surface (tangential, radial and axial). Their results indicate that the axial surface was far superior to the tangential and radial surface by almost doubling each value, and the tangential and radial surfaces were generally similar in value. It was find out that the hardness of a specimen was related to its density as all specimen results indicated a rise in hardness as the density becomes greater.

Regarding the mechanical characteristics, due to the complex microstructure and anisotropy, the material is stiff and strong in the axial direction (cell length direction) and relatively compliant and weak in the tangential and radial directions (Zhang, 2013; Osei-Antwi, 2014; Da Silva & Kyriakides, 2007). However, all mechanical properties strongly depend on the balsa density.

A study by Shishkina et al. (2014) indicated that balsa elasticity is dependent on its density, where a decrease in the porosity of balsa –therefore increasing density– increases the Young's moduli. Kyriakides et al. (2007) found out that the axial elastic modulus, governed by axial deformation of the cells, is proportional to the relative density. But, by contrast, the moduli in the radial and tangential directions that are governed by transverse bending deformation of the cells, go as the cube of the relative density, been the radial modulus stiffer than the tangential one. In Table 9 are show the elastic and Poisson's ratio for each direction.

Table 9. Elastic and Poisson's ratios at approx. 12% moisture content

	E_T / E_L	E_R / E_L	G_{LR} / E_L	G_{LT} / E_L	G_{RT} / E_L	
Elastic ratio	0.015	0.046	0.054	0.037	0.05	
	μ_{LM}	μ_{LT}	μ_{RT}	μ_{TR}	μ_{RL}	μ_{TL}
Poisson's ratio	0.229	0.488	0.665	0.231	0.018	0.009

Moreover, various studies carried out by Goodrich et al. (2010) and Kotlarewski et al. (2016) indicated that the compressive resistance of a specimen was greater with higher densities both directions, parallel and perpendicular to the grain. In addition, they observe that the compressive strength was greater parallel to the grain than in the radial direction. Vural et al., (2001) additionally exposed that the correlation between density and strength is such that the latter increases as much as 15 times from 3 to 45 MPa as the density increases from the low end to the high end of spectrum. Osei-Antwi et al. (2013) presented that balsa wood also exhibits a significant energy absorption capacity when subjected to compression in the fibre direction, which was attributed to the cellular/porous microstructure of the cells. Kyriakides et al. (2007) declared that the specific energy absorption was found to be comparable to that of metallic honeycombs of the same relative density. In Figure 20 can be observed the variation in the compressive strength with the increase in density.

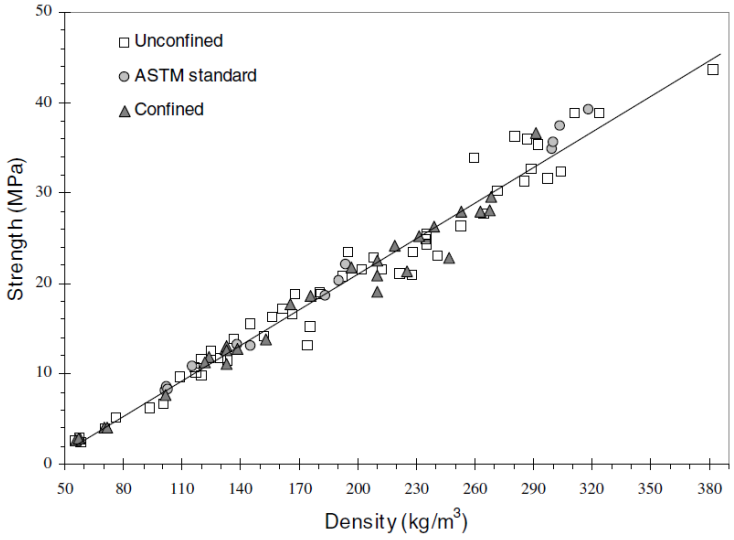

Figure 20. Variation of compressive strength (longitudinal direction)

Respect to the shear performance, due to the anisotropic nature of the material the shear stress–strain behaviour depends on the shear plane (Osei-Antwi, 2014). Shear stiffness and strength has to be characterized respect to the three relevant planes of: plane parallel to the end grain, Eg, plane parallel to flat grain, Fg/P, and plane transverse to flat grain, Fg/T. In the research made by Osei-Antwi et al. (2013) the highest values were obtained for the Eg shear plane (parallel to end grain), intermediate

values for the Fg/P plane (parallel to flat grain) and lowest values for the Fg/T plane (transverse to flat grain). Furthermore, Kyriakides et al. (2007) and the previous author prove that shear stiffness and strength increased with increasing density of the balsa (Figure 21). In addition, it was notice that the presence of the adhesive joints between the lumber blocks may influence the shear response of the panels.

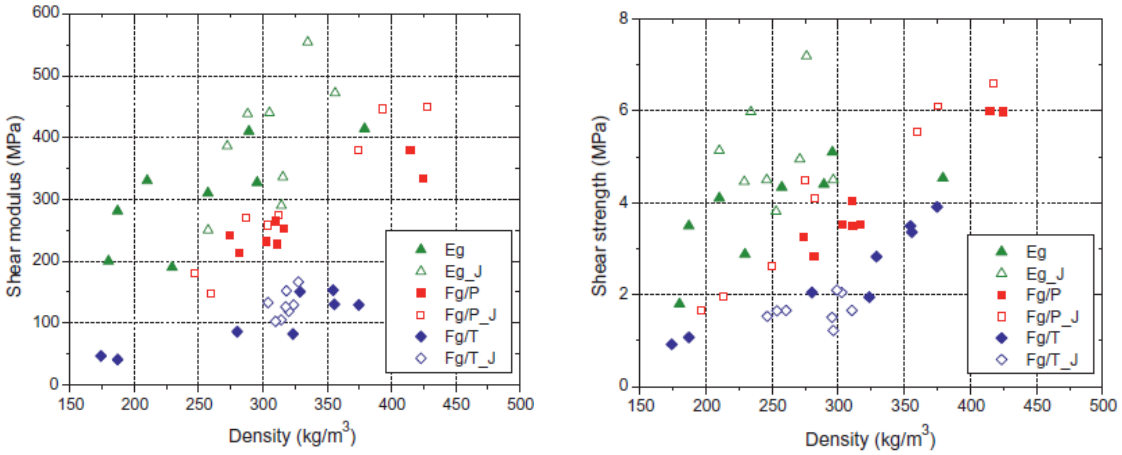

Figure 21. Shear modulus and shear strength vs. density for all shear planes

Table 10 summarises the average mechanical properties for each density class tested in Kotlarewski et al. (2016) study.

Table 10. Balsa mechanical properties per density class

Density class	Light 80 ≤ 120 kg/m^3	Medium 120 ≤ 180 kg/m^3	Heavy 180 ≤ 220 kg/m^3
MOE (MPa)	1222.14 (246.93)	2037.07 (374.85)	*
MOR (MPa)	9.83 (1.72)	16.63 (2.74)	*
Hardness tangential surface (N)	196.59 (17.95)	307.35 (92.06)	585.70 (84.91)
Hardness radial surface (N)	233.17 (37.15)	290.60 (69.96)	566.02 (42.08)
Hardness axial surface (N)	313.44 (38.79)	426.17 (88.83)	686.76 (83.89)
Compression parallel to the grain (MPa)	*	9.24 (0.61)	14.88 (0.42)
Compression perpendicular to the grain (MPa)	0.64 (0.19)	1.14 (0.39)	*
Shear (MPa)	1.56 (0.09)	1.90 (0.25)	*

3.2.3 Thermal properties

The thermal properties of wood are essential physical properties, especially in the processes of drying, producing heat energy by combustion and other processes, which include the transfer of heat through wood (Radmanović, et al., 2014). The thermal properties of wood are as follows: specific heat capacity

(c), coefficient of thermal conductivity (k) and thermal diffusivity (α). These three properties are interconnected by the expression given by:

$$\alpha = \frac{k}{c * \rho} \qquad [5]$$

Where:

α: thermal diffusivity, m^2/s,

k: coefficient of thermal conductivity, W/m · K,

c: specific heat capacity, J/kg · °C,

ρ: density, kg/m^3.

Thermal conductivity (λ) is critical for the evaluation of the insulating value of wood. This property is affected by its density, porosity, moisture content, mean temperature difference, grain direction, and extractives content. Bootle (1983) highlighted that an increase in density and moisture content increases the thermal conductivity value as it is shown in the study made by Kotlarewski, et al., (2014) (Figure 22) . Moreover, since balsa is cellular by nature and vessels run along the axial direction, heat flow could travel through the vessels along the axial grain. The rate of heat flow in the axial direction is two and a half times greater than the rate through the radial and tangential directions.

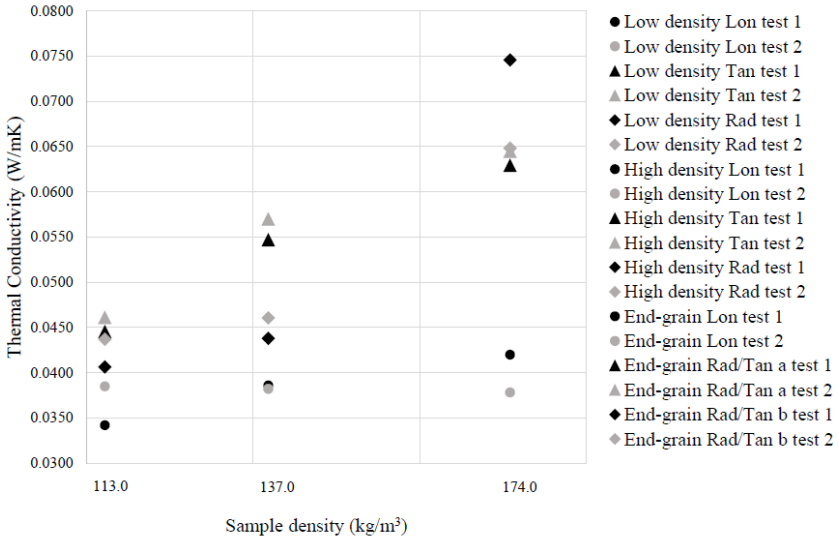

Figure 22. TC graphed against density (Kotlarewski, et al., 2014)

Results presented in Kotlarewski, et al., (2014) paper reveal that the main value was in the range of 0.0381 W/mK to 0.0665 W/mK, similar to other materials currently used as insulators in the construction industry. This result reveals that even balsa samples with less desirable thermal conductivity can compete with manufactured materials (plywood and plaster board) that possess higher densities, more weight, and exhibit a less superior and artificial thermal conductivity value.

Specific heat capacity (c) is a value used to compute the heat storage capacity of the material. This value depends on the moisture content on the moisture content of the wood (Zürcher, 2016).

3.2.4 Properties function of temperature

Balsa wood exhibits as much complexity thermally as it does physically due to the biological nature and multiple components of balsa wood (lignin, cellulose, and hemicellulose). Reductions in the high-temperature strength properties are related to physical transformations and phase changes of the balsa grains (Goodrich, 2009; Goodrich, et al., 2010).

Regarding the elastic modulus of the balsa core, Goodrich et al. (2010) found experimentally the elastic modulus of balsa for temperatures lower than 280 ºC, is related to the temperature via the empirically-derived linear equation:

$$E_C(\mathrm{T}) = E_{C0} - (\ \phi_E * T) \qquad [6]$$

Where:

E_{c0}: elastic modulus of the core at room temperature,

Φ_E: material constant that defines the modulus softening rate.

The material constant must be determined experimentally by elevated temperature tests. This equation is only valid between room temperature and the decomposition temperature of the core material, for T< 280 ºC. Above the decomposition temperature, the modulus of balsa is negligible.

However, balsa is an anisotropic material in which the elastic properties are different in the grain and anti-grain directions. Therefore, the elastic properties of the balsa must be determined for each one. Figure 23and Figure 24 show the temperature dependent elastic and shear modulus. It should be noted that in-plane elastic modulus are equal due to transverse isotropy assumption.

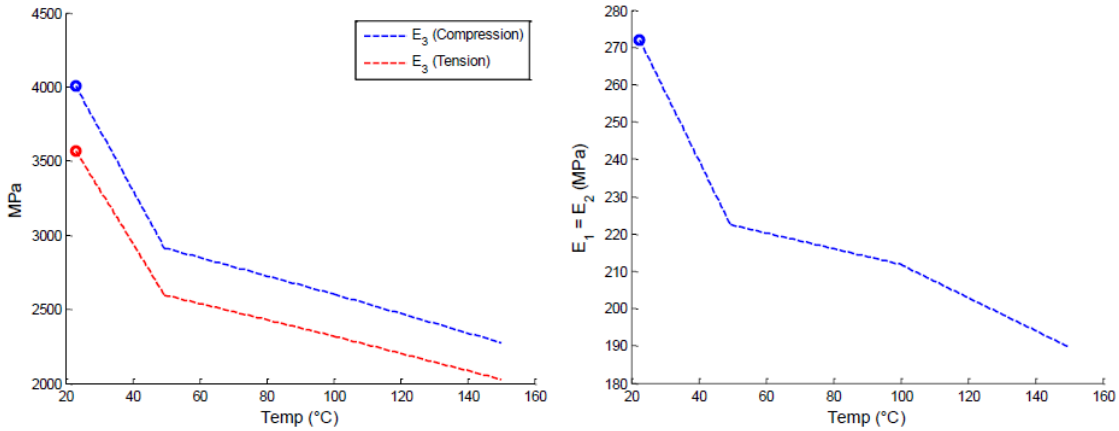

Figure 23. Transverse elastic modulus for tension and compression and in-plane elastic modulus (Cholewa, 2015)

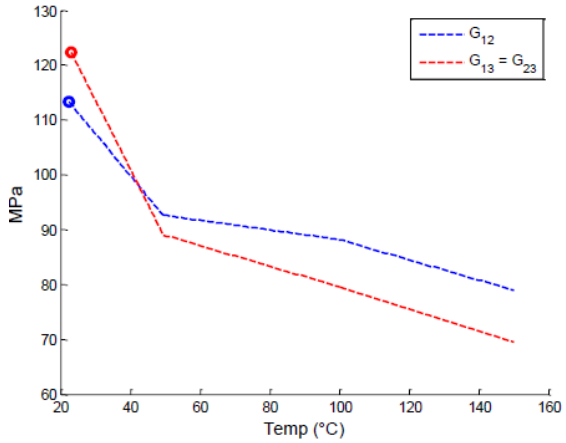

Figure 24. In-plane and transverse shear moduli. (Cholewa, 2015)

In the research made by Goodrich et al. (2010) it was found that the compression strength of balsa decreases at a quasilinear rate with increasing temperature up to the point of decomposition (250°C) in both directions. Furthermore, they discovered that the average softening rate of the balsa was not dependent on the load direction, although the high-temperature strength properties were higher in the axial direction. In the investigation, they exposed that the wood was nearly completely softened (with 90% loss in strength) at the decomposition temperature (250°C) and this was due to the softening of the hemicellulose and lignin, which undergo glass transition phase changes beginning at ~50° and 120°C, respectively.

Figure 25 shows the effect of temperature on the compression strength in the axial and radial grain directions of balsa. Figure 26 compares the normalized high-temperature strengths of balsa measured in the axial and radial directions.

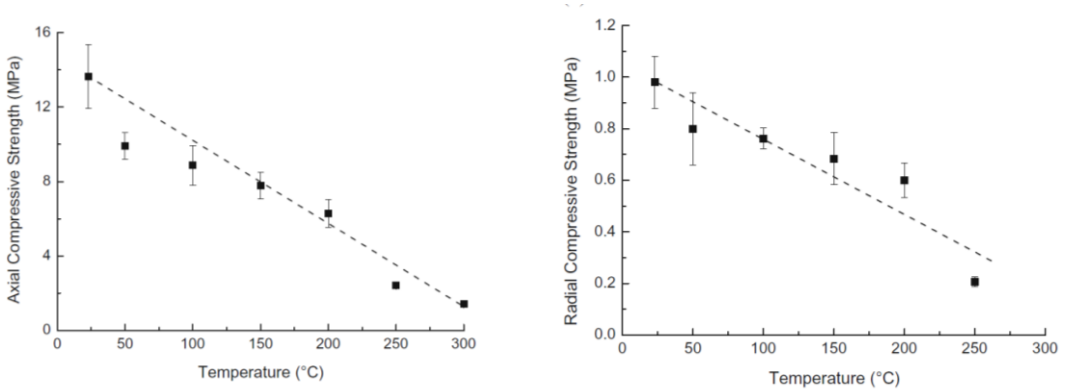

Figure 25. Effect of temperature on compression strength (Goodrich, et al., 2010)

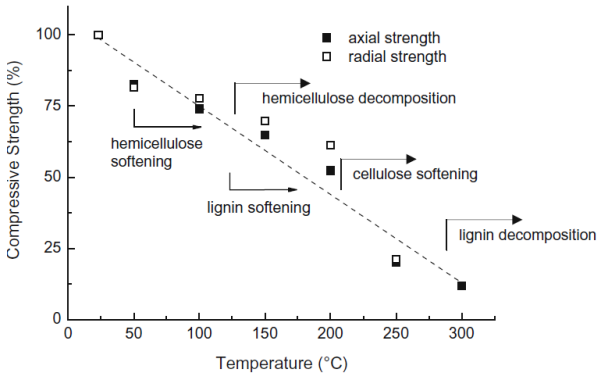

Figure 26. Normalized high-temperature strength (Goodrich, et al., 2010)

Figure 27 show the results for compressive strength of balsa core from experiments performed by Goodrich et al. (2010).

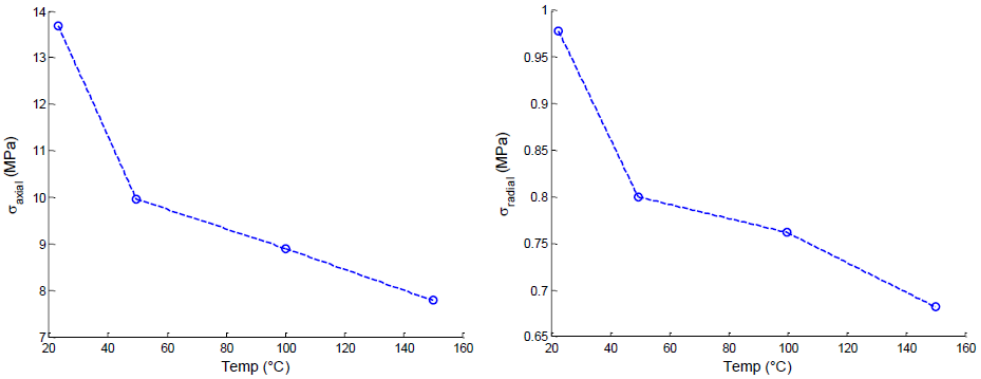

Figure 27. Transverse (axial) and in plane (radial) compressive strengths (Cholewa, 2015)

For the reduction of the tension strength the same authors found that was linearly related to the temperature according to:

$$\sigma_C(\mathrm{T}) = \sigma_{C0} - (\ \phi_\sigma * T) \qquad [7]$$

Where:

σ_c (0): core strength at room temperature

Φσ: defines the linear strength loss rate up to the decomposition temperature.

As well as in the case of the elastic modulus, above decomposition temperature, the tensile strength of balsa is negligible.

Form the research made by Rahman (2015) it is presented Figure 28 related with the strength and stiffness loss of the end-grain balsa core with increasing temperature. Due to the variation of density in balsa core, the room temperature properties are scattered and the failure occurred either in the adhesive bond-line between the balsa blocks or in a low density region of the wood (Rahman, 2015). It is clear the steady decline in strength and stiffness with increasing temperature.

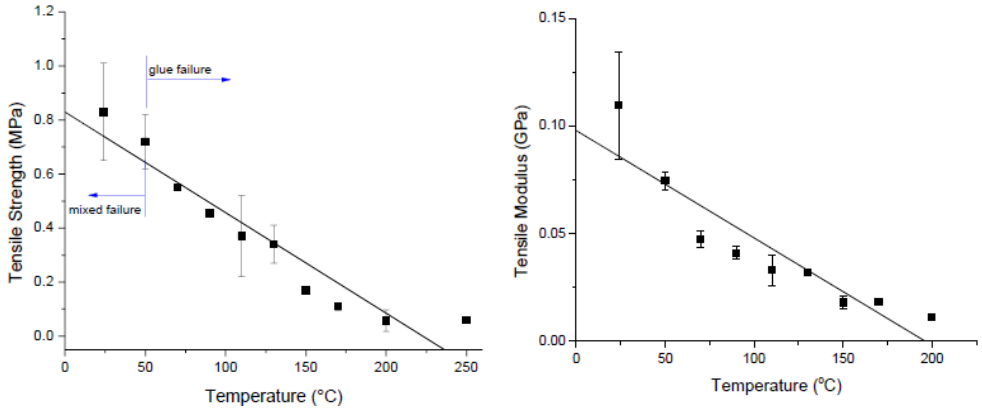

Figure 28. Effect of increasing temperature on the tensile strength and modulus of balsa (Rahman, 2015)

Figure 29 shows the tensile stress-strain curves for the balsa core at elevated temperature. It is shown that the failure stress and stiffness decreased with increasing temperature.

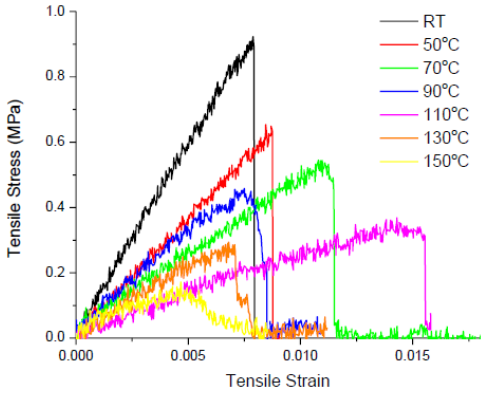

Figure 29. Tensile stress vs strain curves at different temperatures (Rahman, 2015)

The thermal conductivity and specific heat capacity vary with temperature and the decomposition state of the material. Prior to decomposition, the properties are those of the virgin material, while after decomposition the properties are those of the decomposed material (Lattimer, et al., 2009).

Regarding the specific heat capacity Goodrich (2009) studied this property at constant pressure (cp), using a thermogravimetric analysis (TGA) (Figure 30).

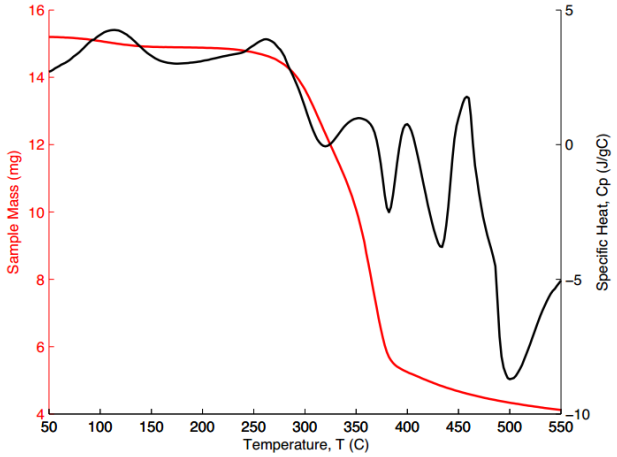

Figure 30. Specific heat and TGA data for balsa wood (20°C/min) (Goodrich, 2009)

Furthermore, Feih et al. (2008) (Cholewa, 2015) determined some relevant thermal properties of balsa cores related with temperature including the specific heat capacity:

$$C_p(\mathrm{T}) = 1420 + 0.68\ (T) \qquad [8]$$

Lattimer et al. (2009) also determined the empirical relationship between specific heat capacity and temperature for the core including the temperature the balsa decomposition temperature:

$$C_p(\mathrm{T}) = 3194 + 1.33\ (\mathrm{T}) \qquad [9]$$

These researchers (Lattimer, et al., 2009) also experimentally determined the thermal conductivity of this material up to about 600ºC. Is defined as a function of temperature for the temperatures below and above balsa decomposition temperature, respectively:

$$k_{x(c)} = 9.211 * 10^{-8} * T^{2.503} + 0.06 \qquad [10]$$

$$k_{x(c)} = 2.223 * 10^{-6} * T^{1.89} + 0.0008 \qquad [11]$$

3.2.5 Fire behaviour

Behaviour in fire has been one of the key aspects of the performance of core materials that needs to be taken into consideration for its use. Fire properties can generally be categorised into fire reaction and fire resistance (Gibson, 2003).

3.2.5.1 Fire reaction

Fire reaction relates to the response of the material, especially in the early stages of a fire, and to its interactions with the environment. Properties considered under fire reaction can be subdivided into properties influencing the growth and spread of fire and properties that are critical to human survival in fire. These can be regarded as characteristics of the material and usually can be determined from samples of material (Rahman, 2015; Gibson, 2003).

Some of the most important fire reaction properties are time-to-ignition, heat release rate, peak heat release rate, smoke density, limiting oxygen index, and flame spread rate (Rahman, 2015; Easby, 2007; Mouritz & Gibson, 2006).

Organic core materials such as balsa wood can thermally decompose with the release of flammable volatiles that can increase the heat release rate of the composite (Rahman, 2015). On the other hand, of the conventional core materials, end-grain balsa is probably the most attractive in terms of integrity and toxicity (Gibson, 2003). When balsa wood is exposed to high temperatures, the wood is able to develop a small char layer on the exposed side of the core. This charred layer has nearly negligible mechanical properties, but thermally it is of great benefit to the remaining undamaged core and face sheet. Because the char acts as an insulating layer, further damage to the core is limited and the unexposed face sheet temperature is significantly lower than the fire-exposed facesheet (Cholewa, 2015). And it is the natural cellular structure of the wood itself that gives it the advantage.

3.2.5.2 Fire resistance

Fire resistance defines the softening and damage caused to materials, including the loss of mechanical properties during fire and the post-fire properties after the flame has been extinguished. Fire resistance is critical to the safe use of load-bearing composites as their structures may collapse or fail due to losses in strength, stiffness and creep resistance.

Strength and stiffness decrease when wood is heated and increased when cooled. The temperature effect is immediate and, for the most part, reversible for short heating durations. However, if wood is exposed to elevated temperatures for an extended time, strength is permanently reduced because of

wood substance degradation and a corresponding loss in weight. The magnitude of these permanent effects depends on moisture content, heating medium, temperature, exposure period (Zürcher, 2016).

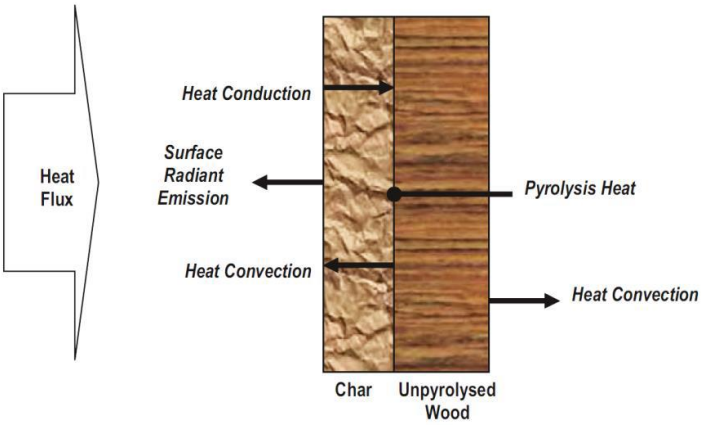

Figure 31. Schematic of a burning wood

Goodrich et al., (2010) exposed in their study that only less than 2% of decomposition mass loss occurred by 250°C, appearing to be thermal softening processes the primary mechanism for strength loss up to this temperature (Figure 32). Above this temperature the properties decreased rapidly due to irreversible decomposition of the grain structure.

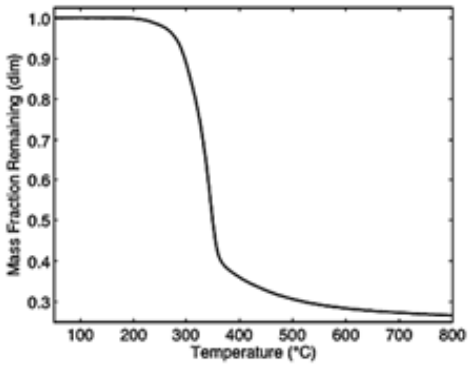

Figure 32. Mass loss-temperature curve (Goodrich, et al., 2010)

They also reported that wood components, cellulose and lignin, will recover when cooled from below 210° and 280°C respectively and that the loss of water, which occurs between 60 °C and 180 °C, will also be recovered within the air (humidity) within a short time (less than 24 h). Furthermore, the onset of hemicellulose decomposition in wood occurred at around 120 °C, but it was found not to significantly affect the post fire properties of balsa. Therefore, it appears that balsa wood has good post fire mechanical properties for maximum exposure temperatures below 250 °C.

3.2.6 Degradation, decomposition and deterioration

Softening and failure of the balsa core is critical to the structural survivability of sandwich composites in fire. The structural properties of sandwich composites under through thickness compression and in-plane shear loads are dependent on the core properties, and any thermal softening or decomposition of balsa will reduce these properties (Goodrich, et al., 2010).

Table 11. Thermally induced changes in wood shows the thermally induced changes in Douglass Fir compiled by Schaffer and used by Goodrich (2009) to explain the behaviour of balsa wood.

Table 11. Thermally induced changes in wood (Goodrich, 2009)

Temperature (°C)	Phenomenon
55	Natural lignin structure is altered Hemicellulose begins to soften
70	Transverse shrinkage of wood starts
110	Lignin slowly begins to lose weight
120	Hemicellulose content begins to decrease Lignin begin to soften
140	Bound water is freed
160	Lignin is melted and starts to harden
180	Hemicelluloses begin rapid weight loss after losing 4% lignin in porous flows
200	Wood begins to lose weight rapidly
210	Lignin hardens Cellulose softens and depolymerizes
225	Cellulose crystallinity decreases and recovers
280	Lignin reaches 10% weight loss Cellulose begins to lose weight
300	Hardboard softens irrecoverably
320	Hemicelluloses have completed degradation
370	Cellulose has lost 83% of initial weight
400	Wood is completely carbonized

Moreover Feih et al., (2008), found that balsa core showed an initial loss in mass at 100 ºC (predecomposition due to the evaporation of water). Then, it remained stable until the temperature exceeded 200-220 ºC when a large loss in mass occurs due to decomposition of the organic structure. After the primary decomposition ends at around 350 - 400ºC, a gradual decomposition continues. Mass loss continues to at least 1100°C, the highest temperature at which balsa wood was tested.

In Goodrich (2009) decomposition of balsa wood was measured to include both directions, pararel and grain cross-section. The same phenomenon took place at similar temperatures. The remarkable difference is that in primary decomposition, in parallel grain direction, the grain cell walls began to pull apart and shrunk leaving the grain cell walls eroded and full of voids. And in grain cross section, at this temperature, the grain cells began to grow larger until about 320°C.

He also exposed that the primary gas transport mechanism through balsa wood along the grain is through water transport vessels that extend through the thickness of the wood and that porosity rises significantly with mass fraction due to erosion of grain cell walls during decomposition.

Figure 1 shows the original microstructure micrographs (SEM) of the balsa and following heating within the decomposition temperature range. During decomposition the balsa become highly porous due to the break-down of the organic constituents such as cellulose, hemicellulose and lignin.

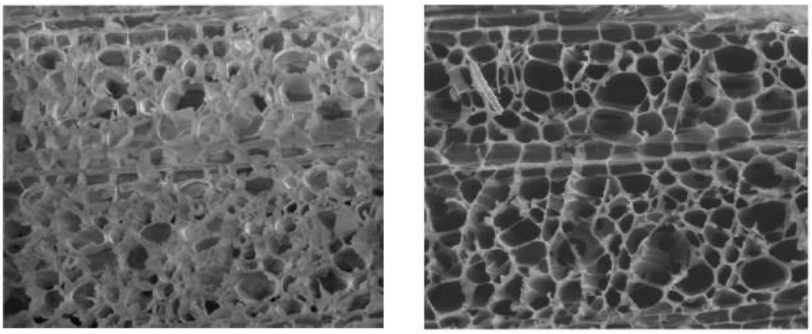

Figure 33. Microstructure of the balsa before and after thermal decomposition (Goodrich, et al., 2010)

3.3 Glass Fibber Reinforced Polymer

3.3.1 Glass fibres

Glass fibres are the most widely used reinforcement accounting for more than 90 % of all composite materials containing fibreglass (Mouritz & Gibson, 2006; Kontopanos, 2001). Maybe this is due to their good electrical insulating properties, low susceptibility to moisture and good mechanical properties. Moreover, they have the advantage of low price, availability and ease of processing (Mei, 2000; Kontopanos, 2001).

Glass fibres are manufactured by drawing those melted oxides into filaments ranging from 3 μm to 24 μm. There are five forms of glass fibres used as the reinforcement of the matrix material: chopped fibres, chopped strands, chopped strand mats, woven fabrics, and surface tissue. Glass fibre strands and woven fabrics are the forms most commonly used in civil engineering application (Casas Rius, 2011).

E-glass fibres can be obtained from E-glass which is a family of glasses with a calcium aluminoborosilicate composition together with other raw materials (such as limestone, fluorspar, boric acid, clay) (Casas Rius, 2011; Mei, 2000). The composition of E-glass is shown in Table 1Table 12. E-glass compositions .

Table 12. E-glass compositions (Mei, 2000)

Components	E-glass range
Silicon dioxe	52-56
Aluminum oxide	12-16
Boric oxide	5-10
Sodium Oxide and Potassium oxide	0-2
Magnesium oxide	0-5
Calcium oxide	16-25
Titanium oxide	0-1.5
Iron oxide	0-0.8
Iron	0-1

Mouritz and Gibson (2006) found that glass fibres are chemically inert in fire and retain chemical and physical stability at high temperature and heat flux. They remain unaffected by fire until heated to approx. 830 ºC when softening and viscous flow starts and melting occurs at approx. 1070 ºC. However, the mechanical properties decrease over range of temperatures well below the softening temperature (Mouritz & Gibson, 2006).

The disadvantages that are found in glass fibres are a relatively low Young´s modulus Table 13, low humidity and alkaline resistance as well as low long-term strength due to stress rupture (Casas Rius, 2011; Mei, 2000).

Table 13. Typical fibre properties

Material	Elastic Modulus (Gpa)	Tensile Strenght (MPa)	Ultimate Strain (%)
Glass	55-81	2.8-4.1	3-4.8
Carbon	170-310	1.4-6.8	1.3-2
7u Aramide	62-83	2.8	3.6-4
Polyethylene	117	2.6	3.5

3.3.2 Vinyl ester

Vinyl ester resins are the addition product of an epoxy resin and an unsaturated carboxyl acid with a molecular structure quite similar to that of the polyester resin (Sobrinho, et al., 2009). It is said that vinyl-ester resins were created as a hybrid that combines the benefits of unsaturated polyester resins (ease of processing) with those of epoxy resins. The resulting material offers improved mechanical toughness and excellent corrosion resistance combined with better handling and faster curing time (Kontopanos, 2001; Mouritz & Gibson, 2006).

The structure of the most common vinyl ester pre-polymer is shown in the Figure 34:

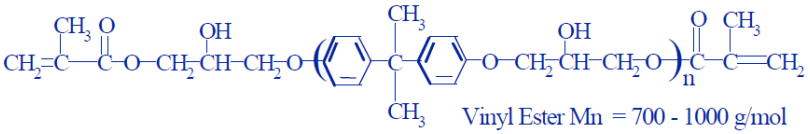

Figure 34. Structure of vinyl ester pre-polymer. (Hui, 1998)

The thermal decomposition of vinyl esters is governed, at least initially, by decomposition of the styrene component. Decomposition and pyrolysis yield a large mass fraction of flammable volatiles that provide fuel to a fire. Most of the polymer is decomposer into volatiles and only 5-10 % of the original mass is converted into char. The fire behaviour (time-to-ignition, heat release and smoke generation) is higher to polyesters due to the content of styrene (Mouritz & Gibson, 2006).

Some properties for composite matrix materials are shown in Table 14:

Table 14. Typical properties of matrix materials.

Material	γ	Elastic Modulus (GPa)	Tensile Strength (MPa)	Coeff. of Linear Expansion ($10^{\wedge 6}$ º C^{-1})
Polyester	1.28	2.5-4	45-90	100-110
Vinylester	1.07	4	90	80
Epoxy	1.03	3.5-7	90-110	45-65
Phenolic	1.6	5.5-8.3	45-59	30-45

3.3.3 Physical and mechanical properties

The properties of GFRP profiles are intrinsically related to their constituent materials: type, orientation and glass fibre volume fraction, the formation of the polymeric matrix and the interaction between fibres and the matrix. On the other hand, there are external factors such as type of loads and environmental exposure which also influence the properties of GFRP materials (Rodrigues Morgado, 2012; Mei, 2000; Casas Rius, 2011).

As an example of the of this anisotropic behaviour, in Table 15 are presented examples of three types of composite materials and the variation of longitudinal modulus, transverse modulus, shear modulus and Poisson's ratio. In this kind of composites, fibres are straight and parallel.

Table 15. Typical values for unidirectional FRP composites (cited by (Casas Rius, 2011).

Composite (fibres/resin)	$E_{Transverse}$ (Gpa)	$E_{Transverse}$ (Gpa)	G (GPa)	υ
Glass /Polyester	54,1	14,05	5,44	0,25
Carbon/Epoxy	181,00	10,3	7,17	0,3
Aramide/Epoxy	75,86	5,45	2,28	0,34

Compeering values of Table 15, it is clear that material composed of glass fibres and polyester resin has a higher Young's modulus in the direction transverse to the fibres, making them more useful for elements subjected to loads in both directions.

In Figure 35 it is shown the influence of the angle of inclination of the fibres in the value of elastic modulus.

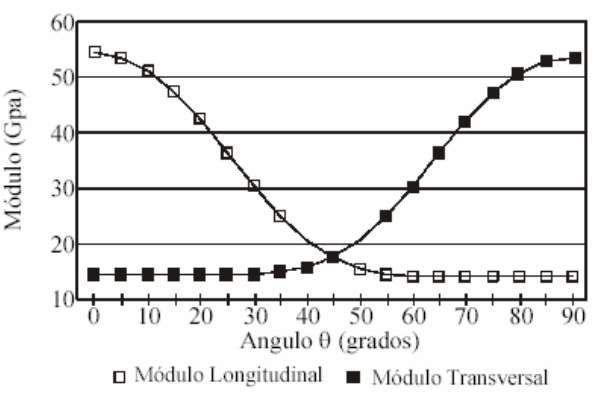

Figure 35. Longitudinal and transverse modulus as a function of angle inclination of the fibres (cited by (Casas Rius, 2011)

Moreover, Poisson's ratio of a composite material may vary considerably depending on the orientation of the fibres. When the angle between the direction of the fibres and the direction of the load is 0°, Poisson´s ratio usually has the values similar to metals, in the range of 0, 25 to 0, and 35. For different orientation of fibres, Poisson´s ratio can vary considerably, reaching 0, 02 ‑ 0, 05 for the angle of 90°. The figure below shows how Poisson's ratio varies with the angle of inclination of the fibres.

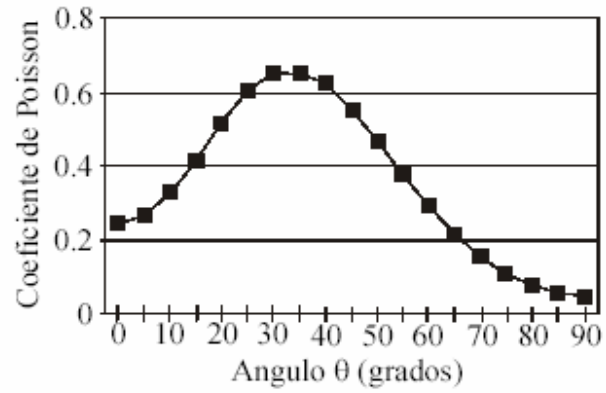

Figure 36. Poisson's ratio as a function of angle of inclination of the fibres (cited by (Casas Rius, 2011)

Taking into account that its production is carried out in a non-standard mode, the values corresponding to the mechanical characteristics are not displayed in the form of absolute values but are characterized by typical values of interval. In Table 16, the ranges of typical values of the main mechanical properties of GFRP profiles produced by major manufacturers are indicated.

Table 16. Mechanical properties of GFRP profiles (Rodrigues Morgado, 2012)

Properties	Standards	Paralel direction	Transversal direction
Traction resistence (MPa)	ISO 527, ASTM D638	200 - 400	50 - 60
Compression resistence (MPa)	ISO 14126, ASTM D695	200 - 400	70 -140
Shear resistance (MPa)	ISO 14129, ASTM D3846	25 - 30	
Elastic modulus (GPa)	ISO 527, EN 13706-2	20 - 40	5 - 9

Rodrigues Morgado (2012) made a comparative analysis between the GFRP properties and other materials such as steel (Fe360 class), wood (spruce species), aluminium and PVC. According to his study, steel is the major competitor of GFRP profiles both having similar tensile fracture stress (400 MPa). However, although the GFRP present an interesting mechanical behaviour, these materials have a low modulus of elasticity (<50 GPa), about 15% of that observed in steel, and lack the ductile behaviour observed in the metallic material.

3.3.4 Thermal properties

During the heating process, density, specific heat capacity and thermal conductivity experience significant changes that influence the temperature distribution inside the material (Bai, 2009).

The specific heat capacity and the thermal conductivity of a mixture is determined by the properties of the different phases and their mass and volume fraction. In Table 17 are presented thermal properties displayed by GFRP materials suppliers.

Table 17. Thermal properties of GFRP (Casas Rius, 2011)

Properties	Standards	Paralel direction	Transversal direction
Density (g/cm^3)	ISO 1183, ASTM D792	1,5 - 2	
Thermal Conductivity (W/K*m)	ISO 22007, ASTM D5930	0,2 – 0,58	
Expansion coefficient (K^{-1})	ISO 11359-2, ASTM D696	$8 – 14* 10^{-6}$	$16 – 22* 10^{-6}$

Studding both materials separately, Mouritz and Gibson (2006) stablished a value of thermal conductivity for E-glass fibre of 1.13 W/K*m and a value of 0.19 W/K*m for Vinyl ester resin.

3.3.5 Properties function of temperature

Generally, the elastic modulus and strength of a polymer drops significantly with temperature and the viscosity of the resin increases when the temperature reaches and exceeds the glass transition temperature (Bai, 2009).

Many authors have proposed various types of functions to try to describe the behaviour of the material. Figure 37 illustrates the relationship which typically occurs when a mechanical property (P) of the FRP material is subjected to a variation in temperature, considering that, on the one hand, the temperature is constant through the thickness of the material and, on the other hand, the temperature variation corresponds to values between ambient temperature and the decomposition temperature of the matrix (Mouritz & Gibson, 2006). For reduced temperatures the composite has a maximum resistance (PU) which decreases with temperature increase (PR). If the material is at temperatures higher than their critical temperature (T_{cr}), it is observed a decrease in the material strength. The T_g parameter represents the glass temperature, and T_g, the mech temperature at which the material loses approximately 50% of its strength.

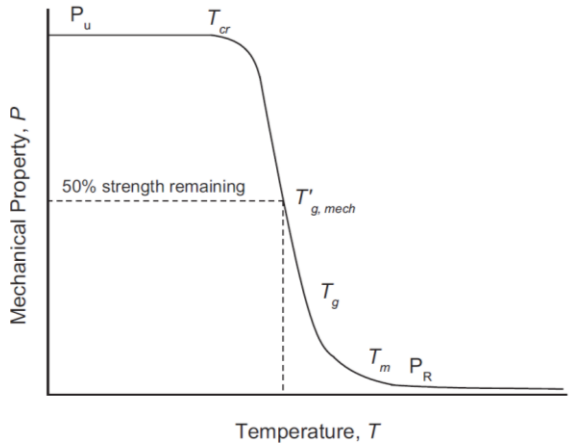

Figure 37. Schematic of the effect of iso-thermal heating on the mechanical property of a laminate (Mouritz & Gibson, 2006).

The expression proposed by these authors that includes an "R" parameter associated with behaviour resins is as follows:

$$P\,(T) = \left(\frac{P_U + P_R}{2} - \frac{P_U - P_R}{2} tanh * (k(T - T'))\right) R^n \qquad [12]$$

Different values to the parameter n are used in order to take into account the variation on properties of the polymeric matrix. The elastic constant and compressive strength are closely related to the matrix polymer, thus they concluded that using n=1 was a good approximation of reality to properties that

depend on polymeric matrix. However tensile strength is deeply related to strength of the reinforcing fibres, a value of n = 0 is used (Gibson, et al., 2012).

Ramroth (2006) exposed that the elastic constants were to be degraded according to equation 13 to account for the loss of stiffness resulting from the glass transition in the matrix resin. In Figure 1Figure 38 is plotted this degradation relation for different elastic constants.

$$\frac{X}{X_0} = 307 - 46\mathrm{T} + 0.276T^2 - 0.000823T^3 + 1.229 * 10^6 T^4 - 7.33 * 10^{-10} T^5 \qquad [13]$$

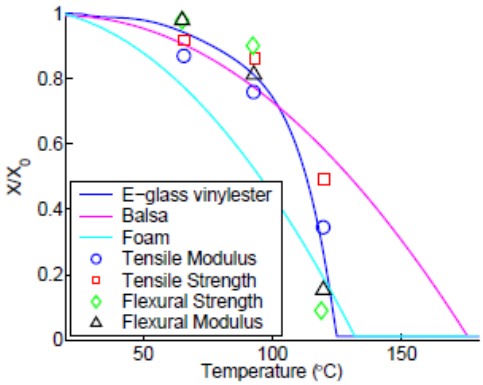

Figure 38. Degradation of elastic constants with temperature (Ramroth, 2006).

In the research made by Yu Bai (2009) he express the time-dependent E-modulus, E_m, as:

$$E_m = E_g * (1 - \alpha_g) + E_r * \alpha_g (1 - \alpha_d) \qquad [14]$$

Where

E_g: the modulus of the glassy state

Er: the modulus of the leathery or rubbery state

α_g: the conversion degree of glass transition

α_d: the conversion degree of glass decomposition

The experimental results obtained by Boyd, S.E. (2006) for the in-plane temperature dependent material properties are shown in Figure 39:

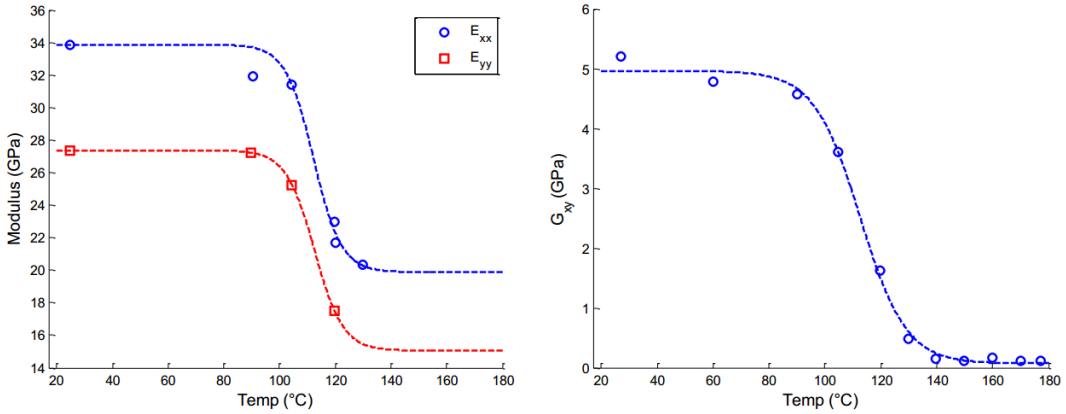

Figure 39. Temperature degradation curves for elastic properties (Cholewa, 2015)

Regarding the tensile strength Yu Bai (2009) exposed that in a lower temperature range, strength is dominated by the fibre tensile strength, while at higher temperatures tensile components may exhibit resin-dominated failure. Figure 40 shows the results of tensile strength on three types on woven fabric laminate being E-glass/vinyl ester composite the one with significant strength retention.

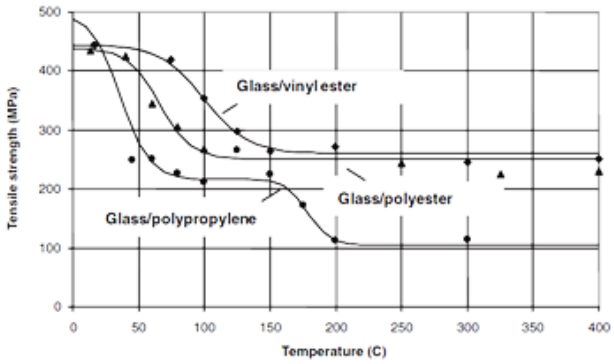

Figure 40. Comparative effect of temperature on the tensile strength of different types of laminates (Mouritz & Gibson, 2006)

Figure 41 shows that the tensile strength of an E-glass/vinyl ester composite with increasing temperature measured, the minimum strength is reached at about 150ºC and then remains constant up to 300ºC.

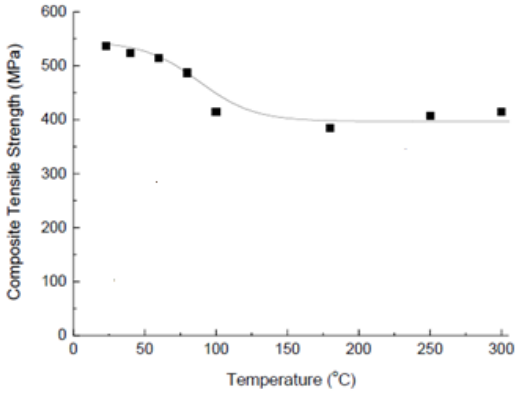

Figure 41. Effect of temperature on the tensile strength of E-glass/vinyl ester composite (Feih, et al., 2007)

As regards the compression strength, this property is more sensitive to temperature variation than the tensile strength as it is observed in Figure 42 or in the comparison between Figure 41 and Figure 43a or Figure 40 and Figure 43b. All the figures denote an early compressive strength loss for even relatively low temperatures and quickly reduction of resistance.

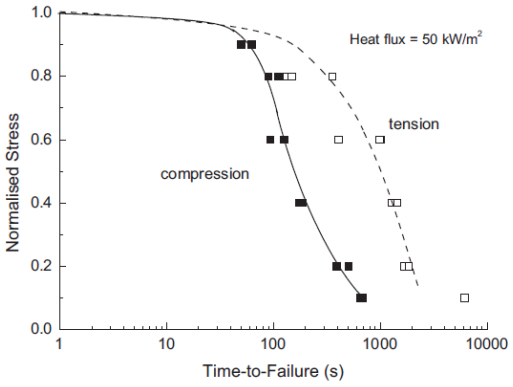

Figure 42. Comparison of the failure times for a glass/vinylester under tension or compression (Mouritz & Gibson, 2006)

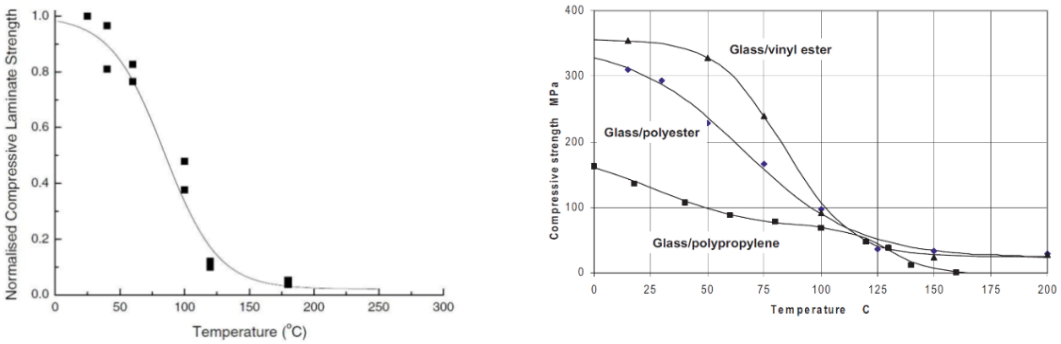

(a) (b)

Figure 43. Effect of the temperature on the compressive strength of a glass-vinyl ester laminate (a) (Feih, et al., 2010) & (b) (Mouritz & Gibson, 2006)

Thermophysical properties (thermal conductivity, specific heat, thermal diffusivity, etc.) are commonly highly temperature-dependent. Furthermore, in the literature, many authors have developed different models in order to estimate these properties (Bai, 2009; Keller, et al., 2006; Dimitrienko, 1997). A review of models for thermal conductivity of composite materials con be found in Pietrak et al. (2015).

Yu Bai (2009) concluded that specific heat capacity and thermal conductivity does not change significantly or increases only slightly with the temperature before decomposition. Thus, consequently, could be described as linearly dependent on temperature or assumed to be a constant before decomposition.

Values for theses parameters for the char and virgin composite are available from research conducted by Lattimer et al. (2009). In particular, specific heat capacity values and thermal conductivity values are obtained as a function of temperature via the data provided in Figure 44 and in Figure 45, respectively:

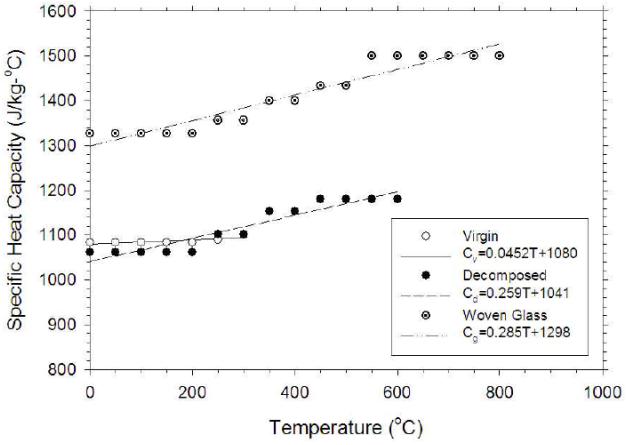

Figure 44. Specific heat capacity of char and virgin composite (E/glass/vinylester) as a function of temperature (Ramroth, 2006)

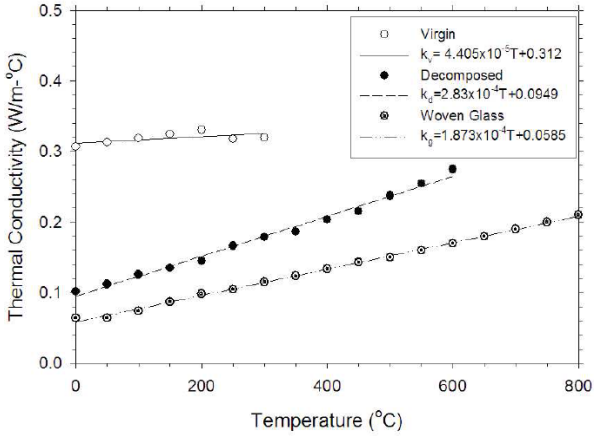

Figure 45. Thermal conductivity of char and virgin composite (E/glass/vinylester) as a function of temperature (Ramroth, 2006)

In addition, other properties such as permeability and porosity allows to assess the gas flow properties through the different stages of composite material in temperature (virgin, partially degraded, and fully degraded). According with the experiments carried out for Goodrich (2009) the permeability of E-glass/ VE was initially zero, with no gas flow possible, and increased to a final value of 1.56E-10 m^2 and the porosity increased from approximately 0 to a final value of 0.68.

3.3.6 Fire behaviour

The behaviour of composite materials in fire is governed largely by the chemical processes involved in the thermal decomposition of the polymer matrix and fibres (Keller & Bai, 2014; Mouritz & Gibson, 2006). A composite material can undergo changes to its physical, chemical and mechanical condition in fire.

Many authors (Alos-Moya, et al., 2014; Bai, 2009; Correia, 2015; Mouritz & Gibson, 2006; Lattimer, et al., 2009; Goodrich, 2009) have described the behaviour of composites under fire. The first event to take place is the conduction of heat into the material that causes expansions or contractions in the material depending on the temperature. The first changes occur at the heat distortion and glass transition temperatures of the matrix, which are usually in the range of 80–180ºC. The load-bearing properties are severely degraded within this temperature range. Decomposition of the polymer occurs between 300–500 º C, although depends on the composition and chemical stability of the organic material. Above this temperature, the matrix and fibres degrade endothermically to a porous carbonaceous char, yielding gaseous products. Eventually the matrix becomes sufficiently porous and cracked. If the temperature is high enough (excess of 1000ºC) pyrolysis reactions will be induced between the char and silica network of the degraded reinforcement resulting in considerably mass loss. Ablation can also occur at this high temperatures, which is accelerated by high velocity air flow over the surface (Easby, 2007).

The main processes are described in Table 18 and Figure 46 shows the approximate temperatures over which the different processes occur:

Table 18. Main processes when a composite is exposed to fire (Easby, 2007)

Anisotropic heat conduction through virgin material and char
Thermal induced strains
Decomposition of polymer matrix and organic fibers
Pressure rise due to formation of combustion gases and vaporization of moisture
Flow of gases from reaction zone through the char zone
Formation of delamination and matrix cracks
Reactions between char and fiber reinforcement
Ablation

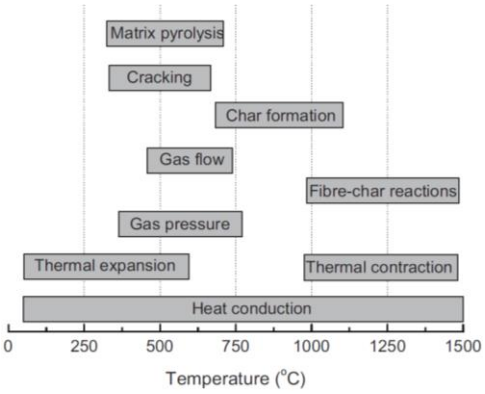

Figure 46. Effect of temperature on the various responses of a fiberglass composite (Mouritz & Gibson, 2006)

3.3.6.1 Fire reaction

The flammability and fire hazard of composite materials are determined by their fire reaction properties. Properties that describe flammability include time-to-ignition, limiting oxygen index (LOI), heat release rate (HRR), mass loss and flame spread rate. Properties that determine the fire hazard are smoke density and toxicity (Mouritz, 2007).

Time-to-ignition defines the start of flaming combustion, is the minimum time required to promote ignition and continuous flaming of a combustible material (Mouritz & Gibson, 2006). Ignition usually occurs when the surface of a composite is heated to about the pyrolysis temperature of the polymer matrix (250–400 ºC) (Mouritz, 2007). The ignition time depends on a variety of physical factors (oxygen availability, chemical and thermos-physical properties of the matrix and fibres, thickness of the composite…) and on the heat flux of the fire.

According to Mouritz (2007) the ignition time for vinyl ester matrix composite is short and it will ignite within 1-2 min. when exposed to a heat flux of 50 kW/m^2. Mouritz & Gibson (2006) exposed that glass fibers are inert to fire when heat flux is under 1000-1200 ºC altought the emulsion binders and other organic agents applied to fibres during manufacture will thermally decompose and contribute to the ignition process. Figure 47 shows the effect of external heat flux on ignition times for fiberglass laminates with different resin matrices.

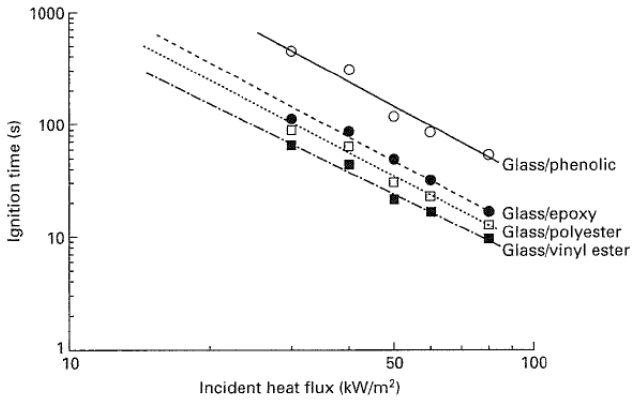

Figure 47. Heat flux against time-to-ignition for 4 composite materials (Mouritz, 2007)

The limited oxygen index (LOI) may be considered as a measure of the ease of self-extinguishment of a burning material. The index values increase with temperature up to 100ºC but a higher temperatures there is a study reduction because less heat is needed to sustain decomposition and burning. Figure 48 shows the LOI values for different composite materials.

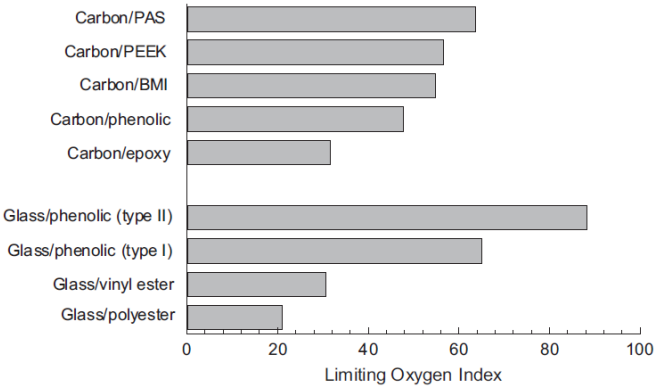

Figure 48. LOI values for several thermoset and thermoplastic composite materials (Mouritz & Gibson, 2006)

Regarding the heat release rate (HRR) is considered the single most important fire reaction property because it can provide the additional thermal energy required for the growth and spread of the fire. The heat released can be affected by fibre reinforcement in several ways; less polymer matrix material is available to generate heat during thermal decomposition. Figure 49 shows the HRR for a vinyl/ester composite material over time exposed to a het flux of 50 kW/m^2.

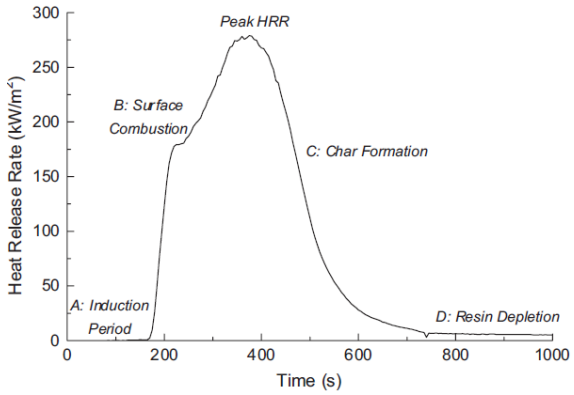

Figure 49. HRR profile for a glass/vinyl ester composite (Mouritz & Gibson, 2006)

The HRR is high for vinyl/ester composites because the matrix releases great amount of hydrocarbon volatiles into the flame.

Regarding the properties that determine the fire hazard, the smoke of polymer composites can be extremely dense and thereby reduce visibility, cause disorientation and make it difficult to fight the fire. Smoke released from a burning composite is dependent on a variety of factors, including the amount and type of resin and fibre reinforcement, heat flux of the fire, heat release rate properties of the composite material and char formation (Mouritz & Gibson, 2006).

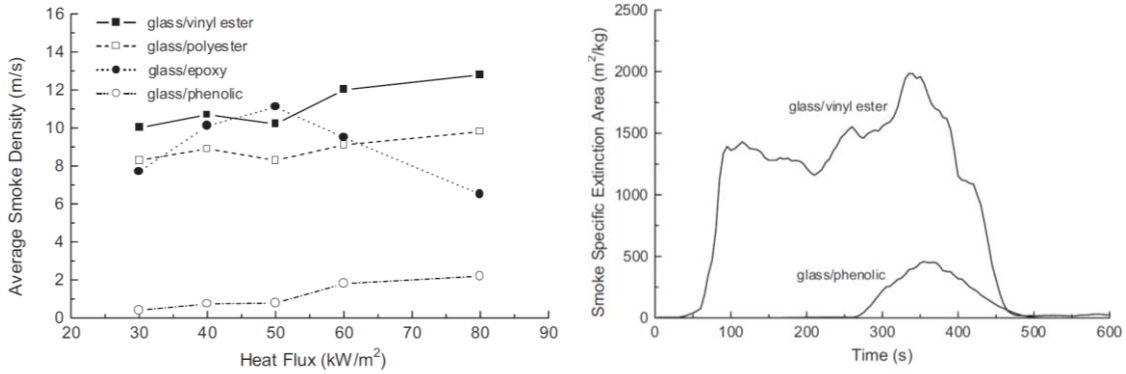

Figure 50. Effect of incident heat flux on the smoke yield and smoke generation verses time (Mouritz & Gibson, 2006)

As it can be observe in the Figures N, from de studies of Mouritz & Gibson (2006), glass/vinylester has the highest average smoke density compering to other composite laminates. Furthermore, the SEA of the vinyl ester laminate increases rapidly at the onset of combustion, and then remains high until the polymer matrix is completely consumed after about 500 seconds. This results should be taken into account for its use in high fire-risk applications.

Mass loss gives a quantitative measure of the amount of materials that will decompose in fire and is one of the few fire reaction properties that can be calculated by thermochemical modelling (Gibson, et al., 2003). According to the study of Mouritz & Gibson (2006) in mass loss curves can be identified

four stages that represents the different events in the fire response of the material as it is show in Figure 51; initially, before reaching the decomposition temperature of the polymer matrix, the mass loss in the material is approximately zero. Following this initial phase, the resin begins to decompose producing a rapid mass loss. Finally, once the resin has been totally degraded, the slope of mass loss is less pronounced and the mass loss curve tend to a constant value.

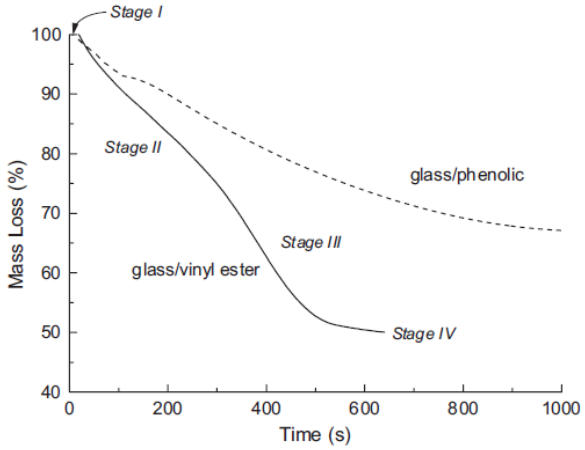

Figure 51. Mass loss curves for glass/vinylester and glass/phenolic (Mouritz & Gibson, 2006)

Observing Figure 51 a greater mass loss is observed in glass/vinylester laminate due almost entirely to the loss of the resin matrix. The mass loss in the composites depends primarily on the type of resin, the combustibility of the fibres and the resin content of the material, taking into account that a larger resin content cause greater mass loss. According to the study realised by Goodrich (2009) the rate of mass loss is also dependant on the rate at which the sample is heated.

3.3.6.2 Fire resistance

The fire resistance of combustible materials is often defined by the time taken for the back-face temperature to reach 160ºC, at which point the fire is likely to spread. The time to reach 160ºC increases rapidly with the panel thickness being capable of withstand severe temperatures for a considerable time. This is achieved due to their low thermal conductivity and the endothermic nature of the resin decomposition reaction that slows heat transmission through the laminate (Mouritz & Gibson, 2006).

However the post-fire tension, compression, flexure and interlaminar shear properties suffer large and rapid reductions with increasing heat flux or duration of a fire. The char produced by decomposition of the polymer matrix is the major cause for the reduced post-fire properties (Mouritz & Gibson, 2006;

Rahman, 2015). Figure 52 show the retained flexural strengths of various thermoset laminates following fire testing at the heat flux of 25 kW/m^2 for twenty minutes.

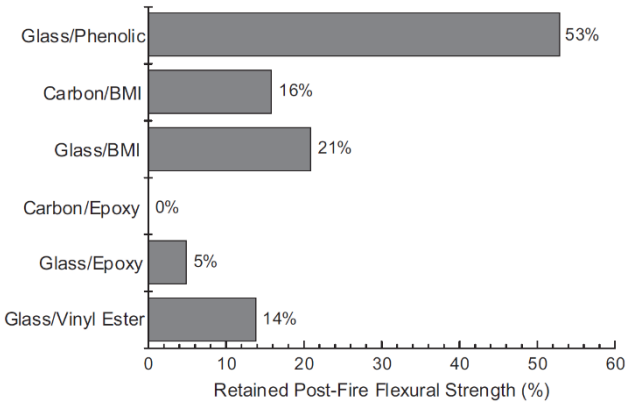

Figure 52. Retained Post-fire flexural strength (%) (Mouritz & Gibson, 2006).

Fire damage is consistently found to have a greater influence on the post-fire compressive properties compared to the tensile properties as it can be appreciated in the Figure 53.

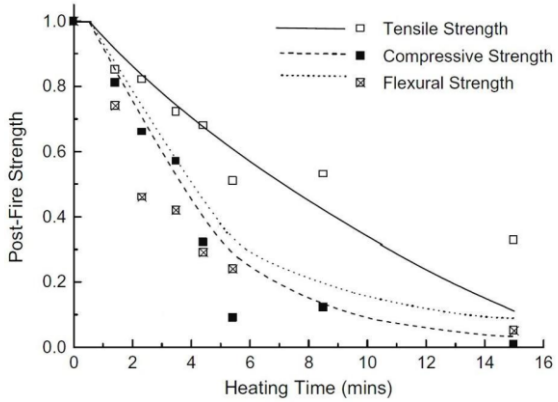

Figure 53. Tensile, compressive and flexural strength for glass/vinylester (Rahman, 2015)

3.3.7 Degradation, decomposition and deterioration

When the material is exposed to a sufficiently large heat flux radiated from a fire, the polymer matrix and organic fibres will thermally decompose to yield volatile gases, solid carbonaceous char and airborne soot particles (smoke) (Mouritz & Gibson, 2006). The chemical composition and amount of the volatiles is dependent on the polymer matrix, oxygen content and temperature.

It is these volatiles that decompose at the fire/composite interface that produce heat that sustains the decomposition process. They react with oxygen in the fire atmosphere leading to the formation of final combustion products providing a rich source of fuel to sustain and grow a fire

The main decomposition reactions that reduce molecular weight are random chain scission, chain-end scission ('unzipping') and chain stripping (removal of side groups). But the dominant reaction in most polymer systems is random chain scission.

The thermal decomposition reactions of polymers may proceed by oxidative processes or simply by the action of heat. The decomposition process is often accelerated by oxygen, the cycle stops when the fuel source has been exhausted, which is usually when the organic matrix has completely decompose or the oxygen is insufficient.

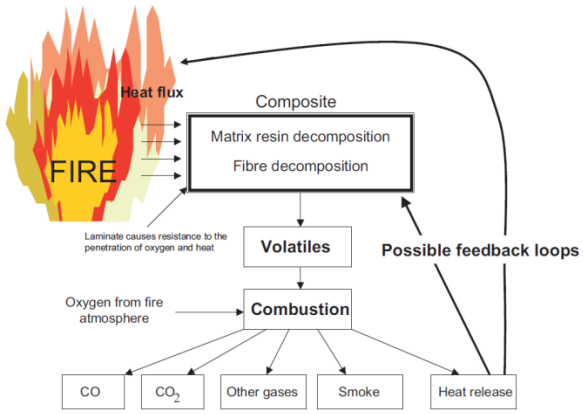

Figure 54. Mechanisms involved in the thermal decomposition (Mouritz & Gibson, 2006)

In the case of E-glass/Vinylester composite, Goodrich (2009) found that only minor surface changes were observed in the Eglass/VE sample up to 400°C in contrast to the resin sample. Above this temperature, decomposition became apparent with pores forming in the gaps between fibres and some fibre motion over the temperature range 380-460ºC. In his study was exposed that the size and geometry of the pores depended most on the arrangement of the adjacent fibres, as they tend to conform to adjacent shapes with a typical range of pore sizes of 20-200 μm.

The composite continued to degrade beyond 460°C, finally appearing to largely stop around 520°C with only 7% of the resin in the material. There was a clear transition from the fairly smooth resin surface into a final char pore structure at this temperature.

In Figure 55 it is shown the results of his study, it can be appreciated the difference between a virgin sample of E-glass/Vinylester and a degraded one:

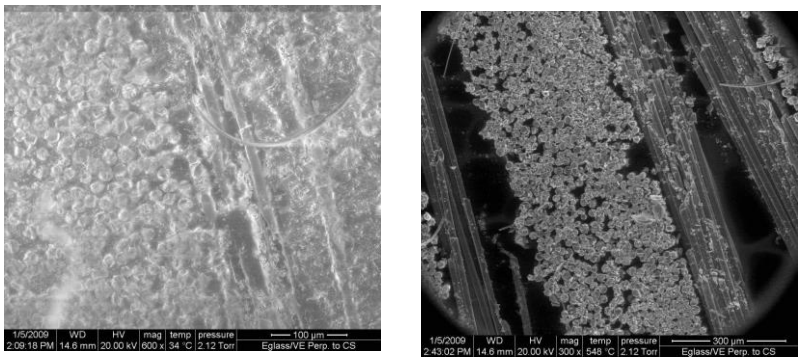

Figure 55. Imagen of E-glass/VE virgin sample and the same sample heated up to 548 ºC at 20º C/min (Mouritz & Gibson, 2006)

In the research made by Rahman (2015) when the laminate was exposed directly to the heat flux (*35 kW/m²*) the decomposition temperature was reached very rapidly (in less the 100 seconds). Decomposition reaction transformed the laminate face skin into a highly porous material consisting mostly of the glass fibre reinforcement and a small amount of char as can be appreciated in figure N.

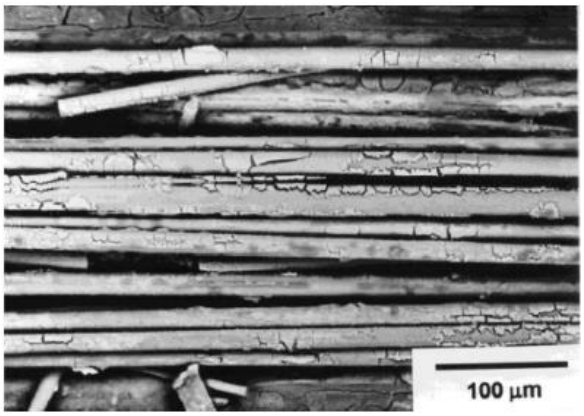

Figure 56. Microstructure of the laminate after thermal decomposition of the polymer matrix (Rahman, 2015)

4. FE MODELIZATION AND CASE STUDY

4.1 Background

4.1.1 Heat transfer model

In predicting the thermal response of FRP composites, numerous heat transfer model can be found in the literature. Those thermal models differ in capability and accuracy to account for the effects of the decomposition reaction and fire damages on heat transfer.

The initial work on thermal modelling of organic material in fire was performed for wood, since processes of the burning wood are fundamentally similar to a burning composite (Gibson, 2003). These models have been adapted for composites in fire due to their capability to calculate the temperature profile distribution through a composite.

The simplest model to calculate temperature in an FRP panel is the standard one-dimensional heat conduction equation, where decomposition's effects are neglected (Mouritz & Gibson, 2006; Yu, 2012).

Mouritz and Gibson (2006) provided a good review of thermal models of FRP composites exposed to fire or high temperature. As stated in their book, one of the earlier models regarding this subject was developed by Pering and co-workers (1980), and consisted in a one dimensional model that took into account the heat conduction and pyrolysis of the matrix.

Later on, Henderson and co-workers (1985) developed an improved model in which the effect of diffusion of decomposition gases was taken into account as well. Other main features of this model are that it is sensitive to transversal conductivity changes with temperature and that takes into account the reactions between carbon-silica that can occur between glass fibres and char.

Afterwards and based on the original work by Henderson et al (1985), Florio, Henderson, Test and Hari Haran (1991) developed a remarkable model in which in addition, the effects of thermal expansion and internal pressure were considered.

More recently, a simplified version of the model developed by Henderson et al. (1985) was proposed by Gibson and colleagues (1995). A one-dimensional, non-linear equation that incorporates the processes of conductive heat transfer through the material, endothermic decomposition of the polymer matrix, and convective mass transfer of volatile products from the reaction zone to the hot composite surface.

In literature, other heat transfer models, in addition to the aforementioned, have been developed but with little difference. Because too many factors affect heat transfer, it is acknowledged that there is no single heat transfer model suitable for all applications. However, some models are mathematically capable of accounting for many phenomena in decomposition but need a large quantity of data (material properties) difficult to obtain.

4.1.2 Structural model

Until recently, models to analyse the fire structural integrity of sandwich composites were not available. Instead, the conventional approach to assess the structural behaviour was to perform fire tests on sandwich composite components (Rahman, 2015). However it is not possible to extrapolate the information obtained for a specific test to predict the structural behaviour of sandwich composites in other fire scenarios.

Nowadays, with knowledge of temperature profile and thermal decomposition from thermal response models, the mechanical response of FRP composites, combining thermal and mechanical loading, can be assessed with a mechanical model.

One of the first thermomechanical models for FRP materials was introduced by Springer in 1984. Later, McManus and Springer (1992) used a governing equation to include the influence of thermal expansion, internal gas pressure, and moisture as well as charring expansion.

Mouritz and Mathys (1999) formulated the two-layer model based on rule-of-mixtures to predict the residual tensile strength of polymer laminates under fire. For simplicity, the tensile strength through the char layer is assumed negligible, and the strength through the virgin layer has the value at room temperature.

Gibson et al., (2004) attempted to combine their thermochemical model with Mouritz's "two-layer" post-fire mechanical model to create a thermomechanical model.

Nowadays, it is being developed many advanced models in order to take into account all features of the thermomechanical response of FRP models.

4.2 Case study: Avançon Bridge

4.2.1 Situation and context

On October 2012, a composite bridge deck with a balsa wood core replaced an old concrete bridge built around 1900 in Bex (Switzerland) due to its excessive degradation. In addition, the old deck permitted neither the passage of vehicles above 28 tonnes, nor an easy crossing. Based on these inconveniences, the Roads Service Vaud decided to take advantage of the construction and expand the total width from 5.30 to 7.50 meters plus increasing the maximum traffic load from 280 to 400 KN, as required by the current Swiss standard SIA261. It was the first application of a balsa sandwich road bridge in the country.

Avançon Bridge is located in a mountainous area, on the only road providing access to the valley. Therefore, the time of installation was critical and the deck was mounted in a single day. The entire replacement which would normally take months, was achieved in weeks.

The composite deck was prefabricated in three 40-square-meter pieces by 3A Composites in Altenrhein, Switzerland, then transported across country by truck. Next, the pieces were pre-assembled on the side of the construction site by adhesively bonding the sandwich deck on the upper flanges of two galvanized steel girders. It took five days to assemble the structure at the construction site before its installation. Then the whole bridge was installed in one single piece with a crane.

Figure 57. Images taken during the construction of the bridge (© 2012 EPFL. Alain Herzog)

The road was closed for 10 days: It took two days to remove the old bridge and only a few hours for installation. The remaining road closure was necessary for casting the transition slabs and standard road reconstruction on both sides of the bridge. By comparison, a cast-in-place concrete solution would have required closing the road for six to eight weeks.

Replacing the concrete deck with a composite one comes with several advantages. Besides being lighter, this composite construction is not subject to corrosion, the main cause of deterioration of

concrete structures (Keller, et al., 2014). Additionally, the prefabrication in a factory further increases its quality, improving safety and longevity, while speeding up the onsite installation.

Material and structural testing were the key of the success of this novel project; material properties were tested, fatigue and ultimate strength tests were performed on full-scale samples and construction details were also tested prior to implementing them on the bridge.

The Bex Bridge will serve as a test site to study the feasibility of this type of construction, and its suitability for other similar rehabilitations in the region. And, while concrete bridges have come to dominate the landscape, this technology brings the wooden bridge back to life, just hidden beneath a modern skin (Nendaz & Lavanchy, 2012).

Figure 58. Image of Avançon Bridge (© 2012 EPFL. Alain Herzog)

4.2.2 Structure and composition

The total span of the bridge is 11.45 m and the total width is 7.5 m (Figure 59 and 60). The sandwich structure is composed of two 22-mm-thick GFRP face sheets bonded to 241-mm-thick balsa wood core that were produced on a flat mold by vacuum infusion. The total thickness is of the same order of magnitude compare to a conventional concrete deck but with a significantly lower weight (only 160 kg/m^2 against 700 kg/m^2 for the concrete solution) (Keller, et al., 2014).

The deck, is adhesively bonded on the wings of two welded steel I-girders (S355). It has a transverse span between the welded girders of 3.90 m and it presents an overhang of 1.80 m (Figure 59). These girders are anchored and thus fixed into two concrete cross beams placed onto the abutment. The transverse deck edges are also supported by the cross beams by means of neoprene strips, they are not adhesively bonded together. The rotations and in-plane displacements of these edges meet the deformation limitations of the continuous pavement construction (Keller, et al., 2014; Nendaz & Lavanchy, 2012).

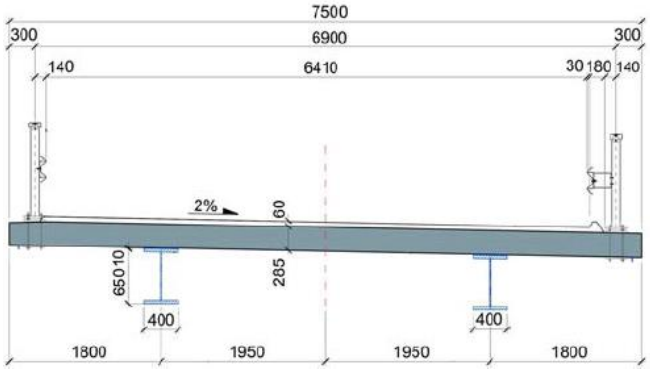

Figure 59. Cross section (mm) (Keller, et al., 2014)

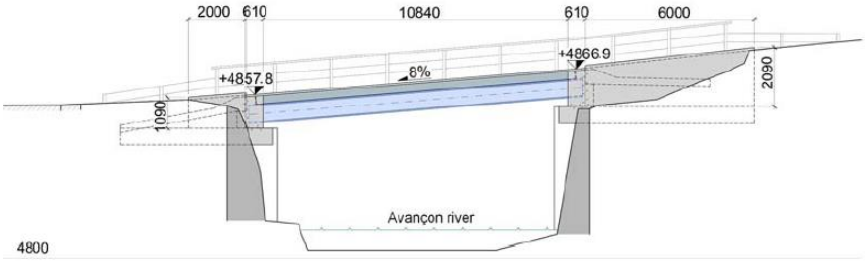

Figure 60. Longitudinal section (mm) (Keller, et al., 2014)

4.2.2.1 Core

The core of the composite deck is made of a structurally-bonded balsa-based material, a laminated veneer lumber (LVL), where thin layers are assembled using a structural adhesive. Due to balsa wood has anisotropic properties, the wood fibres were oriented perpendicular to the plane of the sandwich, taken advantage of the high specific compressive strength and shear strength of the material.

The average density of the LVL-balsa is 250 kg/m^3, which is approximately one tenth of that of reinforced concrete and two to three times lower density than traditional construction wood products.

4.2.2.2 Skin

The E-glass fibre architecture is orthotropic with unidirectional (UD)-layers in the bridge direction (0°, approx. 25%) and transverse to the bridge direction (90°, approx. 75%), resulting in an average fibre volume fraction of 55% in each direction (Keller, et al., 2014). The infusion process under vacuum vinylester resin ensures the cohesion of the sides on the core and a perfect seal, guarantee of

sustainability. Vinylester resin was selected because of its excellent chemical resistance, durability and low cost.

It has been possible optimize the structural behaviour of the sandwich deck using FRP faces with fibers oriented in the direction of the main effort.

4.2.3 Structural design

As mentioned before, the composite sandwich structure used consists of two thin GFRP faces which are bonded to both sides of a lightweight wooden core. This process creates a plate that is light, rigid and strong. The lower and upper faces ensure the bending strength, while the core gets shear forces and provides the distribution of compressive forces perpendicular to the plane of the sandwich (traffic loads).

The design of the structure is based on Swiss standards SIA 260 and SIA 261, which are in line with Eurocode standards (Keller, et al., 2014). The serviceability (SLS) and ultimate limit (ULS) states were verified using the partial safety factor concept, applying load factors on the action and material factors on the material side. Verifications of steel beams and balsa wood core are performed according to standard SIA 263 and SIA 265. With no established standard for building FRP composite materials for adhesive bonds, the recommendations and resistance coefficients proposed by BÜV and EUROCOMP were used.

The actions, their combinations, and associated load factors were determined according to SIA260 and 261. The elastic design strains were limited to 0.20% and the deflection limit to span/500.

4.2.4 Fire protection

Avançon Bridge was not treated with any kind of flame retardant material in order to render the deck resistant to both, the initiation and sustaining of fires. As mentioned in previous sections, bridges can be exposed to fire from a variety of sources, and although the probability is lower than in other kind of structure, the damage is much more devastating due to this lack of fire protection.

The only reference made, regarding the behaviour of composite materials to high temperatures, was at the time of placing the asphalt layer; the composite is not able to withstand the temperatures required for the laying of a traditional asphalt so the composite deck was coated with a layer of 60 mm of warm

asphalt mix type AC 11S (with 1% 'Greenseal additive BT) and the implementation temperature is below 120 °C (Nendaz & Lavanchy, 2012).

4.3 Finite Element Model

Currently there are several finite element programs that can be used in the analysis and design of structures. They are SAP, NASTRAN, NISA, ANSYS and Abaqus, which are capable of treating very complex problems. In this study, package software Abaqus/Standard ver. 6.14 was used because of its extensive capabilities and availability.

This section describes mainly the finite element analysis carried out in order to investigate the bridge fire response in time and its ultimate strength behaviour. It is seek to predict stresses and deflections and assist in the future design of similar single-short-span bridges during fire.

The complete description of the thermomechanical analysis is divide in the description of the structural model and the heat transfer model. In both cases it is include: the types of elements and mesh used, loading, boundary conditions and material properties.

4.3.1 Structural model

A 3D linear elastic finite element (FE) model was constructed: the deck is modelled by a single deck panel, which acts primarily to distribute load to the two supporting steel girders of the same length. A composite action between the deck and girders is assumed, however, the connections between them are not modelled. The geometry of the model can be observed in Figure 61 and 62.

The FE mesh, material properties, boundary conditions and loading is developed in the next sections.

4.3.1.1 Mesh

Figure 61 shows the mesh used for the mechanical analyse. The elements of the core and the facesheets layers were defined by solid 3D continuum elements that had eight-node, integration-reduced, linear brick elements (C3D8R, hourglass control). These elements had three translational degrees of freedom at each node. The use of these elements helped prevent mesh instability, commonly referred to as hourglassing, which may occur in reduced-integration elements (Tuwair, et al., 2016; Peris-Sayol, et

al., 2015). Moreover, the use of 3D elements is motivated by the need to capture local phenomena such as web buckling in the beams.

The size of the solid elements used to model the top and bottom structural faces was so that their nodes coincided with the nodes of the solid elements used to model the core. Moreover, a perfect bond was assumed to exist between the sandwich panel components modelled by the use of tie constraints.

Figure 61. Mesh used in the FE model

The geometry of the mesh of the asphalt layer, as can be seen in the figure above, is altered by the partition made in order to introduce the 8 axle loads.

On the other hand, as Figure 62 shows, in each layer of the model the mesh was seeded in several parts in order to accurately define the distribution of the stresses; asphalt and GFRP layers were divided in 4 parts and core layer was divided in 6 parts.

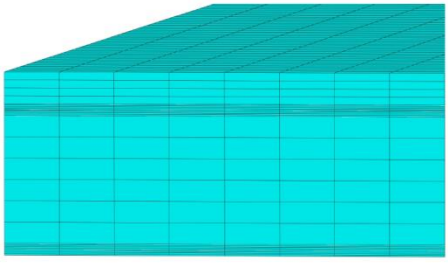

Figure 62. Detail of the division of the mesh

Table 19 show the number of nodes and finite elements in the FE model:

Table 19. Mesh features

Layer name	Element type	Elements	Nodes
Asphalt	C3D8R	36592	46695
Top GFRP layer 90	C3D8R	34500	44080
Top GFRP layer 0	C3D8R	34500	44080
Core Layer-1	C3D8R	51750	61712
Bottom GFRP layer 0	C3D8R	34500	44080
Bottom GFRP layer 90	C3D8R	34500	44080
HEB 800	C3D8R	1495	3248
HEB 800	C3D8R	1495	3248

4.3.1.2 Mechanical properties

In order to define the mechanical resistance limit of the bridge, the model must have as an input the following mechanical properties: elasticity (Young's Modulus and Poisson's Ratio (υ)), density (ρ) and expansion coefficient (α). Since in a following step (thermomechanical study) there will be the need to define these characteristics temperature dependent, it was decided to incorporate them in the mechanical step as they will not affect the results of the model.

There is plenty information about properties in codes and standards for wood materials (Eurocode 5). However, mechanical properties for balsa wood were taken from results found in literature for being more accurate.

Regarding the mechanical properties of the GFRP layers, likewise balsa wood characteristics, they have been taken from the literature. Nevertheless, in this case is due to the lack of standards and because of the paucity of experimental data. The GFRP layers were assumed to be linear elastic orthotropic materials.

The steel used is S355 with a yielding limit of 355 MPa. Engineering values of stresses (σ) and strains (Ɛ) were converted into true stress strain laws (σ_n- $Ɛ_n$) and introduced in Abaqus. Figure 63 represents the variation with temperature of the modulus of elasticity and Yield strength and Figure 64 represents the variation with temperature of thermal expansion and Poisson's Ratio for structural steel S355.

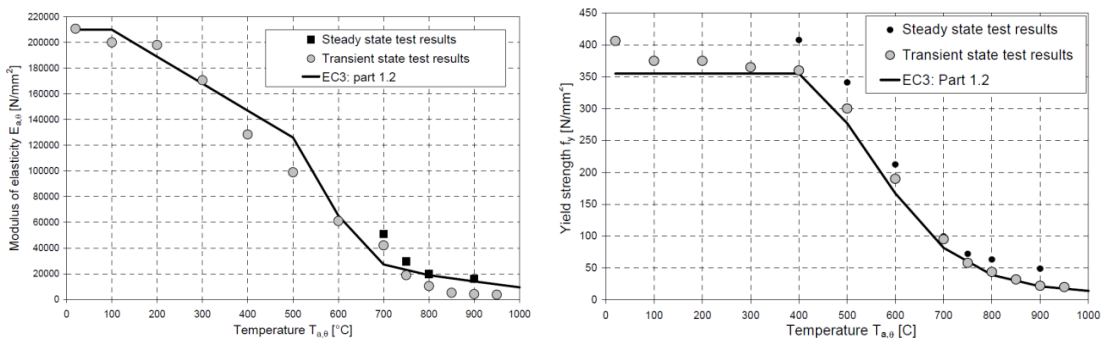

Figure 63. Temperature dependent modulus of elasticity and Yield strength of S355 (Outinen, 2007)

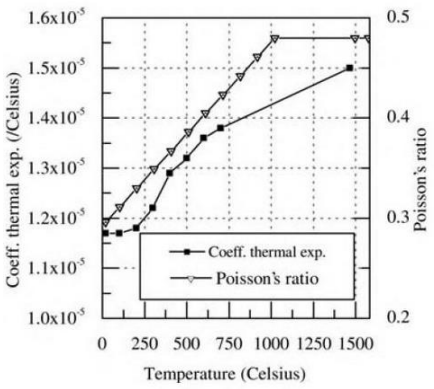

Figure 64. Temperature dependent coefficient of thermal expansion and Poisson's Ratio of S355 (Leroy Gardner, 2012)

In Table 20 are defined the mechanical properties incorporated to the model:

Table 20. Mechanical properties of the materials

Poperties	Asphalt Layer			Skin Layer			Core Layer		Steel Beams	
Young's Modulus (Mpa)	15000-7900*LOG(T)		[116]	Figure 39		[13]	Figure 23	[13]	Figure 63	[87]
Poissons Ratio	20ºC	0.35	[103]	0.3			Table 9	[65]	Figure 64	[68]
	30-100ºC	0.45	[103]							
Density (kg/m3)	2100		[103]	1875		[57]	185	[122]	7850	[68]
Expansion Coefficient	3.00E-05		[103]	T< 350 ºC	0.0094*T+11.024	[102]	0.0019		Figure 64	[68]
				T> 350 ºC	0.0404*T+22.013					

4.3.1.3 Boundary conditions

The boundary conditions were defined as a pin support at one end and a roller support at the other end. The restrictions of both supports are not applied on a point or a line but on a surface that represents the support.

The extent of roller motion is not a parameter in the study thus the bridge is allowed to freely expand without any restraint. Although, as explained by Payá-Zaforteza and Garlock (2012), it is important to consider that elevated temperatures can provoke deck expansion movements which might be eventually restrained by the abutments or an adjacent span and affect stress distribution. Therefore, the maximum longitudinal displacement of the girder should be restricted to the width of the expansion joint.

Moreover, as named previously, a perfect contact was assumed to exist between the steel beams and the surface of the sandwich panel.

4.3.1.4 Gravity loads

In order to meet the requirements of the current Swiss standard SIA 216 (Swiss Standards Association, 2003b) the bridge was designed for the critical load position; two groups of two axle loads and uniformly distributed load.

The two higher axle loads were at mid-span perpendicular to the bridge edge. The load was equal to 135 kN for each axle. The second axle group was placed next to the first one, on the other lane, with a load of 90 kN for each axle. These loads, in both cases, were distributed over a 04 × 0.4 m^2 area. A representation of the geometry can be seen in Figure 65:

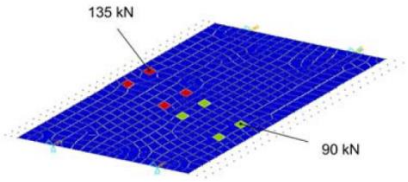

Figure 65. Critical load position according to SIA261 (Keller, et al., 2014)

Furthermore, a uniformly distributed load of 8.1 kN/m^2 was applied on one lane (higher axle loads) and 2.25 kN/m^2 on the second lane. In addition, the self-weight of the steel girders and the deck is considered by Abaqus automatically from their dimensions and from materials density.

4.3.2 Heat transfer model

In this study the one-dimensional heat transfer theory is applied. It is assumed that the composite is subjected to a one-sided heat flux that is applied uniformly over the surface.

For the heat transfer analysis all the features defined for the mechanical model are equal except for the type of elements used in the mesh, for material properties and for the load type that are described in following sections.

The fire load affects the bottom part of the structure that is exposed to a constant heat flux of 2400kW/m² heating the faces with temperature distribution shown in Table 22. Thus, the thermal boundary condition applied to the lower part of the bridge, is the adiabatic surface temperatures obtained with the FDS (see section 4.3.2.3). The model can consider any thermal boundary condition for the cold face.

Furthermore, the heat flux from a fire includes convection and radiation, which are described by the heat transfer coefficient (h_c) defined in the model as 35 W/m^{2}K and the emissivity coefficient (ε) equal to 0.7. These values correspond to a petrol fire according to EC-1 (CEN 2004) and EC-3 (CEN 2011b).

4.3.2.1 Mesh

During the heat transfer analysis response analysis, the FE mesh was kept the same as that used in the mechanical preceding (number of elements and nodes, division of each layer), but the stress elements were replaced with thermal elements, which were the eight-node linear heat transfer brick (DC3D8).

4.3.2.2 Thermal properties

Several thermophysical properties are required as input for the model. Thermophysical properties generally include thermal conductivity, specifc heat, thermal difusivity, etc. Thermal conductivity and specific heat capacity depend on temperature and the decomposition state of the material. At two material states, virgin material and decomposed material, GFRP and Balsa wood have different thermal properties. Thus, in the present model, thermal conductivity of the virgin composite (k_v) and char (k_{ch}) was defined, as well as the specifc heat (at constant pressure) of the virgin composite (c_{pv}) and char (c_{pch}).

Table 21 summarizes the thermal properties of the materials that were utilized in the FEM

Table 21. Thermal properties of the materials

Poperties	Asphalt Layer		Skin Layer			Core Layer			Steel Beams	
Thermal conductivity (W/mC)	1.35	[103]	T< 250ºC T >250ºC	$4.405*10^{-5}*T+0.312$ $2.83*10^{-4}*T+0.095$	[102]	T< 200ºC T >200ºC	$9.211*10^{-8}*T^{2.503}+0.06$ $2.223*10^{-6}*T^{1.89}+0.008$	[65]	EC3 Figure 66	[27]
Specific Heat (J/ kgK)	820	[103]	T< 250ºC T >250ºC	1080+0.0452*T 0.259*T+1041	[102]	T< 250ºC T >250ºC	1042+0.068*T 3194+1.33*T	[13]	EC3 Figure 66	[27]

The definition of theses two properties for the steel girders are shonw in Figure 66:

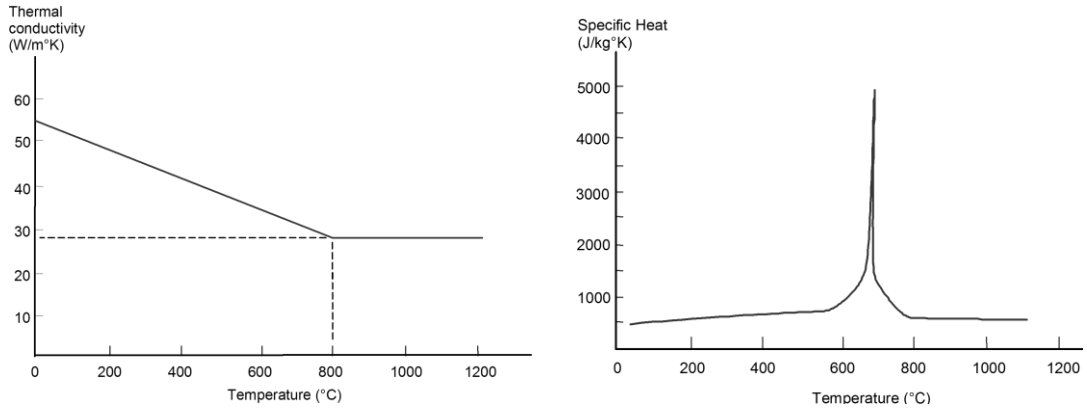

Figure 66. Eurocode 3 values for thermal conductivity and specific heat

4.3.2.3 Thermal loads

The thermal input used in the model was obatined from the Fire Dynamics Simulator (FDS) modelation developed by Peris-Sayol, G. (Peris-Sayol, 2013) in Polytechnic University of Valencia (UPV). The FDS model predicts numerically in a control volume fire engineering variables such as temperatures, heat fluxes or gas pressures involved in a fire event.

With the FDS were obtained the adiabatic surface temperatures (T_a); fictitious temperature obtained assuming that the structural element is a perfect insulator. Moreover, is an equivalent fire temperature when calculating the heat flux to an exposed temperature (Peris-Sayol, et al., 2015). This resource serves to transfer the results from the fire models to thermal or thermo-mechanical models.

The geometric model developed in FDS is shown in Figure 67. For this case of study, it has been chosen the worst possible fire scenario (tanker truck carrying gasoline) along with the least favourable location (mid-span of the bridge). The tanker truck was modelled as a horizontal surface of 25 m^2 (12 x 2.5m) at one meter above the road level. The heat release rate (HRR) was equal to 2400 kW/m^2, which is the HRR corresponding to a gasoline pool fire with a diameter exceeding 3 m.

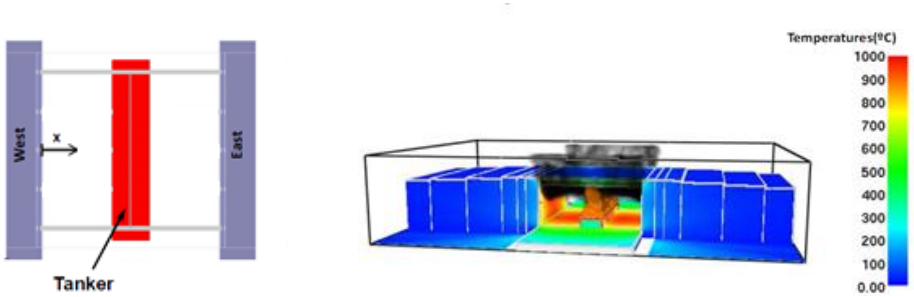

Figure 67. Images of FDS simulation

In this case, adiabatic temperatures vary along the axis of the bridge and also within the girder cross section. However, and given a certain cross section of the girder, all the points located in the same face of the girder (north, south or bottom face) have a very similar adiabatic temperature.

In order to simplify the calculation, the bridge has been divided in three diferent zones: two lateral zones of 3,91m and a central area of 3,68m. In each zone there are applied two different range of temperatures, one for bottom flange of the girders and one for the deck, web and upper flange of the beams.

In Table 22, and Figure 68 and 69 the distribution of temperatures incorporated to the thermal model are shonw.

Table 22. Temperature distribution along the structure

Zone 1			Zone 2			Zone 3		
Time	Temperature 1	Temperature 2	Time	Temperature 1	Temperature 2	Time	Temperature 1	Temperature 2
0	20.00	20.00	0	20.00	20.00	0	20.00	20.00
30	996.56	1150.92	30	1090.42	1234.34	30	1007.07	1154.57
3600	996.56	1150.92	3600	1090.42	1234.34	3600	1007.07	1154.57

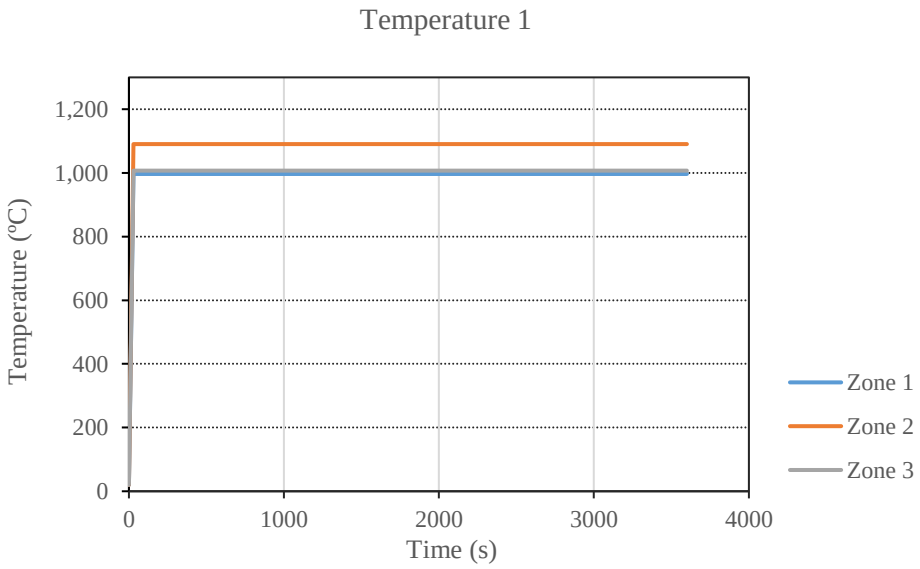

Figure 68. Graphic representation of temperature 1 input

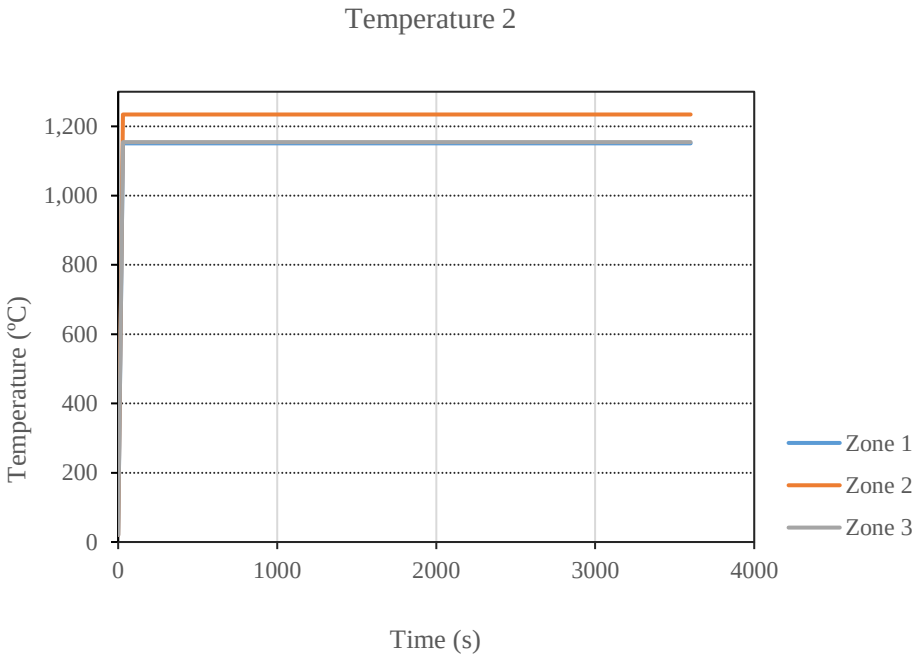

Figure 69. Graphic representation of temperature 2 input

As can be observed from the graphics and Table 22, web temperatures are higher than bottom flange temperatures. This phenomenon occurs in every case and is due to the accumulation of smoke in the space between the girders.

The surface temperature distribution obtained from the FDS simulation will be applied to the non-linear transient heat-transfer analyses.

4.3.3 Thermomechanical model

The response of the bridge is analysed using an uncoupled thermo-mechanical analysis. The model is used to predict the temperature rise, softening rate, failure time and failure mechanisms of the structure under loading and fire. This calculation involves thermal and mechanical analysis of the steel beams and the composite deck.

Thermal analysis, which is the first step in the model, calculates the temperature profile through-the-thickness of the girders and of the sandwich composite when heated from the below part of the structure. The heat transfer method provides the transient nodal temperatures with respect to time using the thermal properties of the material. The thermal model is further described in Section 4.3.2.

In the second analytical step, the nodal temperatures are read from the thermal analysis and corresponding temperature dependent mechanical material properties are used to find the equilibrium of the structure. The mechanical model is out-lined in Section 4.3.1.

Mechanical models are used to calculate reductions of the tensile stiffness and strength due to heat transfer from the lower part of the bridge to the upper (colder) part. By calculating the residual tensile stiffness and strength at critical locations of the structure, it is possible to calculate the residual tensile properties and predict the failure mechanism.

This analysis will give fire protection engineers or structural engineers, critical information related to structural integrity and fire resistance, such as: deflection and strain as a function of time, residual stiffness and strength of the structure, stability and integrity of the structure, and time-to-failure estimation of the structure.

4.3.3.1 Failure Criteria

Fire resistance describes the ability of a material or structure to restrict the spread of fire and to retain mechanical and physical integrity. In this study, the following three criteria were used to assess fire resistance of the composite bridge. The temperature limit criterion measures the thermal insulation of the materials and the stress and deflection criteria measure its ability to resist collapse.

Temperature limit

In this study fire resistance is defined as the time taken for the unexposed surface temperature of one layer to reach the decomposition temperature, at which point load bearing capacity of the material is very low.

Stresses criterion

The FE model was assumed to have failed when the stresses in the materials reached the ultimate stress value. Stresses checked were: Von Misses stresses and stresses in the x direction of the main girder, since is the most critical point.

Von Misses stress criteria considers all the principal stresses that act in all directions on a 3D-body when loaded and gives it as an equivalent stress. Von Misses stress is then compared with the yield stress of the material to see if the material will yield.

On the other hand, when ultimate strain is reached, it can be identified as a rapid increment of the maximum vertical deflection, as a movement of roller support towards the centre of span or as instability due to either lateral or web buckling.

Deflection limit

The structure is assumed to fail when it becomes unstable based on a drastic increase in the rate of vertical deflections or an inward movement of the roller support towards the centre of the span.

5. RESULTS AND DISCUSSION

5.1 Mechanical behaviour

5.1.1 Deflection

In the serviceability limit state the local and global deflection of the structure is the design criteria. The structure needs to fulfil the limit of l/500 (SIA 260) where l is the length of the section being studied. Conditions in SLS are satisfied as long as the deflection is under the limit.

The maximum global deflection and deflection in the two girders and the deck were obtained. The values for each deflection are compared for the model and the allowed limit at that section. The maximum deflection was located on one edge of the deck, where the largest wheel load and the largest uniformly distributed load is located, see Figure 70.

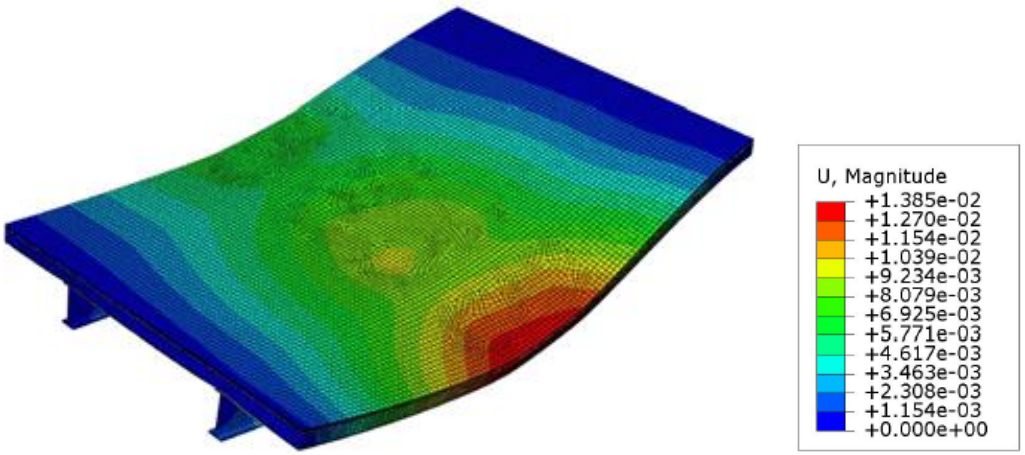

Figure 70. Deflection contour of the composite bridge

From the Figure 71 it can be stated that longitudinal deflection in the most loaded edge of the deck is almost the double of the value of that in the middle span. This can be explained for the overhang of 1.80 m, if the girder were situated closer to the edge, the maximum deflection would be in middle span. Similar results were observed by Osei-Antwei, M. in his study.

In adittion, as can be seen in the figure the maxiimum deflection does not take place in the middle of the span but are displaced towards the roller support. If the boundry conditions were simetric (two fixed supports, two rollers…) The maximum deflection would take place at mid-sapn.

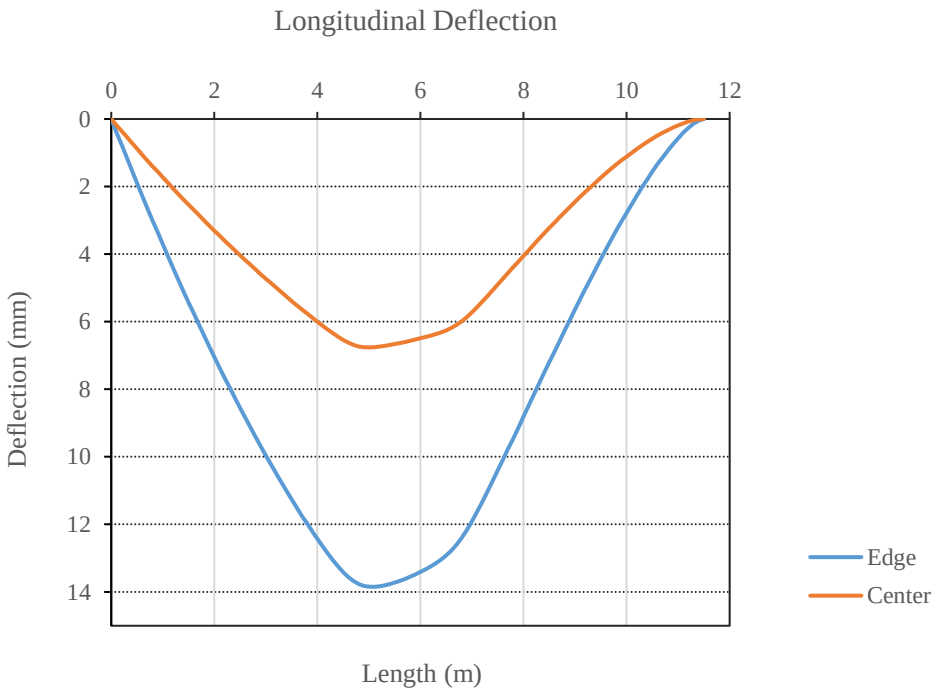

Figure 71. Longitudinal deflection of the deck

Regarding to the transversal deflection of the deck, in Figure 73 is plotted the values for the section where the global deflection is maximum. The deflection in the weakest edge is more than the double of the other edge however this is not a limitant factor since both values amply fulfill the deflection limit.

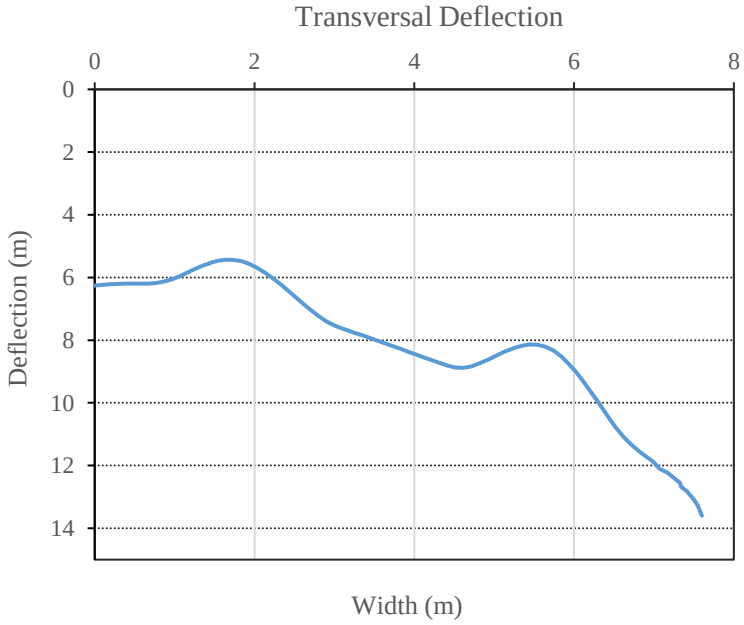

Figure 72. Transversal deflection of the deck

In Figure 73 the deflection values of the two steel girders are plotted. As could be spected the deflection in beam 1 is higher than the deflection in the other beam. This deflection is in consordance with the deformations in the bridge deck.

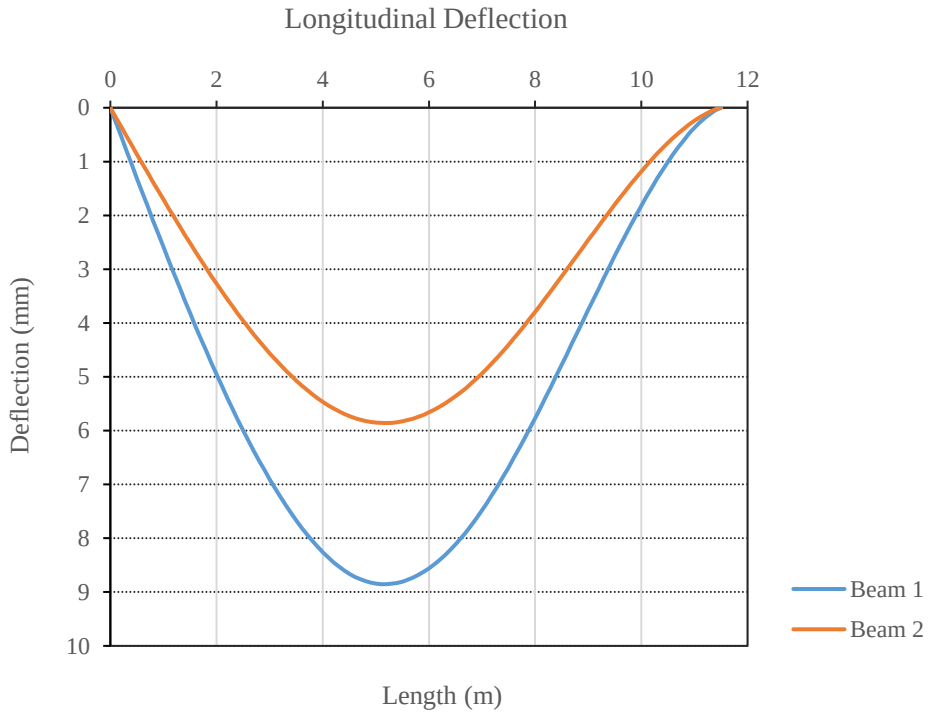

Figure 73. Longitudinal deflection of the girders

Figure N show the location of the maximum deflections on the girders and on the deck. In order to appreciate the deformations, the deflections has been augmented with multiplier factor of 100.

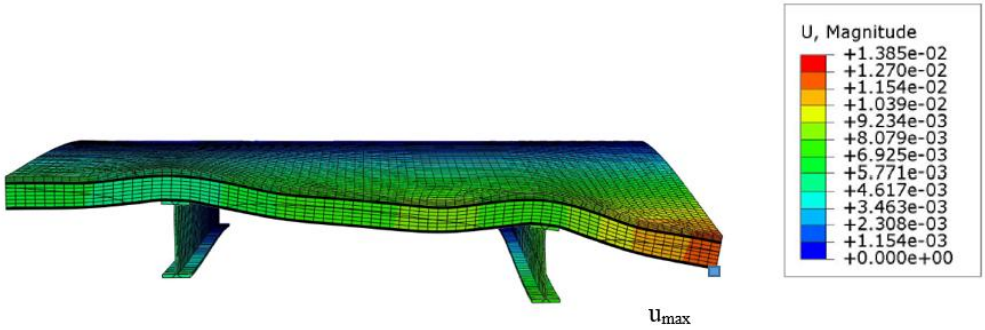

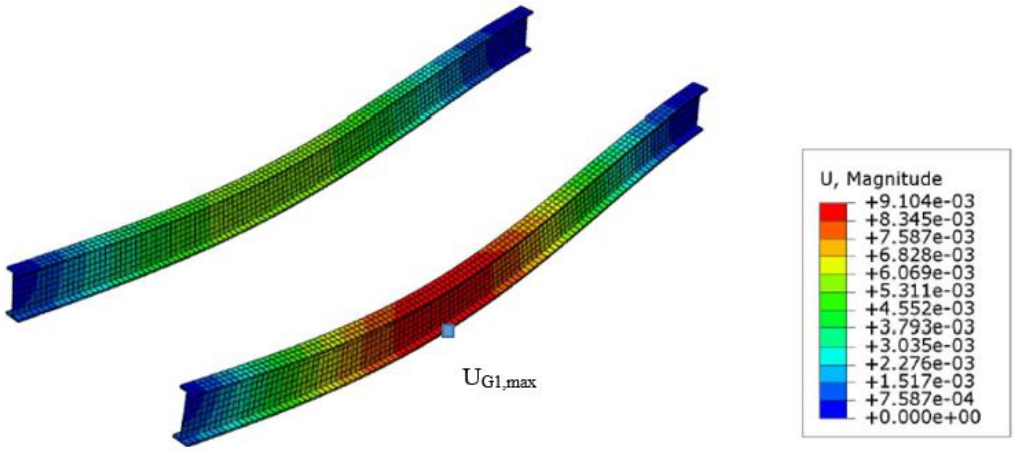

Figure 74. Illustration of the maximum deflection u_{max} at the deck and maximum deflection in girder 1, u_g

By last Table 23 gives the deflection values for the longitudinal and transversal deflection for the deck and the deflection values for each beam.

Table 23. Deflection values

Deflection (mm)			
Deck			
Longitudinal	Middle span	$U_{L,m}$	6,76
	Edge	u_{max}	13,8
Transversal (x= 5.1 m)		$U_{T,max}$	13,8
		$U_{T,min}$	6,26
Girders			
Longitudinal	Beam 1	$U_{G1,max}$	9.1
	Beam 2	$U_{G2,max}$	5.86

5.1.2 Stresses

The stresses were obtained from the load case in which all the loads described in section 4.3.1.4 are acting simultaneously. In Figure 75, it has been plotted the normal stress values of the two beams. It is verify that the higher stress value is consistent with boundary conditions implemented in the model, that is to say, that the stresses are the highest in the fixed support and zero in the roller.

Furthermore, the stresses are also in accordance with the loas case since the stresses are higher in the more loaded beam. Moreover, the more stressed beam is also the beam in which the deflections are higher.

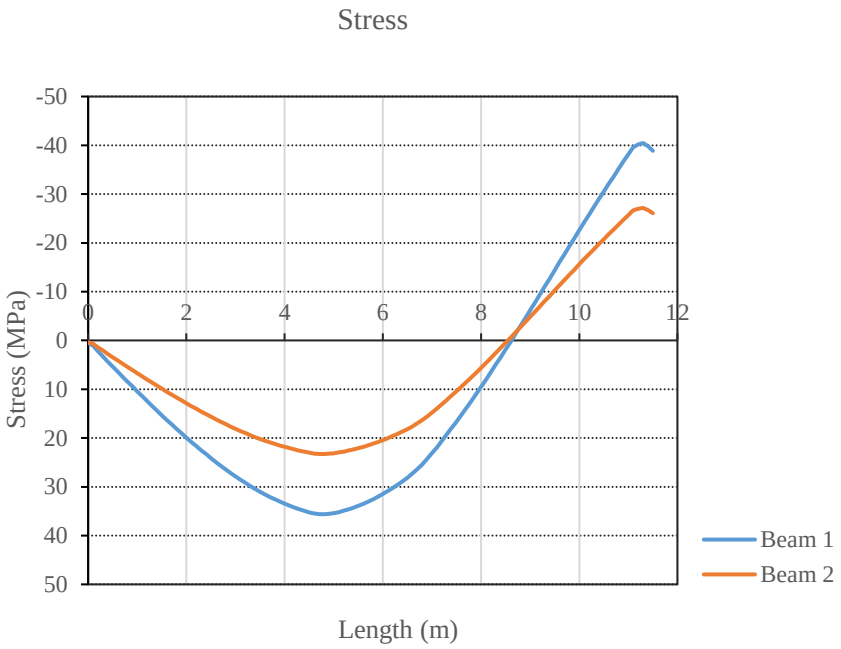

Figure 75. Normal stresses in the girders

In Figure 76 shows an image of the two beams with the values of the normal stresses along with its values.

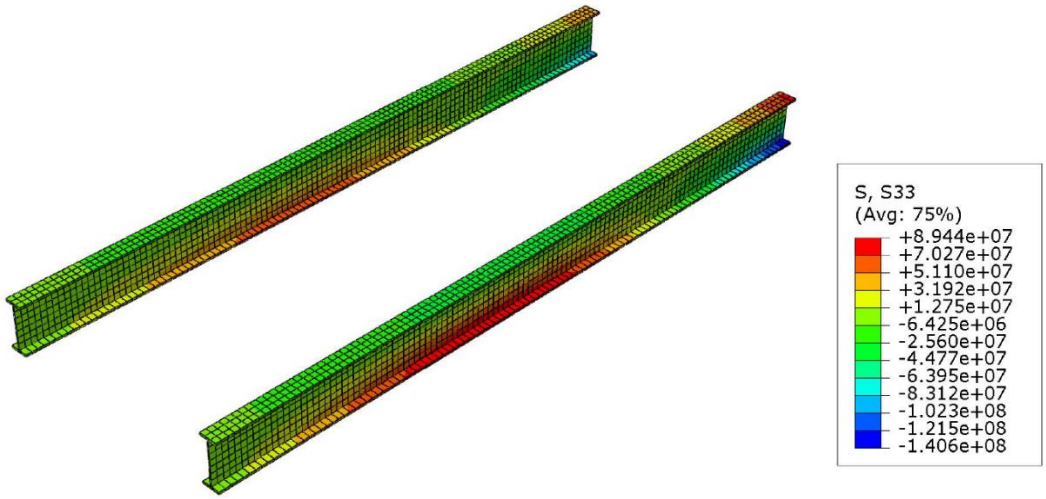

Figure 76. Normal stress contour

In Table 24 can be observed the longitudinal stress value and Von Mises value for Beam 1, since is where the maximum stress take place.

Table 24. Stress values

Stresses σ (MPa)	
σ_{xx}	89,4
	-146
Von Mises	131,7

From the values of the above table, it can be observed that the maximum stresses are well below the yield stress of the steel grade used for the girders (355 MPa), therefore yielding conditions are not reached and the bridge model have enough capacity to carry the loads. In table N values for the longitudinal.

5.2 Thermal behaviour

The results of the thermal response of the GFRP/Balsa composite sandwich deck is analyse in this section. The study of its behaviour is done exclusively under the thermal load applied in the below part of the structure; a gasoline tunker trunk realeasing a heat rate of 2400 kW/m^2.

In this study, one hour time for the analysis of the evolution of temperatures has been set. The reason for this limit is that it has been consider time enough for firefighting response.

Figure 77 shows the temperature contour of the bridge at final step of the analysis. By this time, both, the steel girders and the bottom surface of the deck, have reached the maximum temperature incorporated to the model.

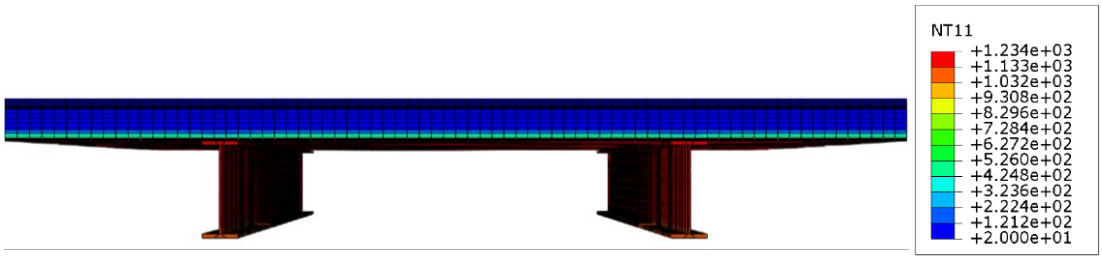

Figure 77. Temperature contour of the bridge

In Figure 78 it can be seen the distribution of temperatures in time for the bottom surface of the deck. It is appreciated how during the first 30 seconds, the surface reaches almost 200 ºC and from this time to the first minute the temperature increases fivefold. From this graphic it can also be notice the insulating effect of the girders. However, by the end of the analysis the contact surface girder-GFRP reaches almost the maximum temperature.

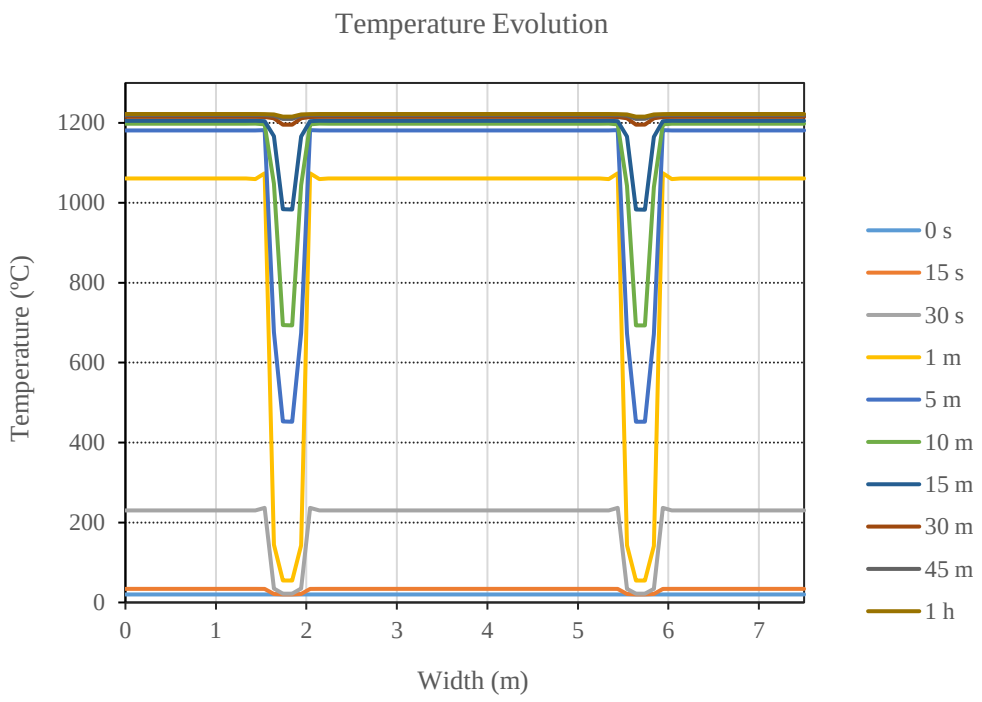

Figure 78. Temperatures evolution along the transversal span

As a result of the differential distribution of temperatures in this GFRP layer, the temperature profile through-the-thickness of the deck is analysed in two locations: in the centre of the bridge at middle span and at the centre of the contact are girder-GFRP. In Figure 79 a detailed imagee of the distribution of the temperatures is shonw.

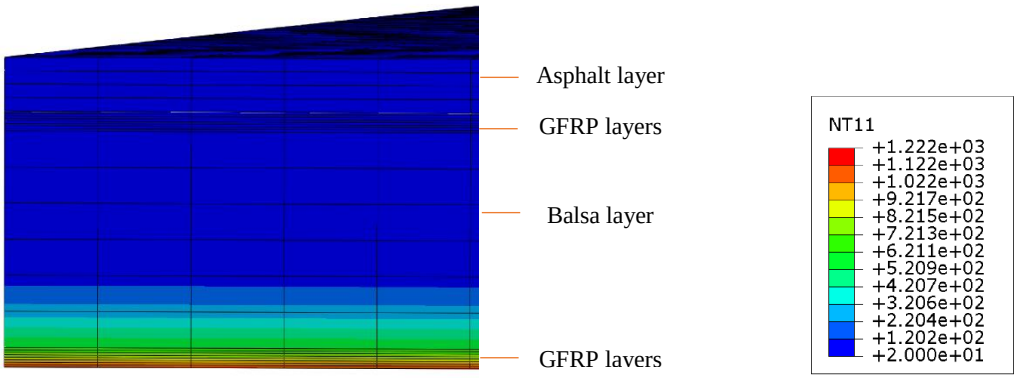

Figure 79. Detail of the temperature contour of the deck

Figure 80 plots the temperatures evolution in time at the centre of the deck. As can be seen, only the 10 first centimetres of the deck are affected by a notable change in temperature. From the first 15 centimetres the temperature of the materials is the ambient temperature established in the model (20º), the upper part of the bridge is completely isolated from the fire action. This effect can be explained for the char layer developed by balsa wood core that acts as an insulating layer, further damage to the core and upper layers is limited.

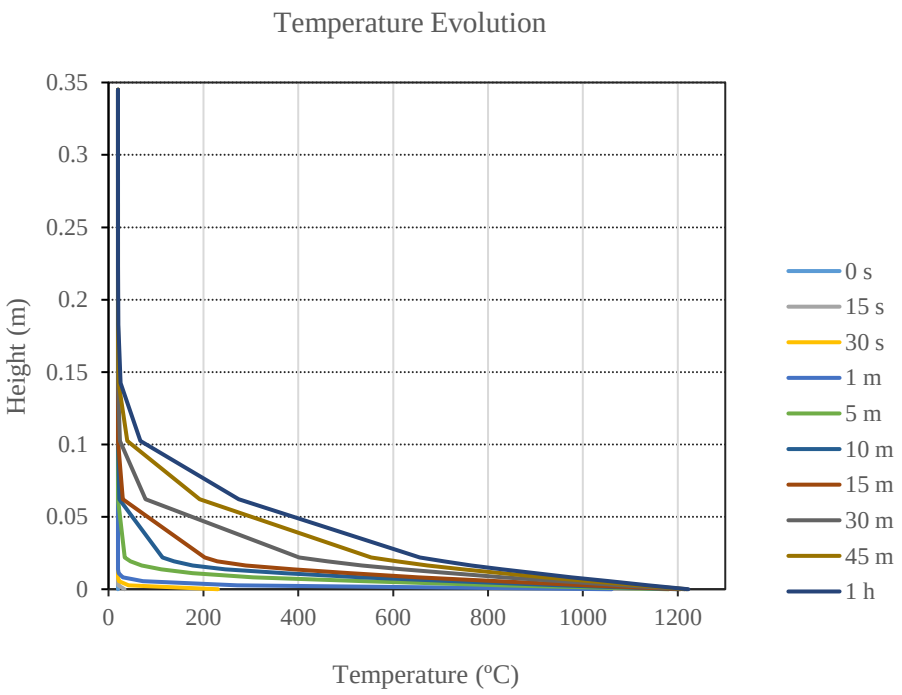

Figure 80. Temperatures evolution through-the-thickness of the deck (middle span)

In Figure 81 the insulating effect of bala wood takes place in addition to the fact that fire high temperatures do not affect directly the surface on the composite. Therefore the temperatures are lower than in the center zone as can be observed.

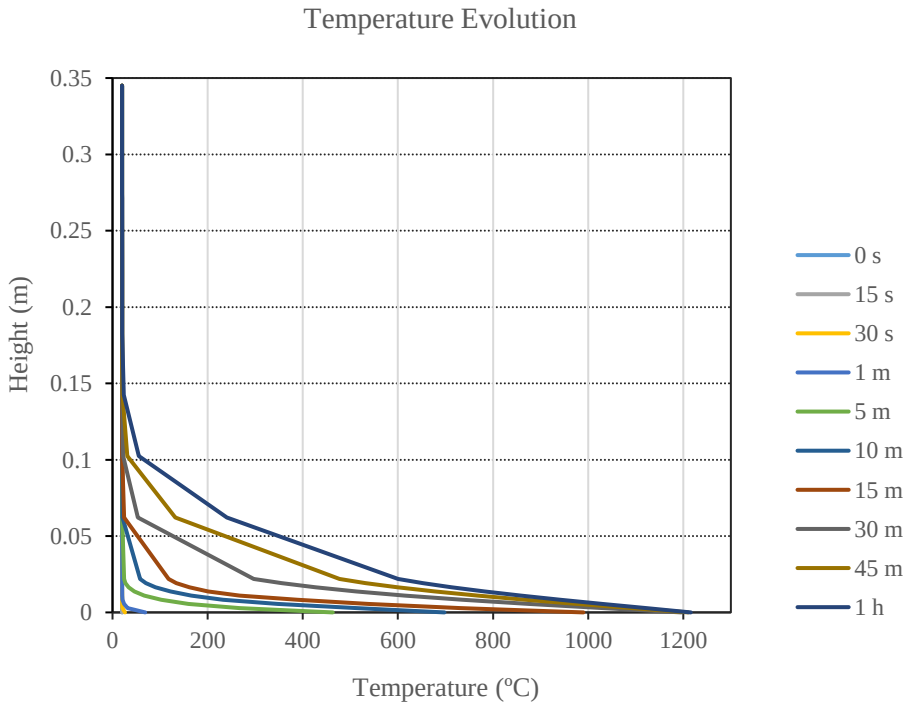

Figure 81. Temperatures evolution through-the-thickness of the deck (interface GFRP-deck)

Figure 82 displays the temperatures along the length of one beam at the last step time, the values of temperatures in both girders are equal due to the centred position of the fire below the structure. There is not a large variation of the temperatures along the bridge length, in fact, it can be clearly appreciated 3 different areas coinciding with the three different temperature zones defined in the model. In an hour, the maximum temperature is achieved.

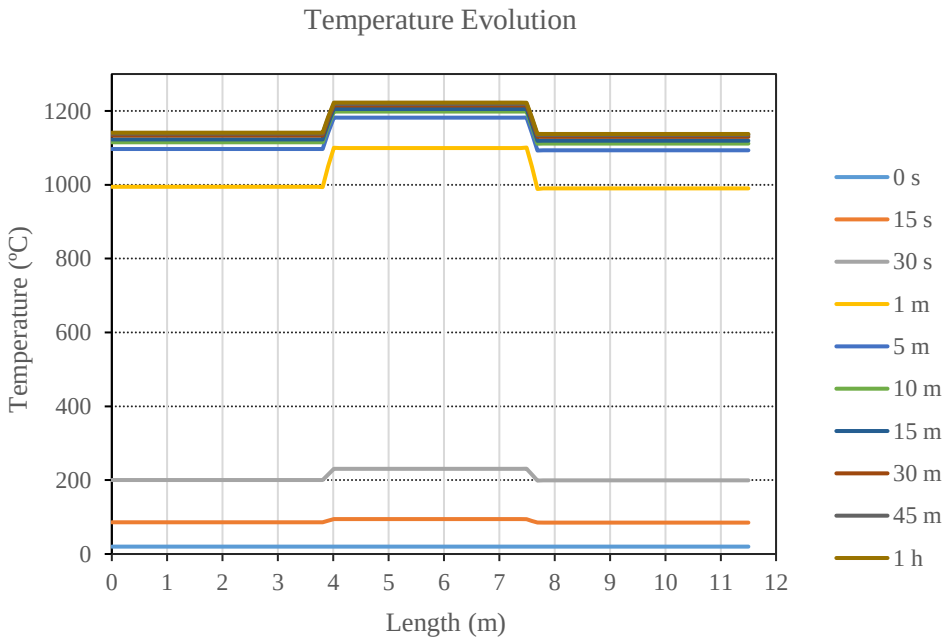

Figure 82. Temperatures evolution along the girders

From Figure 83 it is clear that a non linear thermal gradient exists in the beams which causes mechanical strains (and therefore stresses) even if the structure is statically determinate and no gravity load is applied. In this figure is shonw the evolution along time of the temperature at middle span (section where temperatures were maximal). Moreover, it can be seen that the distribution of temperature in the cross section varies in height, the maximum temperature is located in the middle region of the web and it is significantly higher than those in the flanges. In addition, the upper flange always has temperatures below the lower flange as a result of the exposition to lower temperatures but also the high thermal inertia of the concrete slab.

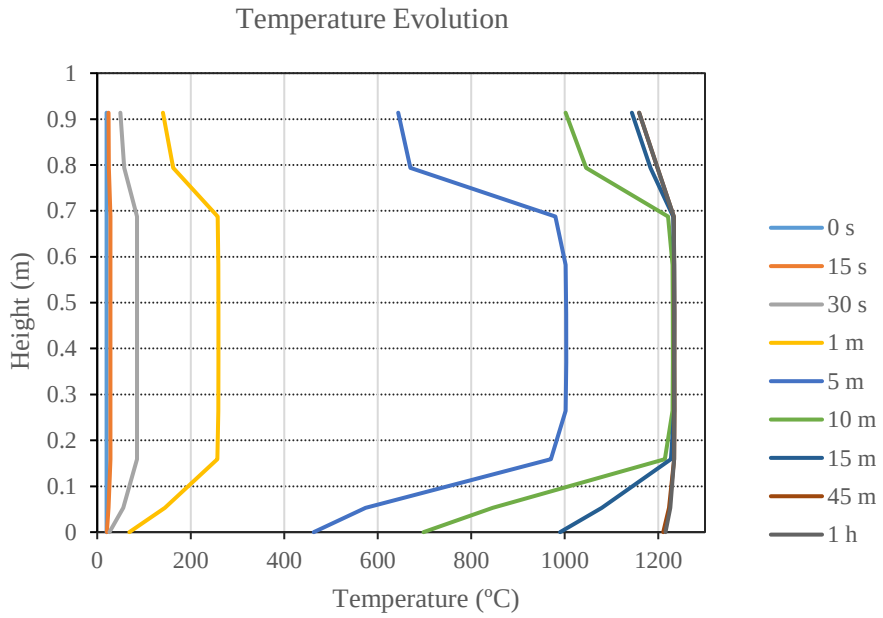

Figure 83. Temperature evolution in the cross section of the girder

On the other hand, the structure is supposed to act as a composite bridge, both elements, the steel girders and the composite slab work together to sustain the loads acting on the bridge. However, temperatures caused by the fire can deteriorate the adhesive bonded connexion between them and reduce the load bearing capacity of the structure. Figure 84 shows that soon after reaching 5 minutes of fire action, the temperatures in the interface between the steel girder and the deck are higher than 500ºC, temperature above the decomposition temperature for the majority of resins. This phenomenon is not part of the scope of this study, however it should be emphasized the importance of the failure of this connexion.

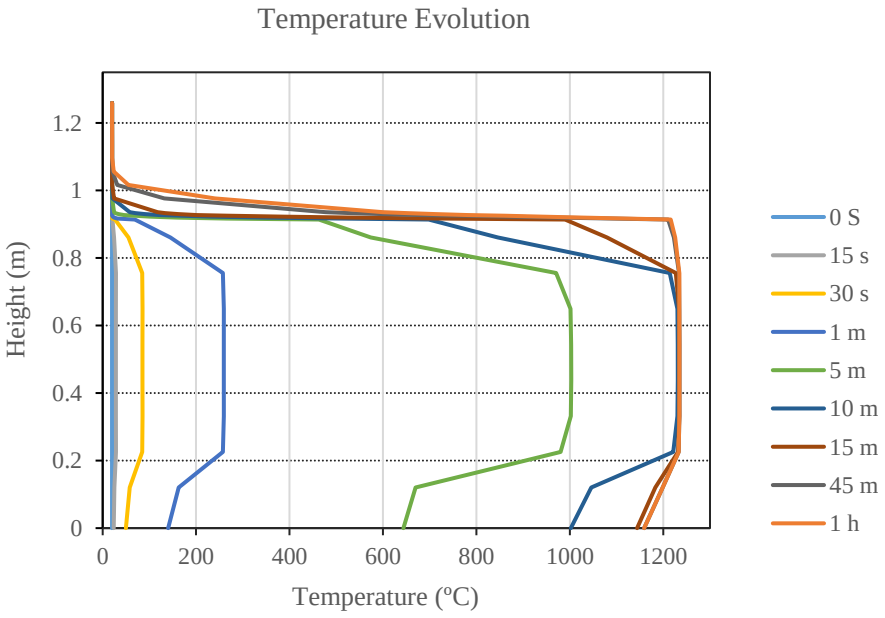

Figure 84. Temperature evolution of the deck and the girder

5.3 Thermomechanical behaviour

The objective of the thermo-structural model is to determine the failure load at each time step. The mechanical response of the composite bridge in the combined thermal and mechanical loading can be assessed.

In first place, the results of the vertical displacement are presented and discussed. In Figure 85 it is shown the deflection contour for the structure at the moment of failure along with their corresponding values. From this figure it is observed that the maximum value in the deck is located arround the mid-span, where the the temperature is hihger, but slighly diverted to where the higher axle traffic load is located.

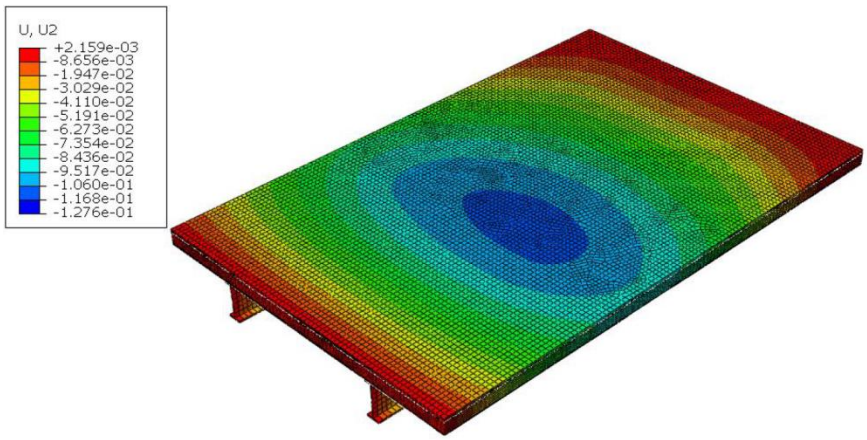

Figure 85. Global deformation contour

If this image is compared with Figure 86, the one showing the defletion contour but only for the mechanical analaysis, it is clear how the temperature increase affects the location of the critical point, from the edge of the deck to the centre.

Table 25. Deflection thermo-mechanical values

Deflection (mm)		
	Gravity loads	Gravity + thermal loads
Middle span	6,76	103
Edge	13,8	95

In order to understand how the rise in temperature affects deformation, in Figure 86 is plotted the deflection-in-time for the Girder 1, since is where the maximum values take place. It is clear that as the temperature increases so does the vertical deformation.

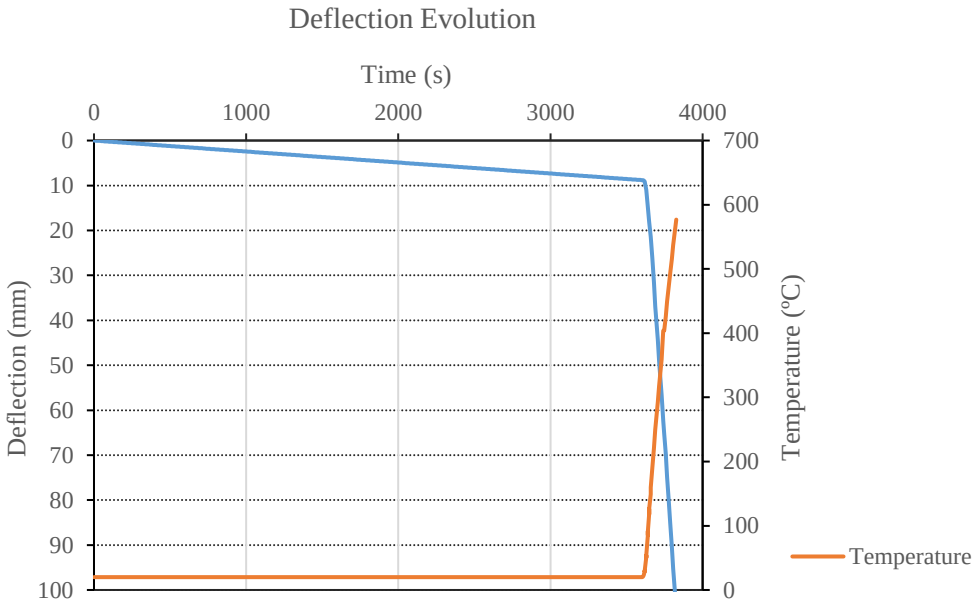

Figure 86. Deflection evolution in time for girder 1

Table 26 shows the maximum values of deflection for the deck and for Girder 1 at the time of failure. The deformations are consistent with the type of constraint implemented in the model; the deflection in the upper flang of the girder is equal to the deformation in the deck, however, the deformation in the lower flang of the beam is higher that the one in the deck due to the deformation ability of the steel material.

Table 26. Deflection values at failure time.

Deflection (mm)	
Deck	103
Girder 1	127

Regarding the stresses, yielding conditions in the critical point of Girder 1, located in the web at mid span, is reached in the first 66 seconds once the fire is started as it is desplayed in Figure 87. However, the structural model used considers load redistributions, so it is not until second 240 when the failure of the bridge takes place.

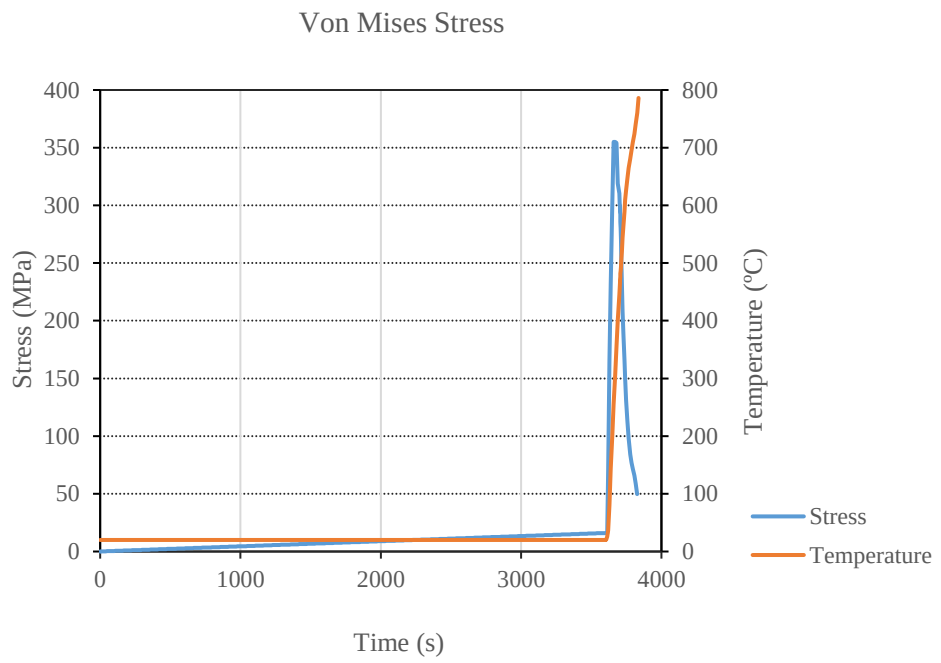

Figure 87. Von Mises stress in temperature for Girder 1

As can be observed in Figure 88, actually, there are to critical points that are plasticized almost at the same time, second 66 and 67, at different locations of the same girder for different conditions. One point is located in the web of the beam at mid-span and the other is located at the fixed edge. The first point reaches its plastification at the same time due to the deterioration of the material in higher temperatures while the point at the edge is the one that is carring more stress during all the analysis.

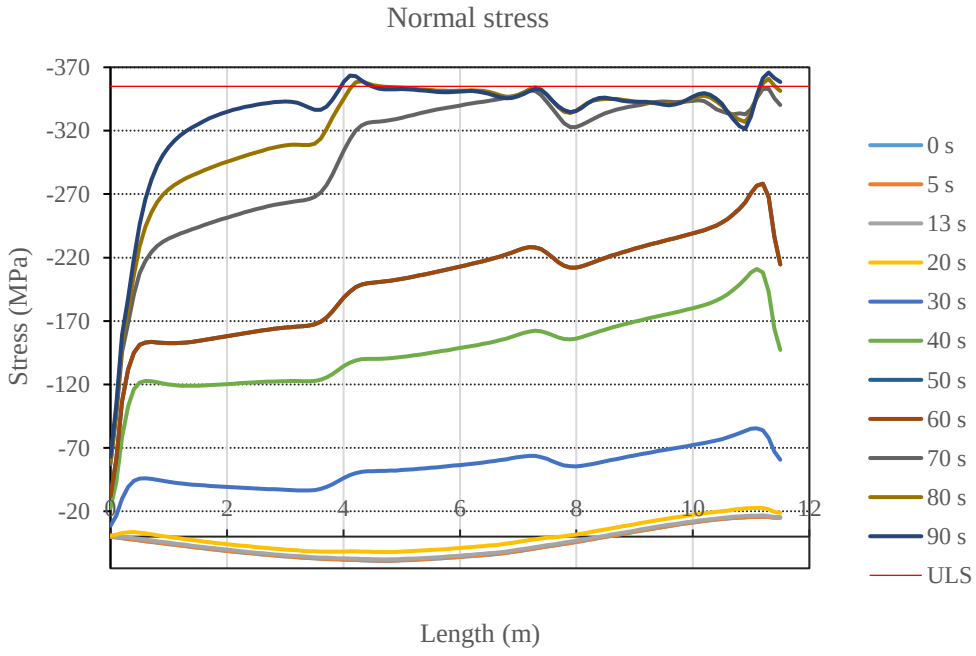

Figure 88. Normal stress evolution in time for Girder 1

Furthermore, the stresses caused the out-of-plane displacement of the web as is observed in Figure 89.

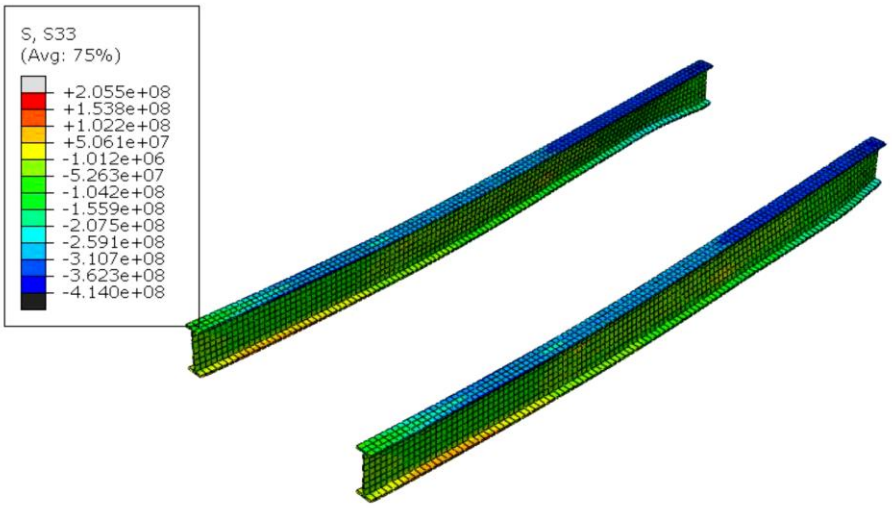

Figure 89. Temperatures distribution through-the-thickness of the deck

Finally, in order to asses what causes the final failure of the structure the three failure criteria are compared. In first place all the results are shonw and later are contrasted and analyced.

Figure 90 shows deflection values in time for Girder 1 and Figure 91 shows these values but for the deck.

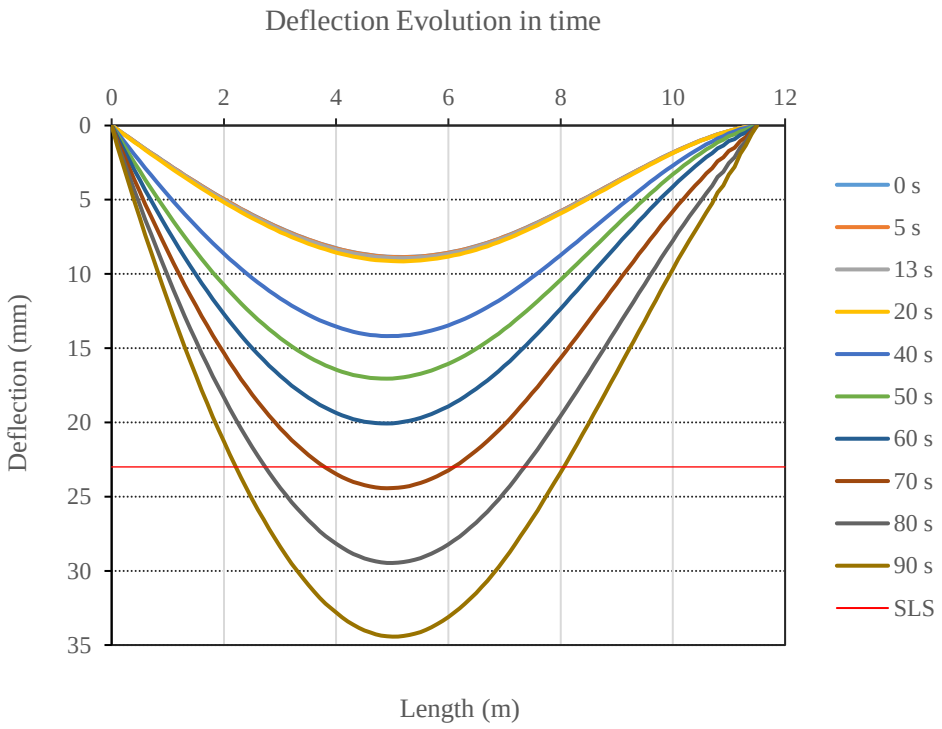

Figure 90. Deflection evolution in time for the girder

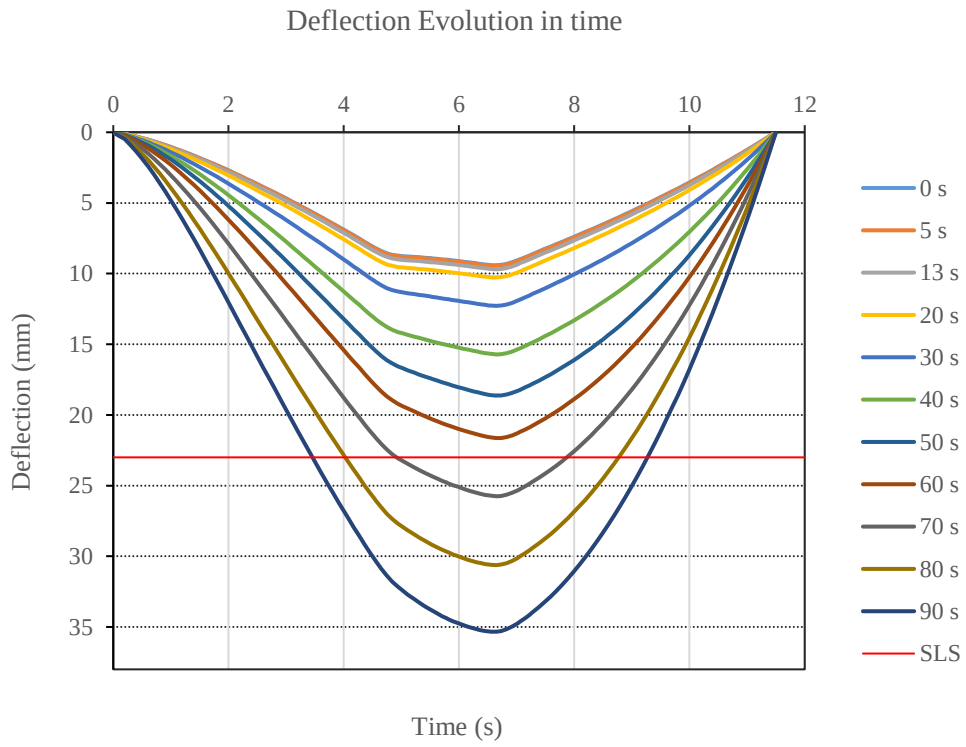

Figure 91. Deflection evolution in time for the deck

Next, for Girder 1, Von Mises stresses are displayed in Figure 92. These values are obtained for the mid web of the beam since is the weakest part.

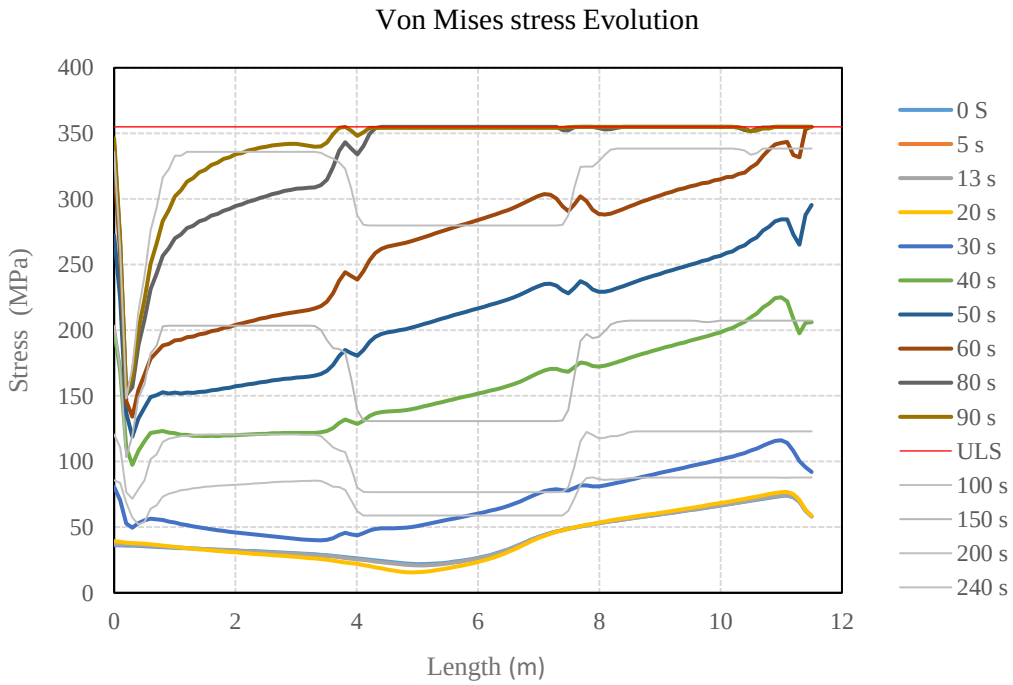

Figure 92. Von Mises stresses for Girder 1

Moreover, it has been asses the temperature distribution through-the-thickness of the deck but at the time of failure of the structure, since from the thermal analysis it was observed that this criteria was not the most limiting one.

What can be observed is that only the first layer of GFRP is completely degraded and only the first 7 cm of th deck have increased their temperature.

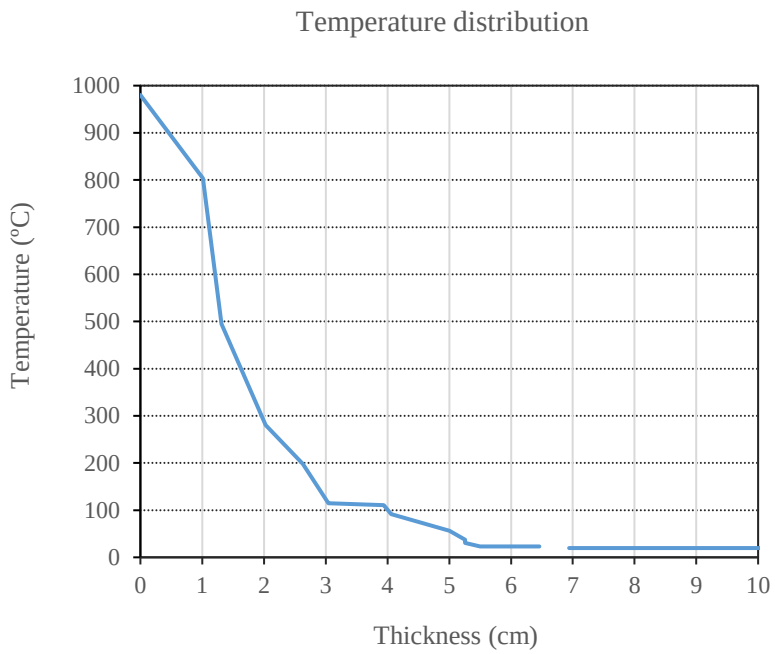

Figure 93. Temperatures distribution through-the-thickness of the deck at failure time

The failure of the bridge occurs at second 240 once the fire is ignited. The reason of the breakdown of the structure is the failure of the girders. However the SLS is reached in the first minute almost at the same time that the first point of the beam reaches its yielding conditions. Therefore the failure criteria that is reached in the first place is the deflection limit.

6. CONCLUSIONS AND FURUTE WORK

6.1 Conclusions

The behaviour composite bridges at high temperatures are currently a major concern due to the rise in number of fire events and the corresponding social and economic consequences. However, there are very few studies on this topic and, in addition, experimental studies are difficult to conduct due to the large dimensions that bridge elements and the fire loads required. Therefore, it is of major importance to develop numerical models to characterize composite bridges fire response and, on the other hand, check its response with data coming from real fire events.

Based on the foregoing, this research is focused on the analysis of the thermal and thermo-mechanical responses of composite sandwich decks exposed to high temperatures. For this purpose, a numerical model has been developed using as a case of study the Avançon Bridge (Switzerland).

A thorough bibliographical study provided the information needed about the time dependent characteristics of the materials based on experimental results conducted by other authors. Moreover, this research helped to determine the best approach to study and to model the behaviour of the structure.

Results of the study show that:

- The time to failure of the bridge exposed to a hydrocarbon fire being fully loaded was less than 5 minutes (240 seconds), not even close to the necessary time to fire fighter response or for evacuating people.
- It may be necessary to use a fire retardant or a flame retardant matrix since the GFRP layer exposed directly to fire, at failure time, was already decomposed.
- It is necessary to use passive fire protection in the girders in order to insulate steel from the effects of the high temperatures, namely sprays, boards, intumescent coatings.
- The position of the fire load and the possible existence of the spill are essential variable in the characterization and location of the critical point in the more thermally heated beam.
- The fixed support generates high stress concentration, if the introduced compression (restriction of longitudinal movements) is too high it will cause the mobilization of buckling mechanisms and lateral buckling.

- The connection between the steels girders and the composite deck must be studied in depth since the temperature reached in the interface is higher than 500 ºC in the first 5 minutes which is a critical factor when considering bonded connections.

Finally, the numerical model proposed in this paper can be used to perform an engineering analysis of a bridge damaged by a fire and to study how bridge performance in fire events can be improved. Additionally, and if complementary experimental research and extensive parametric studies are carried out, this numerical model can be used to develop simpler design methodologies to assess the effects of fire on composite bridges.

6.2 Future work

Sandwich panels are a relatively new material in construction industry therefore the research field of this type of material, particularly for fire, is wide and full of uncertainties. Hence, many aspects have to be further studied in order to contribute to a better understanding of the behaviour of the composite bridges in fire. In this chapter some suggestions that may be investigated in future developments are indicated:

- Development of an analytical model that includes some type of fire protection in order to compare and test if the thermomechanical response of the bridge is improved.
- To model the bonded connection between the girders and the deck and to assess its behaviour in high temperatures
- To discretize the bridge in smaller sections when importing fire curves
- Study and development of models capable of taking into account the influence of an adjacent span or abutment since fire sometimes induces longitudinal movements higher than the width of the expansion joint
- Analyse the influence of the location of fire and its load (heat release).
- The need to incorporate in standards tools and simplified models that enable bridge design with an approach similar to that used in building design.

BIBLIOGRAPHY

[1] Britannica Academic, 2010. *Encyclopædia Britannica Online.* [Online] Available at: http://www.britannica.com/bcom/eb/article/5/0,5716,119325+2,00.html [Accessed 11 June 2016].

[2] Transportation research board of the national acedemies, 2006. *Field Inspection of In-service FRP Bridge Decks, N 564,* Washington, D.C.: American Association of State Highway and transportation Off.

[3] Alos-Moya, J. et al., 2014. Analysis of a bridge failure due to fire using computational fluid dynamics and finite element models. *Engineering Structures,* Issue 68, p. 96–110.

[4] Anjang, A. et al., 2014. Tension modelling and testing of sandwich composites in fire. *Composites Structures,* 1(13), p. 437–445.

[5] Avó de Almeida, M. I., 2009. *Structural behaviour of composite sandwich panels for applications in the construction industry,* Lisbon, Portugal: Technical University of Lisbon.

[6] Bai, Y., 2009. *Material and Structural Performance of Fiber-Reinforced Polymer Composites at Elevated and High Temperatures,* Suisse: s.n.

[7] Battles, E. P., Dagher, H. J. & Abdel-Magid3, a. B., 2000. Durability of Wood-FRP Composite Bridges. *Advanced Technology in Structural Engineering.*

[8] Birman, V., Kardomateas, G., Simitses, G. & Lib, R., 2006. Response of a sandwich panel subject to fire or elevated temperature on one of the surfaces. *Composites: Part A,* Issue 37, p. 981–988.

[9] Casas Rius, J., 2011. *Use of Fibre Reinforced Polymer Composites in Bridge Construction. State of the Art in Hybrid and All-Composite Structures.,* Barcelona: Universitat Politècnica de Cataluña.

[10] Chandler, R., 2009. *Fire investigation.* USA: Delmar Cengage Learning.

[11] Cheng, L. & Karbhari, V. M., 2006. New bridge systems using FRP composites and concrete: A state-of-the-art review. *New Materials in Construction,* Issue 8, p. 143–154.

[12] Chen, L. D. & Zhao, L., 2014. Deck Panels and Griders for bridbe Applications. In: M. Zoghi, ed. *The International Handbook of FRP Composites in Civil Engineering.* s.l.:CRC Press, pp. 155-167.

[13] Cholewa, N., 2015. *Debond Buckling of Woven E-Glass/Balsa Sandwich Composites Exposed to One-Sided Heating,* Blacksburg, VA: Virginia Polytechnic Institute.

[14] CIB Report, 2000. *European Recommendations for Sandwich Panels. Part 1: Desing.* s.l.:Joint Committee. European Convention for Constructional Steelwork and International Council for Research and Innovation in Building and Construction.

[15] Código Técnico de la Edificación de España (CTE), 2010. *Comportamiento frente al fuego,* Madrid, Spain: CTE.

[16] Correia, J. R., 2015. Fibre-Reinforced Polymer (FRP) Composites. In: F. Margarido & M. C. Gonçalves, eds. *Materials for Construction and Civil Engineering: Science, Processing, and Design.* s.l.:Springer, pp. 501-556.

[17] Cote, A. E. & Bugbee, P., 1988. *Principles of fire protection.* USA: NFPA.

[18] Da Silva, A. & Kyriakides, S., 2007. Compressive response and failure of balsa wood. *International Journal of Solids and Structures,* Issue 44, p. 8685–8717.

[19]Davalos, J. F., Qiao, P. & Shan, L., 2006. Advanced fiber-reinforced polymer (FRP) structural composites for use in civil engineering. In: H. C. Wu, ed. *Advanced civil infrastructure materials.* s.l.:Woodhead Publishing Limited.

[20]Dehghan-Manshadi, B., 2011. *Biaxial Wrinkling of Thin-Walled GFRP Webs in Cell-Core Sandwiches,* Lausanne: École Polytechnique Fédérale de Lausanne.

[21]Deng, L., Wang, W. & Yu, Y., 2015. State-of-art Review on the Causes and Mechanisms of Brigge Collapse. *Journal of Performance of Constructed,* Issue 13.

[22]Dimitrienko, Y. I., 1997. Thermomechanical behaviour of composite materials and structures under high temperatures: I. Materials. *Composites Part A,* Issue 28, pp. 453-461.

[23]Easby, R. C., 2007. *Fire Behaviour of Pultruded Composites,* Newcastle: University of Newcastle.

[24]European Committee for Standardization (CEN), 2000. *EN 1363-2: 1999, Fire resistance tests. Alternative and additional procedures.*, Brussels, Belgium: CEN.

[25]European Committee for Standardization (CEN), 2002. *EN 1991-1-2: 2002. Eurocode 1: Actions on Structures. Part 1.2 General Action—Action on Structures Exposed to Fire,* Brussels, Belgium: CEN.

[26]European Committee for Standardization (CEN), 2002. *EN 13501-1: Fire Classification of Construction Products and Building Elemnets,* Brussels, Belgium: CEN.

[27]European Committee for Standardization, 2008. *Design guide Single-Storey Steel Buildings; Part 7: Fire Engineering,* Brussels, Belgium: CEN.

[28]Feih, S., Mathys, Z., Gibson, A. & Moritz, A., 2010. Modeling Compressive Skin Failure of Sandwich Composites in Fire. *Journal of Fire Sciences,* Issue 28, pp. 141-160.

[29]Feih, S., Mouritz, A., Mathys, Z. & Gibson, A., 2007. Tensile Strength Modelling of Glass Fibre- Polymer Composites in fire. *Journal of Composite Materials,* 41(19), pp. 2387-2410.

[30]Fire Safety Technical Guide, 2015. *USER GUIDE TO THE CLASSIFIC User guide to the classification of fires for extinguishing purposes,* U.K.: UCL Fire Technical Note - TN024.

[31]Florio, J., Henderson, J., Test, F. & Hariharan, R., 1991. Measurement of the thermochemical expansion of porous. *International Journal of Heat & Mass Transfer,* 135-147(34).

[32]Forestry Commission of New South Wales, 1991. Seasoning of Timber.

[33]Garlock, M., Paya-Forteza, I., Venkatesh, K. & Gu, L., 2012. Fire hazard in bridges: Review, ssessment and repair strategies. *Engineering Structures,* Issue 35, pp. 89-98.

[34]Gibson, A., Browne, T., Feih, S. & Mouritz, A., 2012. Modeling composite high temperature behavior and fire response under load. *Journal of Composite Materials,* 16(46), p. v.

[35]Gibson, A. G., 2003. *The cost effective use of fibre reinforced composites offshore,* Newcastle: s.n.

[36]Gibson, A. G., Feih, S. & Mouritz, A. P., 2011. Developments in Characterising the Structural Behaviour of Composites in Fire. In: L. Nicolas, M. Meo & E. Milella, eds. *Composite Materials: A vision for the future.* s.l.:Springer, pp. 187-218.

[37]Gibson, A. G., Wright, P. N. H., W. Y.-S. & Evans, J. T., 2004. *Laminate Theory Analysis of Composites under Load in Fire.* Long Beach, CA (USA), Proceedings of the International SAMPE Symposium.

[38]Gibson, A. et al., 2003. *Validation of the Gibson model for the fire reaction properties of fibre-polymer composites.* Newcastle, s.n.

[39]Gibson, A. et al., 1995. A model for the thermal performance of thick composite laminates in hydrocarbon fires. *Revue de L'Institut Francais du Petrole,* Issue 50, pp. 69-74.

[40]Goodrich, T. et al., 2010. High-temperature mechanical properties and thermal recovery of balsa wood. *The Japan Wood Research Society,* Issue 56, p. 437–443.

[41]Goodrich, T., 2009. *Thermophysical Properties and Microstructural Changes of Composite Materials at Elevated Temperature,* Blacksburg, VA: Virginia Polytechnic Institute.

[42]Gottuk, D. & White, D., 2015. Liquid Fuel Fires. In: Greenbelt, ed. *SFPE Handbook of Fire Protection Engineering.* USA: Springer, pp. 2552-2590.

[43]Grenier, A., 1998. Fire Characteristics of Cored Composite Materials for Marine Use. *Fire Safety Journal ,* Issue 30, p. 137Ð159.

[44]Halliwell, S., 2004. In service performance of FRP structures. In: L. C. Hollaway, M. K. Chryssanthopoulos & S. .Moy, eds. *Advanced Polymer Composites for Structural Applications in Construction.* Guildford, UK: Woodhead Publishing Limited, pp. 719- 726.

[45]Hartin, e. & MS, E. M. C., 2008. *Fire Development and Fire Behavior Indicators,* s.l.: CFBT-US.

[46]Henderson, J., Wiebelt, J. & . Tant, M., 1985. A model for the thermal response of polymer composite. *Journal of Composite Materials,* Issue 19, pp. 579-595.

[47]Hollaway, L., 2003. The evolution of and the way forward for advanced polymer composites in the civil infrastructure. *Construction and Building Materials,* Issue 17, p. 365–378.

[48]Hollaway, L., 2010. A review of the present and future utilisation of FRP composites in the civil infrastructure with reference to their important in-service properties. *Construction and Building Materials,* Issue 24, p. 2419–2445.

[49]Hui, L., 1998. *Synthesis, Characterization and Properties of Vinyl Ester Matrix Resins,* Blacksburg, Virginia: Virginia Polytechnic Institute.

[50]Imam, B. & Chryssanthopoulos, M., 2012. *Causes and Consequences of Metallic Bridge Failures,* Guildford, UK: Faculty of Engineering and Physical Sciences, University of Surrey.

[51]Jain, R., Lee, L., Stephenson, L. & Ramirez, C., 2011. Introduction. In: R. Jain & L. Lee, eds. *Fiber Reinforced Polymer (FRP) Composites for Infrastructure Applications.* s.l.:Springer, pp. 1-22.

[52]Karbhari, V. M. & Chin, J. W., 2001. "Gap Analysis" for Durability of Composites in Civil Infrastructure. *Construction and Materials ,* pp. 35-44.

[53]Keller, T., 2001. Recent all-composite and hybrid fibre-reinforced polymer bridges and buildings. *Progress in Structural Engineering and Materials,* Issue 3, p. 132–140.

[54]Keller, T., 2010. Multifunctional and Robust Composite Material Structures for Sustainable Construction. *CICE 2010- The 5th International Conference on FRP Composites in Civil Engineering.*

[55]Keller, T. & Bai, Y., 2014. *High Temperature Performance of Polymer Composites.* s.l.:Wiley-VCH Verlag GmbH & Co..

[56]Keller, T. & Haas, C., 2008. *Function-integrated GFRP sandwich roof structure – Structural concept and design.* Zurich, Switzerland, Fourth International Conference on FRP Composites in Civil Engineering (CICE2008).

[57]Keller, T., Rothe, J., De Castro, J. & Osei-Antwi, M., 2014. GFRP-Balsa Sandwich Bridge Deck: Concept, Design and Experimental Validation. *Composite Construction,* Issue 18.

[58]Keller, T., Tracy, C. & Zhou, A., 2006. Structural response of liquid-cooled GFRP slabs subjected to fire - Part I: Material and post-fire modeling. *Composites Part A,* 37(9), pp. 1286-1295.

[59]Kepler, J., 2010. Simple Stiffness Tailoring of Balsa Sandwich Material. *Composites Science,* Issue 71, pp. 46-67.

[60]Kodur, V. K. R., Naser, N. & Aziz, E. M., 2015. Strategies for Enhancing fire performance of steel bridges . In: V. K. R. Kodur & N. Banthia, eds. *Response of Structures Under Extreme Loading.* s.l.:DEStech publications, pp. 881-898.

[61]Kodur, V. & Naser, M., 2013. Importance factor for design of bridges against fire hazard. *Engineering Structures,* Issue 54 , p. 207–220.

[62]Kontopanos, P., 2001. *Fiber Reinforced Polymer Bridge Deck Panels,* New York: Massachusetts Institute of Technology.

[63]Kosmatka, J. B., 2008. *Composite Bridging for Military and Emergency Applications,* San Diego: University of California,.

[64]Kotlarewski, N., Ozarska, B. & . Gusamo, K. B., 2014. Thermal Conductivity of Papua New Guinea Balsa Wood Measured using the Needle Probe Procedure. *BioResources,* Issue 9, pp. 5784-5793.

[65]Kyriakide, S. & Da-Silva, A., 2007. Compressive response and failure of balsa wood. *International Journal of Solids and Structures,* Issue 44, pp. 8685-8717.

[66]Lattimer, B., Ouellette, J. & Trelles, J., 2009. Thermal Response of Composite Materials to Elevated Temperatures. *Fire Technology,* Issue 47, p. 823–850.

[67]Lennon, T., Moore, D. B., Wang, Y. C. & Bailey, C. G., 2006. *Designers' Guide to EN 1991-1-2, EN 1993-1-2 and EN 1994-1-2: Handbook for the fire design of steel, composite, and concrete structures to the eurocodes.* s.l.:Thomas Telford.

[68]Leroy Gardner, 2012. *Tubular Structures XIV.* London: Taylor and Francis Group.

[69]Manalo, A., 2013. *Fibre reinforced polymer composites sandwich structure: Recent developments and applications in civil infrastructure,* Australia: University of Southern Queensland.

[70]Manalo, A., Maranan, G. & Erp, G., 2013. *Glue-laminated Composite Sandwich Beams for Structural Engineering and Construction.* Japan, Hokkaido University Collection of Scholarly and Academic Papers.

[71]Mc Grattan, K., Baum, H. & Hamins, A., 2000. *Thermal radiation from large pool fires,* USA: National Institute of Standards and Technology.

[72]McGrattan, K. & Miles, S., 22016. Modeling fires using Computational Fluid Dynamics (CFD). In: M. J. Hurley, ed. *SFPE Handbook of Fire Protection Engineering.* USA: Springer, pp. 1034-1066.

[73]McManus, H. & Springer, G., 1992. High temperature behaviour of thermomechanical behaviour of carbon-phenolic and carbon-carbon composites, I. Analysis. *Journal of Composite Materials,* Issue 26, pp. 206-229.

[74]Mei, L., 2000. *Temperature and moisture effects on composite materials for wind turbine blades,* Bozeman, Montana: Montana state University-Bozeman.

[75]Mhirschler, M. & GBH International, U., 2008. Improving the fire safety of road vehicles. In: A. Horrocks & D. Price, eds. *Advance in fire retardant materials.* s.l.:Woodhead Publishing Limited, pp. 443-466.

[76]Mouritz, A., 2007. Durability of composites exposed to elevated temperature and fire. In: V. Karbhari, ed. *Durability of Composites for Civil Structural Applications.* USA: Woodhead Publishing, pp. 98-125.

[77]Mouritz, A. et al., 2009. Review of fire structural modelling of polymer composites. *Composites: Part A,* Issue 40, p. 1800–1814.

[78]Mouritz, A. & Gibson, A., 2006. *Fire properties of polymer composite materials.* s.l.:Springer.

[79]Mouritz, A. & Mathys, Z., 1999. Post-fire mechanical properties of marine polymer composites. Composite Structures. *Composite Structures,* Issue 47, pp. 643-653.

[80]Mouritz, A. P., 2007. Durability of composites xposed to elevated temperature and fire. In: V. Karbhari, ed. *Durability of Composites for Civil Structural Applications.* s.l.:Woodhead Publishing Series, pp. 98-125.

[81]Nair, A. et al., 2010. *Performance evaluation of a FRP-wrapped balsa wood bridge deck system.* Honolulu, Earth & Space 2010 Conference, pp. 1693-1702.

[82]Naser, M. Z. & Kodur, V., 2015. A probabilistic assessment for classification of bridges against fire hazard. *Fire Safety Journal,* Issue 76, pp. 65-73.

[83]National Fire Protection Association, 2007. *Draft NFPA 556,* USA: s.n.

[84]Nendaz, S. & Lavanchy, S., 2012. Tablier composite du Pont sur l'Avançon. *Tracés,* Issue 22.

[85]Omar, T., Van Erp, G. & Key, P., 2007. *Innovative All Composite Multi-Pultrusion Truss System for Stressed Arch Deployable Shelters.* Egypt, AICSGE 6: 6th Alexandria International Conference on Structural and Geotechnical Engineering.

[86]Osei-Antwi, M., 2014. *Structural performance of complex core systems for FRP-balsa composite sandwich bridge decks,* Suisse: École Polytechnique Fédéral de Lausanne.

[87]Outinen, J., 2007. *Mechanical properties os structural steel at elevated temperatures and after cooling down.* San Francisco, USA, Interscience Communications Limited, UK,.

[88]Pagani, R., Bocciarelli, M., Carvelli, V. & Pisani, M., 2014. Modelling high temperature effects on bridge slabs reinforced with GFRP rebars. *Engineering Structures,* Issue 81, p. 318–326.

[89]Palm, J., 1994. Temperature analysis using ABAQUS. *Fire Technology,* Volume 30, pp. pp 291-303.

[90]Pascoe, D., 2015. *Moisture Meters on Boat Hulls.* [Online]
Available at: http://www.yachtsurvey.com/moisture_meters.htm
[Accessed 11 June 2016].

[91]Payá-Zarforteza, I. & Garlock, M., 2012. A numerical investigation on the fire response of a steel girder bridge. *Journal of Constructional Steel Research,* Issue 75, p. 93–103.

[92]Pering, G., Springer, G. & Farrel, P., 1980. Degradation of tensile and shear properties of composites exposed to fire or high temperature. *Journal of Composite Materials,* Issue 14, pp. 54-66.

[93]Peris-Sayol, et al., 2015. *Analysis of the Influence of Structural Models in Fire Responses of Steel Girder Bridges.* s.l., Structures Congress 2015.

[94]Peris-Sayol, G., 2013. *Análisis del colapso del paso superior situado entre las calles Hodge y Bayard, en la localidad de Princeton, NJ, USA",* Valencia: Polytechnic University of Valencia.

[95]Pintea, D., 2016. *Design Approaches: Performance: Thermal Analysis.* [Online] Available at: dan.ct.upt.ro/fire/files/ThermalAnalysis.doc [Accessed 27 April 2016].

[96]Potyrała, P. B., 2011. *Use of Fibre Reinforced Polymer Composites in Bridge Construction. State of the Art in Hybrid and All-Composite Structures.*, Barcelona: Universitat Politecnica de Catalunya.

[97]Promat Internacional , 2013. *PROMAT.* [Online] Available at: http://www.promat-tunnel.com/en/advices/fire-protection/fire%20curves [Accessed 14 April 2016].

[98]Quang-Tuan, N., Di-Benedetto, H. & Sauzéat, C., 2012. Determination of thermal properties of asphalt mixtures as another output from cyclic tension-compression test. *Road Materials and Pavement Design,* 13(1), pp. 85-103.

[99]Quiel, S. E., Yokoyama, T., Bregman, L. S. & Mueller, K. A., 2015. A streamlined framework fo rcalculating the response of steel-sup-ported bridges to open-air tanker truck fires. *Fire Safety Journal,* Issue 73, p. 63–75.

[100] Radmanović, K., Đukić, I. & Pervan, S., 2014. Specific Heat Capacity of Wood. *DRVNA INDUSTRIJA,* Issue 65, pp. 151-157.

[101] Rahman, A. A. A., 2015. *Fire Structural Properties of Sandwich Composites,* USA: Royal Melbourne Institute of Technology.

[102] Ramroth, W. T., 2006. *Thermo-mechanical Structural Modelling of FRP Composite Sandwich Panels Exposed to Fire,* s.l.: University of California.

[103] Read, J., 1996. *Fatigue cracking of bituminous paving mixtures,* s.l.: University of Nottingham.

[104] Rodrigues Morgado, T. M., 2012. *Fire resistance behaviour of GFRP pultruded profiles,* Lisbon: s.n.

[105] Rodrigues-Morgado, T., 2012. *Fire Protection Systems for GFRP Pultruded Profiles,* Lisbon: Tecnico Lisboa.

[106] Schollmayer, M., 2009. *Through-Thickness Performance of Adhesive Connections Between FRP Bridge Decks and Steel Main Girders,* Lausanne: École Polytechnique Fédéral de Lausanne.

[107] Silva, J. C. G., Landesmann, A. & Ribeiro, F. L., 2014. *Interface model to fire-thermomechanical performance based analysis of structures under fire consitions.*

Gaithersburg, MD, USA, Fire and Evacuation Modeling Technical Conference (FEMTC) 2014.

[108] Simeoni, A., 2015. Wildland fires. In: M. J. H., ed. *SFPE Handbook of Fire Protection Engineering.* Greenbelt: Springer, pp. 3283-3303.

[109] Sobrinho, L. L., Ferreira, M. & Bastian, F. L., 2009. The effects of water absorption on an ester vinyl resin system. *Materials Research,* 12(3).

[110] Sokol, Z. & Wald, F., 2010. *Sustainable steel and timber constructions (SUSCOS): Design for fire and robustness.* [Online]
Available at: http://steel.fsv.cvut.cz/suscos/PP/2C10-01_Fire-design_Introduction.pdf
[Accessed 27 April 2016].

[111] Springer, G. S., 1984. Model for Predicting the Mechanical Properties of Composites at Elevated Temperatures. *Journal of Reinforced Plastics and Composites,* Issue 1, pp. 85-95.

[112] Spruce, H., 2016. *The Hub.* [Online]
Available at: http://www.highspeedtraining.co.uk/hub/fire-triangle-tetrahedron-combustion/
[Accessed 13 April 2016].

[113] SteelConstruction, 2012. *SteelConstruction.info.* [Online]
Available at: http://www.steelconstruction.info/File:Fire_test_curves.png
[Accessed 14 April 2016].

[114] Swan, B., 2014. *Ignition and spread of fire.* [Online]
Available at: https://www.linkedin.com/pulse/20140715143714-57781373-ignition-and-spread-of-fire
[Accessed 14 April 2016].

[115] Swiss Standards Association, 2003b. *"Actions on structures",* Zurich, Switzerland: SIA 261.

[116] Taha, M. et al., 2013. Study of the Effect of Temperature Changes on the Elastic Modulus of Flexible Pavement Layers. *Research Journal of Applied Sciences, Engineering and Technology,* 5(5), pp. 1661-1667.

[117] Tracy, C. D., 2005. *Fire Endurance of Multicellular Panels in an FRP Building System,* Lausanne: École Polytechnique Fédérale De Lausanne.

[118] Tuwair, H., Volz, J., ElGawady, M. & Chandrashekhara, K., 2016. Modeling and Analysis of GFRP Bridge Deck Panels Filled with Polyurethane Foam. *Journal of Bridge Engineering,* 5(21).

[119] Valbona, M., Reza, H. & Harryson, P., 2014. Bridge decks of fibre reinforced polymer (FRP): A sustainable solution. *Construction and Building Materials,* Issue 50, pp. 190-199.

[120] Vural, M. & Ravichandran, G., 2003. Dynamic response and energy dissipation characteristics of balsa wood: experiment and analysis. *International Journal of Solids and Structures,* Issue 40, p. 2147–2170.

[121] Wright, W. et al., 2013. *Highway Bridge Fire Hazard Assessment Draft Final Report,* s.l.: s.n.

[122] Wu, C., 2016. *Mechanical properties of BALTEK VBC (90o) under elevated temperatures,* s.l.: Postdoctoral Research.

[123] Yu, Z., 2012. *Thermal and mechanical responses of fiber reinforced polymer composites under one-sided fire exposure,* Charlotte: The University of North Carolina.

[124] Zhang, S., 2013. *Thermomechanical Interaction Effects in Polymer Foam Cored Sandwich Structures,* Southampton: University of Southampton.

[125] Zürcher, E., 2016. *Wood: Structures, poperties and uses,* Biel-Bienne: Bern Univerity of Applied Science.